NAVAL POSTGRADUATE SCHOOL
Monterey, California

THESIS

POOL BOILING OF R-114/OIL MIXTURES FROM SINGLE TUBES AND TUBE BUNDLES

by

Thomas J. Murphy

September 1987

Thesis Advisor: P.J. Marto

UNCLASSIFIED
URITY CLASSIFICATION OF THIS PAGE

REPORT DOCUMENTATION PAGE

REPORT SECURITY CLASSIFICATION UNCLASSIFIED	1b RESTRICTIVE MARKINGS
SECURITY CLASSIFICATION AUTHORITY	3 DISTRIBUTION/AVAILABILITY OF REPORT Approved for public release; distribution is unlimited
DECLASSIFICATION/DOWNGRADING SCHEDULE	
ERFORMING ORGANIZATION REPORT NUMBER(S)	5 MONITORING ORGANIZATION REPORT NUMBER(S)
NAME OF PERFORMING ORGANIZATION val Postgraduate School	6b OFFICE SYMBOL (If applicable) Code 69
7a NAME OF MONITORING ORGANIZATION Naval Postgraduate School	
ADDRESS (City, State, and ZIP Code) nterey, California 93943-5000	7b ADDRESS (City, State, and ZIP Code) Monterey, California 93943-5000
NAME OF FUNDING/SPONSORING ORGANIZATION	8b OFFICE SYMBOL (If applicable)
9 PROCUREMENT INSTRUMENT IDENTIFICATION NUMBER	
ADDRESS (City, State, and ZIP Code)	10 SOURCE OF FUNDING NUMBERS

PROGRAM ELEMENT NO	PROJECT NO	TASK NO	WORK UNIT ACCESSION NO

TITLE (Include Security Classification)
OL BOILING OF R-114/OIL MIXTURES FROM SINGLE TUBES AND TUBE BUNDLES

PERSONAL AUTHOR(S)
rphy, Thomas J.

TYPE OF REPORT	13b TIME COVERED	14 DATE OF REPORT (Year, Month, Day)	15 PAGE COUNT
ster's Thesis	FROM _____ TO _____	1987, September	144

SUPPLEMENTARY NOTATION

COSATI CODES		
FIELD	GROUP	SUB-GROUP

18 SUBJECT TERMS (Continue on reverse if necessary and identify by block number)
R-114; Nucleate Pool Boiling; Enhancement; Single Tube; Tube Bundles; Oil Contamination

ABSTRACT (Continue on reverse if necessary and identify by block number)

An apparatus was designed, fabricated and operated for the testing of rizontal tube bundles for boiling of R-114 with various concentrations oil. Preliminary data were taken on the top tube in the bundle, with d without the other tubes in operation. Results showed up to a 37 rcent increase in the boiling heat-transfer coefficient as a result of e favorable bundle effect.

In a separate single-tube apparatus, three enhanced tubes were tested a saturation temperature of 2.2 °C with oil mass concentrations of 0, 2, 3, 6 and 10 percent. The tubes were: (1) a finned tube with 24 fins per meter (26 fpi), (2) a finned tube with 1575 fins per meter 0 fpi) and (3) a Turbo-B tube. These tubes resulted in enhancement

STRIBUTION/AVAILABILITY OF ABSTRACT UNCLASSIFIED/UNLIMITED ☐ SAME AS RPT ☐ DTIC USERS	21 ABSTRACT SECURITY CLASSIFICATION Unclassified
NAME OF RESPONSIBLE INDIVIDUAL of. A. Wanniarachchi	22b TELEPHONE (Include Area Code) (408) 646-3385
	22c OFFICE SYMBOL Code 69Wa

ORM 1473, 84 MAR 83 APR edition may be used until exhausted
All other editions are obsolete

SECURITY CLASSIFICATION OF THIS PAGE
UNCLASSIFIED

#19 - ABSTRACT - (CONTINUED)

ratios in pure refrigerant of 2.8, 3.8 and 5.2, respectively, at a practical heat flux of 30 kW/m^2. With 3 percent oil, these ratios were decreased to 2.6, 3.5 and 5, while with 10 percent oil, these ratios were further reduced to 2.6, 3.2 and 4.7, respectively. Based on these results, the use of Turbo-B tubes is expected to result in significant savings in weight and size of evaporators over the finned tubes presently in use on board some naval vessels.

Approved for public release; distribution unlimited.

Pool Boiling of R-114/Oil Mixtures from Single Tubes and Tube Bundles

by

Thomas J. Murphy
Lieutenant Commander, United States Navy
B.S.Ch.E., Northwestern University, 1977

Submitted in partial fulfillment of the
requirements for the degrees of

MASTER OF SCIENCE IN MECHANICAL ENGINEERING
and
MECHANICAL ENGINEER

from the

NAVAL POSTGRADUATE SCHOOL
September 1987

ABSTRACT

An apparatus was designed, fabricated and operated for the testing of horizontal tube bundles for boiling of R-114 with various concentrations of oil. Preliminary data were taken on the top tube in the bundle, with and without the other tubes in operation. Results showed up to a 37 percent increase in the boiling heat-transfer coefficient as a result of the favorable bundle effect.

In a separate single-tube apparatus, three enhanced tubes were tested at a saturation temperature of 2.2 ^{o}C with oil mass concentrations of 0, 1, 2, 3, 6 and 10 percent. The tubes were: (1) a finned tube with 1024 fins per meter (26 fpi), (2) a finned tube with 1575 fins per meter (40 fpi) and (3) a Turbo-B tube. These tubes resulted in enhancement ratios in pure refrigerant of 2.8, 3.8 and 5.2, respectively, at a practical heat flux of 30 kW/m^2. With 3 percent oil, these ratios were decreased to 2.6, 3.5 and 5, while with 10 percent oil, these ratios were further reduced to 2.6, 3.2 and 4.7, respectively. Based on these results, the use of Turbo-B tubes is expected to result in significant savings in weight and size of evaporators over the finned tubes presently in use on board some naval vessels.

TABLE OF CONTENTS

LIST OF TABLES

LIST OF FIGURES

ACKNOWLEDGEMENTS

The author wishes to express his appreciation to Dr. Paul J. Marto and Dr. A.S. Wanniarachchi for their advice and guidance in the research project and towards the completion of this thesis. Additionally, the assistance rendered by Thomas McCord and the Machine Shop personnel of the Mechanical Engineering Department was invaluable.

The author also wishes to express his sincere gratitude to his wife, Rosanne, for her patience and unwavering support throughout this endeavor.

I. INTRODUCTION

A. BACKGROUND

Throughout the U.S. Navy a wide array of heat-exchanger applications exists on board both surface and submerged vessels. Because of the significant cost, the weight of such components, and the premium associated with shipboard space, considerable effort has been expended in recent years to design more compact and efficient heat exchangers. While the Navy's efforts in achieving these goals include a wide variety of heat exchangers, this thesis work concentrates on evaporators used in water chillers on board naval vessels.

The design of compact heat exchangers almost always involves the use of enhanced heat-transfer surfaces. For example, the use of enhanced boiling surfaces that have been developed commercially during the past decade provide up to a tenfold enhancement of boiling coefficients. The Navy presently uses copper finned tubes having 700 to 1050 fins per meter or porous-coated High Flux tubes for shipboard evaporator tubes. The refrigerant is boiled on the outside surface of these tubes, thereby cooling the fresh water that flows inside them. Such finned tubes generally show about a threefold enhancement on the outside when compared to smooth tubes [Ref. 1]. Therefore, the use of a more advanced boiling surface, such as the High Flux surface, which shows

up to a tenfold increase in the boiling heat-transfer coefficient [Ref. 2] results in significant reductions in the size and weight of evaporators the Navy puts to sea. Further, owing to the use of fresh water on the inside of these tubes, it is possible and desirable to use internal enhancements, such as ridges, to further reduce the size and weight of these components. Notice that the use of internal enhancement would not raise serious questions about fouling because of the use of fresh, possibly chemically treated, water through the tubes.

Boiling is a very complex phenomenon. Indeed, this complexity is well demonstrated by the lack of a good model (theoretical or empirical) for the seemingly simple case of single-component boiling from a single smooth tube. Chongrungreong and Sauer [Ref. 3] compare nine equations in an attempt to arrive at a predictive model for this "simple" case. Yet, no truly reliable model exists in the literature. The treatment of boiling from an enhanced surface, which contains reentrant cavities, is even more complex than for a single smooth tube. Also, the performance of any given tube in a bundle can be significantly different from the performance of a single tube in a large liquid pool, thus requiring performance data of tube bundles. The boiling phenomenon is even further complicated by the presence of refrigeration oil mixed with the refrigerant liquid being boiled in the evaporator. Notice

that most refrigeration systems use hermetically sealed compressors, which are cooled by the refrigerant liquid. Therefore, small amounts of oil generally migrate into the evaporator space.

Based on the above discussion, it is essential that a sufficient amount of reliable data be available to designers of refrigeration systems. Such data must include all relevant variables and operating conditions. As discussed in Chapter II, a scarcity of data exists in the literature covering the operating conditions outlined above.

Even though R-11 and R-22 are the most common working fluids being used in industry for large refrigerating and air-conditioning systems, the Navy has been using R-114. The Navy has selected R-114 over other refrigerants based on four important advantages offered by this refrigerant.

The advantages are:

(1) R-114 is a moderate-pressure refrigerant, thus minimizing leakage problems,

(2) R-114 belongs to a group of refrigerants with the least toxicity [Ref. 4],

(3) R-114 is more stable with temperature, and

(4) R-114 is more stable when exposed to water vapor.

Using the data provided by Helmick [Ref. 5], the thermal resistances to heat transfer were calculated for the evaporators on board two recent classes of Navy combatant. Tables 1.1 and 1.2 list most of the design and operating parameters, together with some computed parameters, for the

TABLE 1.1

DESIGN AND OPERATING PARAMETERS FOR CG-47 EVAPORATOR

Design Parameters [Ref. 5]		
Tube material	Copper	
Fin density	748 fins/m	(19 fins/in)
Tube outside diameter	19.1 mm	(0.75 in)
Tube inside diameter	16.6 mm	(0.625 in)
Tube wall thickness	1.25 mm	(0.049 in)
Tube length	3.61 m	(142.0 in)
Number of tubes per pass	113	
Number of passes	2	
Operating Parameters [Ref. 5]		
Water inlet temperature	10.4 ^{o}C	(50.7 ^{o}F)
Water outlet temperature	6.7 ^{o}C	(44.0 ^{o}F)
Saturation temperature	1.9 ^{o}C	(35.4 ^{o}F)
Cooling water flow rate	45.4 kg/s	(100.1 lbm/sec)
Computer Parameters		
Total cooling load	711.2 kW	(2.43 E6 BTU/hr)
Cooling water velocity	1.41 m/s	(4.63 ft/sec)
Overall thermal conductance (U_oA_o)	110.1 kW/K	(58.1 BTU/^{o}R·sec)
Mass of tubes (M)	5052 kg	(11,138 lbm)
Estimated evap. vol. (V)	2.03 m^3	(71.7 ft^3)
Heat-Transfer Capacity		
U_oA_o/M	0.0217 kW/K·kg	(0.0052 BTU/^{o}R·sec·lb)
U_oA_o/V	54.2 kW/K·m^3	(0.81 BTU/^{o}R·sec·ft^3)

TABLE 1.2

DESIGN AND OPERATING PARAMETERS FOR DDG-51 EVAPORATOR

Design Parameters [Ref. 5]		
Tube material	95% Copper 5% Nickel	
Tube type	corrugated, outside coated with High Flux	
Tube outside diameter	15.9 mm	(0.625 in)
Tube inside diameter	13.4 mm	(0.527 in)
Tube wall thickness	1.25 mm	(0.049 in)
Tube length	2.56 m	(100.8 in)
Number of tubes per pass	170	
Number of passes	2	
Operating Parameters [Ref. 5]		
Water inlet temperature	10.4 ^{o}C	(50.7 ^{o}F)
Water outlet temperature	6.7 ^{o}C	(44.0 ^{o}F)
Saturation temperature	5.0 ^{o}C	(41.0 ^{o}F)
Cooling water flow rate	4.54 kg/s	(100.1 lbm/sec)
Computed Parameters		
Total cooling load	711.3 kW	(2.43 E6 BTU/hr)
Cooling water velocity	1.9 m/s	(6.23 ft/sec)
Overall thermal conductance (U_oA_o)	224.3 kW/K	(118 BTU/^{o}R·sec)
Mass of tubes (M)	4416 kg	(9,736 lbm)
Estimated evap. volume (V)	1.15 m^3	(40.5 ft^3)
Heat-Transfer Capacity		
U_oA_o/M	0.0508 kW/K·kg	(0.0121 BTU/^{o}R·sec·lb)
U_oA_o/V	224.3 kW/K·m^3	(2.91 BTU/^{o}R·sec·ft^3)

CG-47 and DDG-51 evaporators, respectively. Since almost all design and operating parameters are different between these two evaporators, a direct comparison of the mass of tubes or the volume of the shell would be inappro-priate. Therefore, in order to make a more meaningful comparison between these two evaporators, Tables 1.1 and 1.2 list U_oA_o/M (i.e., the overall heat-transfer capacity per unit mass of tubes) and U_oA_o/V (i.e., the overall heat-transfer capacity per unit volume of evaporator). As can be seen, the DDG-51 evaporator offers a 134% and 314% increase in these two parameters, respectively, compared to the CG-47 evaporator.

As Figure 1.1 shows, for the Ticonderoga (CG-47) class cruiser, the inside, wall and outside resistances are 52, 1 and 47 percent, respectively, of the overall thermal resistance. For the Arleigh Burke (DDG-51) class destroyer, these resistances are 48, 2 and 50 percent, respectively (see Figure 1.2). As shown in Figure 1.3, the DDG-51 evaporator, due to both interior and exterior enhancement, shows a 51 percent reduction in the overall thermal resistance compared to the CG-47 evaporator. Based on this information, significant savings in size and weight of these evaporators could be achieved by widespread use of more advanced boiling surfaces.

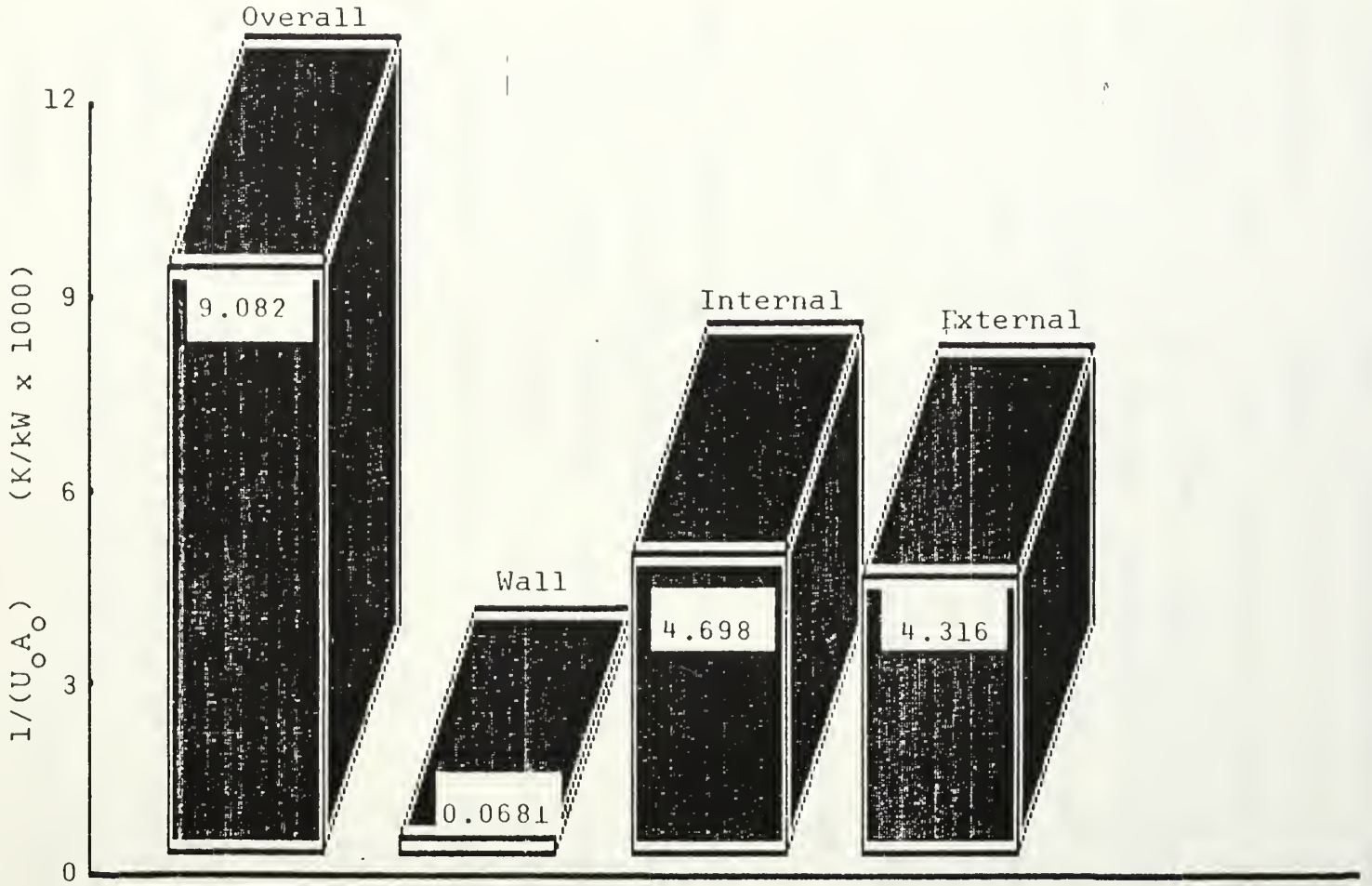

Figure 1.1 CG-47 Evaporator Thermal Resistances

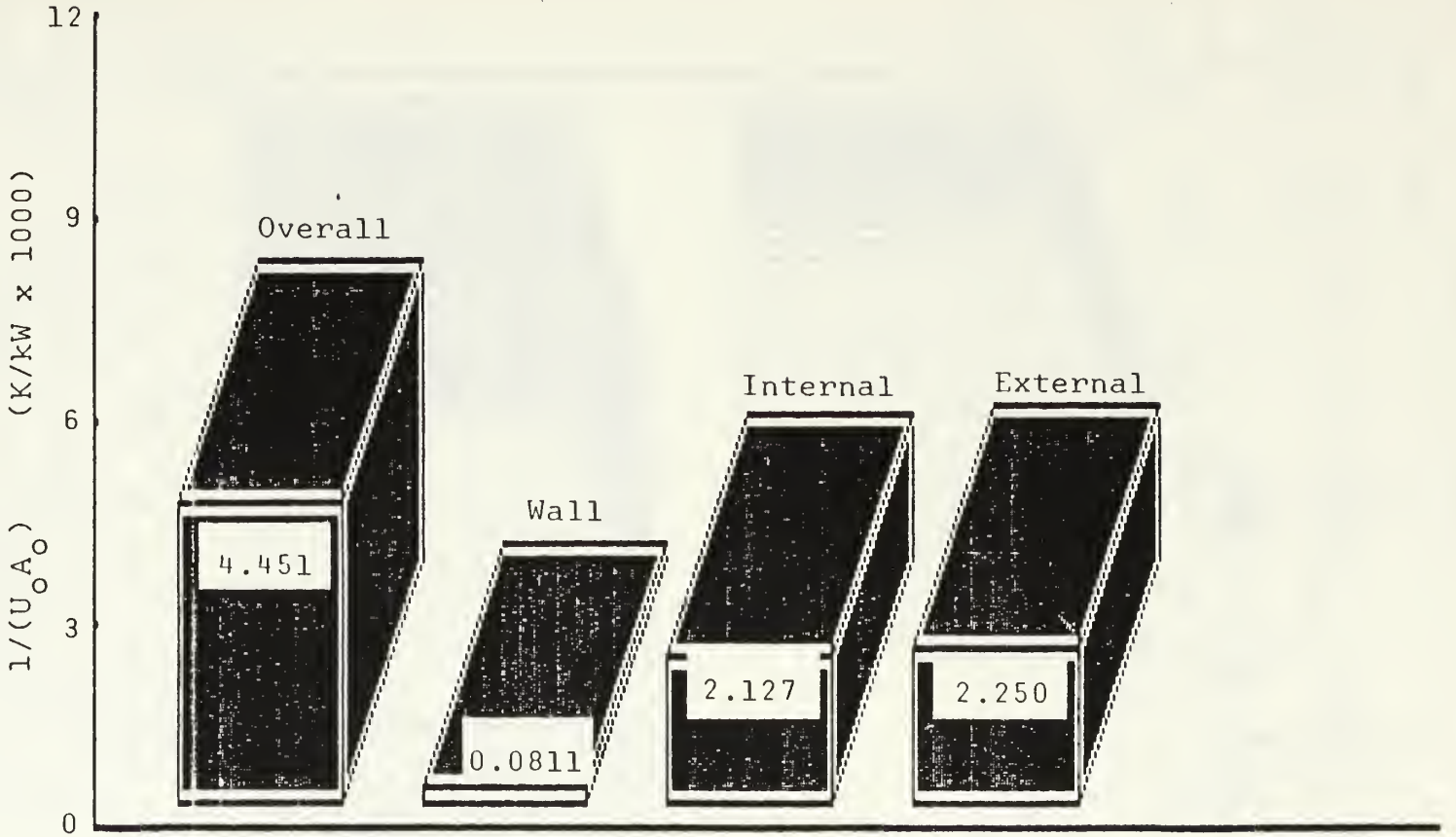

Figure 1.2 DDG-51 Evaporator Thermal Resistances

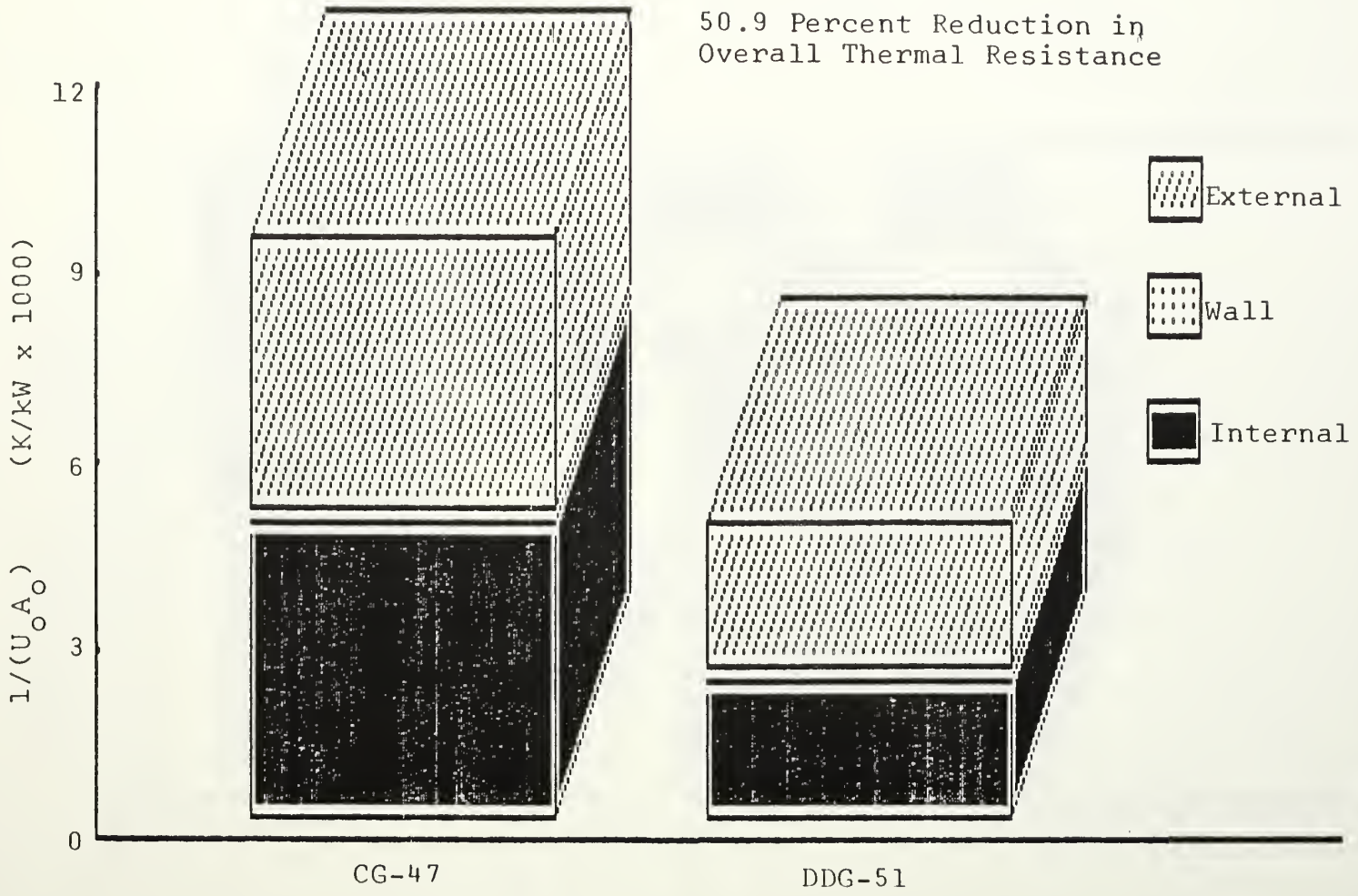

Figure 1.3 Comparison of Thermal Resistances for CG-47 and DDG-51 Evaporators

B. OBJECTIVES

Based on the foregoing discussion, the major objectives of this thesis were:

1. Design, fabricate and operate an apparatus for the testing of a boiling tube bundle with R-114 as the working fluid.[1]

2. Using the single-tube apparatus already in operation at the Naval Postgraduate School, test: (a) a 1024 fpm (26 fpi) finned tube, (b) a 1575 fpm (40 fpi) finned tube, and (c) a Turbo-B tube with 0, 1, 2, 3, 6 and 10 percent by mass of miscible oil.

3. Compare the new data with those taken on this apparatus for a smooth tube and the High Flux enhanced tube.

---

[1]Initially, the primary objective of this study was to test a tube bundle of smooth and externally enhanced tubes in an attempt to obtain the best-performing tubes for the conditions of the Navy's interest. For example, the testing of Turbo-B, High Flux and other enhanced tubes was essential. Unfortunately, owing to considerable delays experienced in receiving funding for this project and further delays with the installation of a large refrigeration unit, it was not possible to fully complete this objective. Therefore, new objectives were established in order to provide achievable goals while at the same time providing important supplementary information.

II. LITERATURE REVIEW

A. INTRODUCTION

Figure 2.1 shows a schematic representation of the heat-transfer performance when a gradually increasing and then decreasing heat flux is applied to a solid surface, which is immersed in a pool of liquid. This figure shows the variation of heat flux with the temperature drop from the average wall temperature to the saturation temperature. This temperature drop is also referred to as the wall superheat, and the resulting curve is referred to as the "boiling curve." The line AB represents the heat-transfer performance while only natural convection is the mode of heat transfer. For this situation, the wall superheat increases rapidly with increasing heat flux, indicative of poor heat-transfer performance. At point B, however, bubbles appear which depart from the surface and this point is normally referred to as the onset of nucleate boiling (ONB). When bubble nucleation occurs, the wall superheat that is required to remove the prescribed heat flux is drastically reduced and, after a very rapid transition period, point C is reached. Further increase in heat flux is represented by curve CD. As is well known, the maximum heat flux obtained under this condition is known as the critical heat flux (CHF) (see point D). Increases in wall

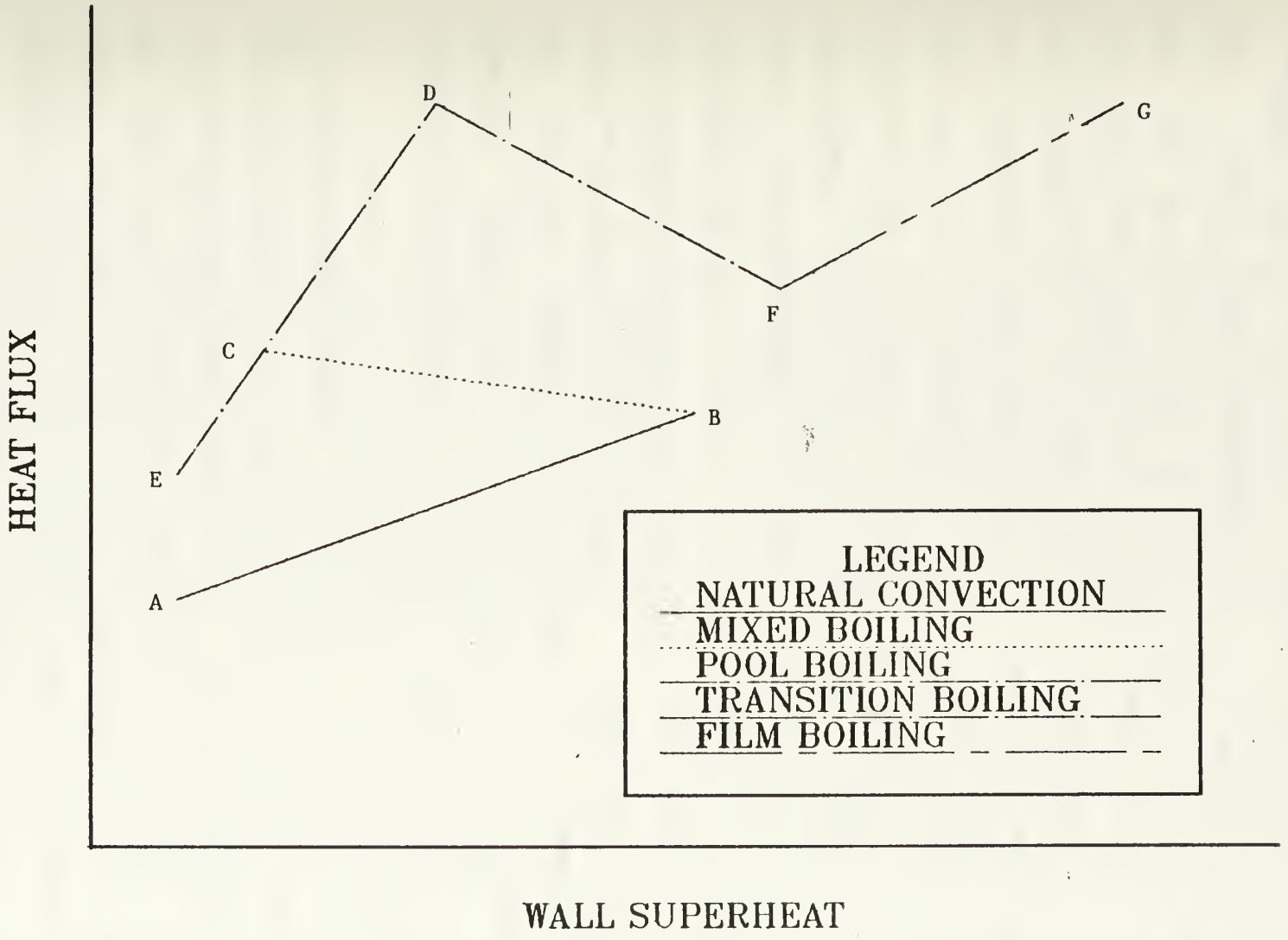

Figure 2.1 Schematic of a Typical Boiling Curve

superheat beyond critical heat flux result in a decrease in heat flux. The resulting regime (line DF) is referred to as the transition boiling regime. Increases in wall superheat beyond point F result in increased heat flux. The phenomenon depicted in line FG is referred to as the film boiling regime. From point D, the critical heat flux, if heat flux is decreased, the heat-transfer performance would be represented by curve DCE. This region is referred to as the pool-boiling region, which represents a much larger heat-transfer performance compared to that in the natural-convection region. The observance that the wall superheat during nucleate boiling in region CE (decreasing heat flux) is less than the superheat that is required in the natural-convection region AB (increasing heat flux) is referred to as boiling hysteresis. Boiling hysteresis is generally more pronounced for highly wetting fluids such as the refrigerants. The nucleate pool-boiling process is very efficient due to bubble pumping, intense mixing and thin-film evaporation from the solid surface.

Usually, the wall superheat necessary to generate a vapor bubble depends on the surface cavity size in addition to fluid properties, such as surface tension and viscosity. In fact, the wall superheat necessary for nucleation increases with decreasing cavity size. Therefore, the cavity size must be large enough to lower the necessary wall superheat, while it should be small enough to sustain

nucleation by retaining a small portion of vapor when a bubble departs from its surface.

Based on the phenomenon briefly discussed above, a number of advanced boiling surfaces have been developed over the past decade. For example, Figure 2.2 shows four enhanced boiling surfaces: (a) GEWA-T surface, manufactured by splitting and rolling the fins of a standard finned tube, (b) High Flux surface, consisting of a coating of sintered particles, (c) Thermoexcel-E surface, manufactured by bending over serrated fin tips to provide triangular cavities and (d) Turbo-B enhanced surface, manufactured by Wolverine Tube. These surfaces offer a high density of reentrant cavities to enhance the pool-boiling performance. During nucleate boiling, the density and the size of the active, reentrant cavities depends on the specific fluid being boiled. Further, single-tube performance can be different from that of tube-bundle performance. In addition, the presence of a less-volatile component mixed with a volatile component changes the boiling performance of the overall mixture. In view of these important aspects, the literature review presented in this chapter will focus on (1) single-tube studies and (2) tube-bundle studies for both the pure-component case and that for boiling of mixtures. Emphasis will be given to the use of enhanced surfaces.

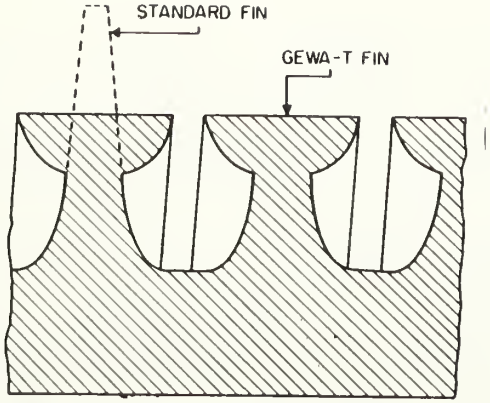

(a) GEWA-T Surface

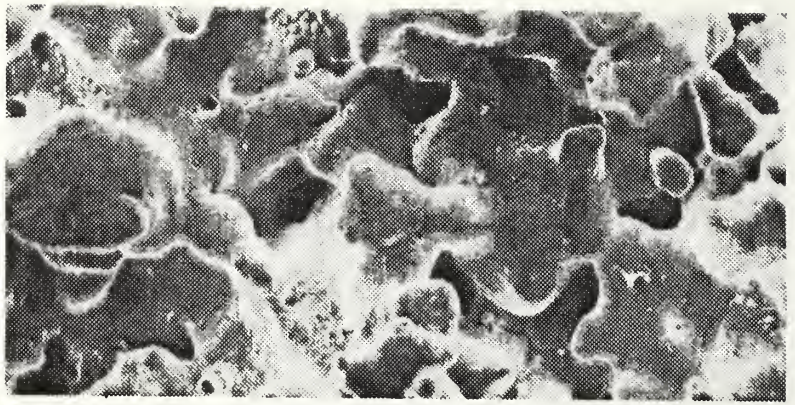

(b) High Flux Surface

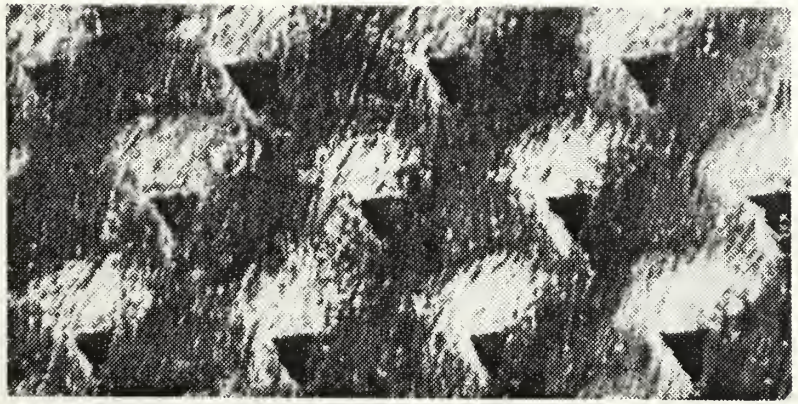

(c) Thermoexcel-E Surface

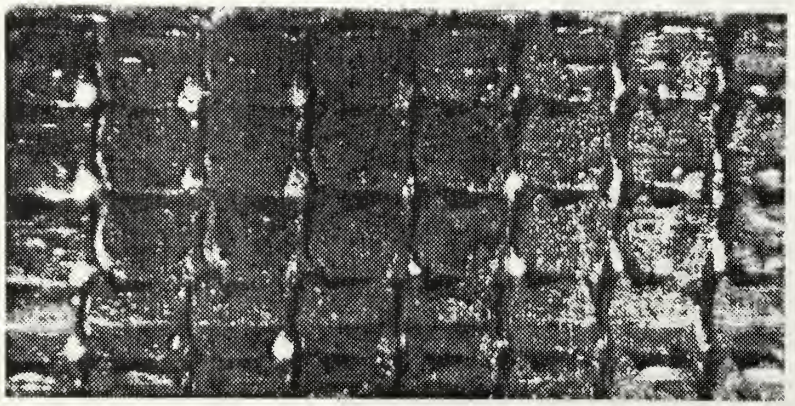

(d) Turbo-B Surface

Figure 2.2 Examples of Enhanced Boiling Surfaces

The study of boiling of mixtures is varied and broad. To adequately review the full spectrum of such a study is beyond the scope of this work. The area of discussion will focus primarily on mixtures in which the saturation temperature of the components is widely separated such that only one constituent is undergoing phase change.

B. SINGLE-TUBE STUDIES

1. Pure-Component Boiling

Rohsenow proposed a correlation in 1952 to predict the pool-boiling heat-transfer performance from single smooth tubes [Ref. 6]. The correlation developed is:

$$\frac{c_\ell (T_w - T_{sat})}{h_{fg}} = C_{sf}\left\{\frac{q}{\mu_\ell h_{fg}}\left[\frac{g_c \sigma}{g(\rho_\ell - \rho_v)}\right]^{1/2}\right\}^r \left(\frac{c_\ell \mu_\ell}{k_\ell}\right)^s \qquad (2.1)$$

where C_{sf} is a tabulated coefficient which depends on the specific fluid and the surface condition, h_{fg} is the specific enthalpy ("latent heat") of evaporation and μ_ℓ is the liquid viscosity. The value of the exponent r is generally accepted to be 0.33 for all fluids, whereas Rohsenow recommends two separate values of s in order to correlate the data for water and for other fluids. For water s = 1.0 while s = 1.7 for other fluids. The correlation has been shown to correlate a variety of heat-transfer data to within 30-40 percent.

Following the development of this correlation, a number of investigators (as discussed by Chongrungreong and

Sauer [Ref. 7]), over the past few decades, have attempted to generate a reliable and generalized correlation. Unfortunately, owing to the lack of understanding of the physical mechanisms involved, a truly representative model does not exist. Based on these observations, a generalized predictive model to represent boiling from enhanced surfaces appears to be an almost impossible task. Therefore, the reliance of experimental data covering the ranges of operating and geometrical parameters has been an essential part of the utilization of enhanced boiling surfaces in designing more compact and efficient evaporators.

Borishanski [Ref. 8] proposed an expression to correlate the effect of pressure on boiling heat-transfer performance:

$$h = A^* \phi^{0.7} f(P) \tag{2.2}$$

where f(P) is a function of reduced pressure and A^* is a constant evaluated at a reduced pressure of 0.0294. Mostinski [Ref. 9] modified these expressions for various refrigerants and proposed:

$$A^* = 0.1011 P_{CR}^{0.69}, \tag{2.3}$$

and

$$f(P) = 1.8\ P^{*0.17} + 4\ P^{*1.2} + 10\ P^{*10} . \qquad (2.4)$$

The Mostinski equations are at least as accurate as any of the physical property correlations [Ref. 10].

Studies of boiling from single tubes have shown that the local heat-transfer coefficient of finned tubes (based upon finned tube area) may be decreased below that of a smooth tube, but this decrease is more than offset by the significant area increase [Ref. 1]. The decrease in local boiling coefficient may be explained, in part, by bubble trapping between adjacent fins. Larger enhancements have been accomplished by the addition of reentrant cavities such as porous coatings or by surface modifications which also increase nucleation site density. In addition, some machining techniques (e.g., GEWA-T surface) provide a convective channeling effect of liquid and vapor, such as in a thermosyphon, thereby reducing the required wall superheat to transfer a given heat flux [Ref. 11].

Enhancement techniques which utilize reentrant cavities to reduce the required wall superheat necessary to induce boiling have shown significant improvement in heat transfer. Yilmaz et al. [Ref. 12] measured the boiling performance of a GEWA-T tube using p-xylene as the working fluid. They reported about a fourfold increase in the pool-boiling performance compared to a smooth tube at a heat flux of 100 kW/m^2. The enhancement increased with decreasing

heat flux. Wanniarachchi et al. [Ref. 2] reported data for a porous-coated (High Flux) surface using R-114 as the working fluid using an electrically-heated single tube. They conducted their experiments with and without the presence of oil, and at boiling temperatures of -2.2 ^{o}C and 6.7 ^{o}C. The effect of oil will be discussed later in this chapter. Their results showed up to a tenfold increase in the pool-boiling heat-transfer performance compared to a smooth tube. Also, Venart [Ref. 13] showed that once these nucleation sites are activated, they continue to allow for nucleate boiling at very low heat-flux values resulting in large boiling curve hysteresis. A High Flux-coated tube was shown by Wanniarachchi et al. [Ref. 2] to undergo onset of nucleate boiling at significantly lower heat fluxes and wall superheats than smooth tubes. Later, with the same apparatus, Wanniarachchi et al. [Ref. 14] tested three additional enhanced tubes at a boiling temperature of 2.2 ^{o}C. These tubes were: a GEWA-T tube with 1.02 fins/mm, a Thermoexcel-E tube and a Thermoexcel-HE tube. At a practical heat flux of about 30 kW/m^2, these three surfaces gave pool-boiling enhancements of about 8.2, 6.8 and 4.4, respectively.

Studies of enhanced surfaces have shown that pore or groove size strongly determines the heat-transfer performance, and that the optimum pore size depends on the boiling fluid properties. Tongze et al. [Ref. 15] conducted

a series of pool-boiling experiments using water and methanol as working fluids on 14 different surfaces at atmospheric pressure. They prepared their specimens by covering the parallel grooves machined on copper surfaces by a sintered cover screen or by a porous cover plate. Their results showed up to a tenfold increase in the boiling heat transfer compared to a smooth surface at a heat flux of up to 100 kW/m^2. Also, they discovered that the pore size of the screen has a stronger effect on the boiling performance than the geometrical parameters of the grooves. They found an optimum pore size of 0.16 mm for water, while the value was between 0.16 mm and 0.22 mm for methanol.

Ayub and Bergles [Ref. 16] studied pool-boiling behavior of water and R-113 from GEWA-T surfaces. They observed that with R-113, the enhancement was a well-behaved function of gap width. Moreover, they observed that a strong interdependence between thermal performance and gap width existed for both fluids regardless of the wetting characteristics.

Nakayama et al. [Ref. 17] studied boiling of water, R-11 and nitrogen on porous enhanced surfaces. They proposed that the increase in surface area of such surfaces was not a major contributor to enhanced heat-transfer performance. Nakayama et al., reasoned that significant vaporization occurred in the interconnecting tunnels existing within the surface and that latent heat transport

was significant. They proposed that net heat flux was the sum of exterior surface heat flux and latent heat flux:

$$q = q_{LH} + q_{ES} \tag{2.5}$$

with

$$q_{LH} = (N_A/A)\ f_b\ h_{fg}\ \rho_v(\pi d_b^3/6) \tag{2.6}$$

and

$$q_{ES} = (\Delta T/C_q)^{3/2}(N_A/A)^{1/4} \tag{2.7}$$

where:

(N_A/A) is the bubble population density,
d_b is bubble departure diameter, and
C_q is an empirical coefficient.

For heat fluxes of 2 to 40 kW/m^2, the predicted heat flux for R-11 and the slope of the boiling curves agree fairly well with data. The prediction is limited by sensitivity to geometric changes. Also, the analysis is based on the assumption that bubble diameter is independent of heat flux.

Czikk and O'Neil [Ref. 18] studied porous surfaces (High Flux) and developed a correlation relating nucleate

boiling performance to the number and size distribution of the pores. Their development of the correlation assumed that active nucleation sites consist of vapor bubbles trapped in reentrant pores, with large pores intermittently filled and smaller pores permanently filled by capillary effect. Czikk and O'Neil assumed that the temperature drop due to matrix conduction and frictional pressure drops was negligible. Lastly, they assumed that the two primary resistances, expressed as the temperature difference to achieve heat transfer, were bubble superheat (caused by surface tension acting on the vapor-liquid interface) and liquid layer superheat.

They proposed the following theoretical model:

$$q = C_1 \int_{d_{b\,min}}^{d_{b\,max}} \delta N_u d_b \left(\frac{\Delta T - C_2 T_{sat}}{d_b}\right) d\, d_b \qquad (2.8)$$

where:

δ is matrix thickness,

N_u is a pore size distribution function, and

C_1 and C_2 are shape factors.

The model correlated boiling performance of liquid nitrogen and water over a wide range of heat flux to within 30 percent.

2. Boiling of Mixtures

In 1986, Schlünder [Ref. 19] compared a model he developed in 1982 for predicting the nucleate-boiling

heat-transfer coefficients for binary and multi-component mixtures. His equation for a binary mixture takes the form:

$$\frac{h}{h_{id}} = \frac{1}{1 + \frac{h_{id}}{q}(T_{ph} - T_s)} \tag{2.9}$$

where:

h_{id} = "ideal" boiling coefficient for pure component,

T_s = boiling temperature of the mixture at bulk concentration, and

T_{ph} = vapor-liquid interface temperature,

which satisfies the following equation:

$$\frac{\tilde{Y}_{iph} - \tilde{X}_i}{\tilde{Y}_{iph} - \tilde{X}_{iph}} = \exp(-\phi_\ell) \tag{2.10}$$

where

$$\phi_\ell = B_o \frac{q}{\rho_\ell \, h_{fg} \, \beta_\ell} \tag{2.11}$$

where:

β_ℓ = liquid-phase mass-transfer coefficient.

While Schlünder selected a value of unity for B_o, the only other adjustable parameter (β_ℓ) was found to be on the order of 10^{-4} m/s. He tested his model with his own data and those from the open literature and found good

agreement between the predicted and measured boiling coefficients. He stated that as the more volatile component is depleted at the heated surface, higher wall superheats are required to maintain a given heat flux. Using binary mixtures of methanol-water, ethanol-water and isopropanol-water, Pandey et al. [Ref. 20] found the resulting nucleate pool-boiling coefficient to be consistently less than the weighted average of the mixture components.

When enhanced surfaces have been studied during boiling of binary mixtures (methanol-water, propanol-water and ethanol-benzene), Shakir and Thome [Ref. 21] showed that generally a much greater activation superheat (i.e., the wall superheat at ONB) was required for mixtures than for pure liquids. They also found the increase in the activation superheat to be a complicated function of mixture composition. Further, they found the activation superheat given by:

$$T_W - T_{sat} = \frac{2\sigma}{r\left(\frac{dP}{dT}\right)_{sat}} \qquad (2.12)$$

was inadequate for the mixtures they tested. Arshad and Thome [Ref. 22] showed that while enhanced surfaces show up to tenfold improvements in the heat-transfer coefficient over smooth tubes for pure liquids, the improvement was only slight for liquid mixtures.

Sauer et al. [Ref. 7] conducted boiling experiments on a single finned tube and on a smooth tube using R-11 as the working fluid. They varied the mass concentration of naphthene-base oil from 0 to 10 percent. With up to 3 percent oil, the effect of oil was minor, and the presence of oil was even seen to slightly increase the pool-boiling heat-transfer coefficient. On the other hand, with oil concentrations in excess of 5 percent, the performance decreased considerably. However, they reported that the performance degradation for the finned tube was no greater than for the smooth tube. They stated that the changes (i.e., increases) in vapor pressure, surface tension and viscosity to be partly responsible for the observed decreased performance with the presence of oil. Sauer et al., discuss two opposing effects which may account for the slight increase in performance with up to 3 percent oil. The oil at high concentrations tends to choke the surface structure, while at lower concentrations the foaming agitation may create an enhancement.

When a contaminating fluid (refrigeration oil) was added to a pool of R-114 liquid, Wanniarachchi et al. [Ref. 2] found a consistent reduction in pool-boiling performance using their single-tube studies. For a porous-coated (High Flux) surface, tested at a saturation temperature of approximately 2.2 ^{o}C, the reduction in the heat-transfer performance was as large as 35 percent with an oil mass

concentration of up to 3 percent over a heat-flux range of 0.5 to 95 kW/m^2. However, with 6 percent or more oil, the heat-transfer performance decreased drastically at high heat-flux values (>30 kW/m^2) [Ref. 2]. At a practical heat flux of about 30 kW/m^2, the enhanced surface retained a factor of seven improvement over the smooth tube up to 10 percent oil, although it suffered a delay in onset of nucleate boiling compared to the oil-free case [Ref. 2]. The degradation in performance for enhanced tubes is due to the collection of an increasingly oil-rich mixture within the porous structure. At high oil concentrations or high heat fluxes, the migration of oil to the vicinity of the tube surface tends to deplete the low-saturation-temperature liquid, increasing local liquid viscosity and surface tension, thus decreasing the heat-transfer performance. This high oil concentration deactivates some nucleation sites on enhanced tubes. This explains why smooth tubes are less susceptible to decreased performance (on a relative basis compared to the oil-free case) due to oil contamination than enhanced tubes [Ref. 23].

3. Forced-Convection Boiling

Many observers, such as Chen [Ref. 24], have noted that boiling heat transfer involving forced convection combines two types of phenomena: pool boiling and convection effects. Which of the two phenomena has the greatest effect depends on both the wall superheat and heat

flux. One region of the q vs (T_w-T_{sat}) curve is dominated by local boiling while the other is dominated by forced convection.

In 1964, Bergles and Rohsenow developed an interpolation equation useful in estimating the heat-transfer performance of single smooth tubes for the mixed boiling region [Ref. 25]:

$$\frac{q}{q_{FC}} = \left[1 + \frac{q_B}{q_{FC}}\left(1 - \frac{q_{Bi}}{q_B}\right)^2\right]^{1/2} \qquad (2.13)$$

They also proposed an alternate superposition equation:

$$q = q_{FC} + q_B - q_{Bi} \qquad (2.14)$$

These equations combine the overall heat-transfer performance, modeling the asymptotes for forced convection, high heat flux and data at incipient boiling.

Chen [Ref. 24], in 1966, published a correlation in which the total heat-transfer coefficient was the sum of the microscopic (nucleate boiling) and macroscopic (forced convection) heat transfer. The following Chen correlation is restricted to heat-transfer inside tubes, but it provides beneficial insight into the combined effects of natural convection and convection driven by an externally induced flow.

For nucleate boiling, Chen modified the Forster and Zuber formulation yielding:

$$h_{NB} = 0.00122\left(\frac{k_\ell^{0.79} C_\ell^{0.45} \rho_\ell^{0.49} g_c^{0.25}}{\sigma^{0.5} \mu_\ell^{0.29} h_{fg}^{0.24} \rho_v^{0.24}}\right)(T_W - T_{sat})^{0.24}(\Delta P)^{0.75} S \qquad (2.15)$$

$$S = \left(\frac{\Delta T_e}{\Delta T}\right)^{0.24}\left(\frac{\Delta P_e}{\Delta P}\right)^{0.75} \qquad (2.16)$$

where S is a suppression factor. This suppression factor is the ratio of effective superheat to total wall superheat; it has a value of unity at no flow and decreases to zero in an infinite flow.

For forced-convection boiling, Chen modified the Dittus-Boelter equation:

$$h_{FC} = 0.023(Re_L)^{0.8}(Pr_L)^{0.4}\left(\frac{k_\ell}{D}\right)F \qquad (2.17)$$

$$F = \left(\frac{Re}{Re_L}\right)^{0.8} = \left(Re\,\frac{\mu_\ell}{DGz}\right)^{0.8} \qquad (2.18)$$

where F is strictly a flow parameter.

Chen then added the two contributions to obtain the resultant boiling heat-transfer coefficient:

$$h = h_{NB} + h_{FC} \qquad (2.19)$$

Chen compared his equations with available data for water and a variety of organic fluids, such as methanol, cyclohexane and pentane. The Chen equations correlated with experimental data to within 15 percent.

Recently, Steiner [Ref. 26] proposed a generalized correlation using a cubic relationship between the nucleate boiling and convection regions of boiling. Like the Chen equations, the Steiner correlations refer to heat transfer inside tubes.

For nucleate boiling, he proposed:

$$\frac{h_{NB}}{h_{p^*=0.3}} = C_F \left(\frac{q}{q_o}\right)^N \left[1.68\, P_*^{0.43} + \frac{P_*^{6.5}}{1 - P_*^{4.4}}\right] \cdot \left(\frac{D_o}{D}\right)^{0.5} \left(\frac{R_p}{R_{po}}\right)^{0.13} \left(\frac{\dot{m}}{\dot{m}_o}\right)^{0.25} \cdot \left[1 - P_*^{0.1} \left(\frac{q}{q_{CR,PB}}\right)^{0.3} X\right] \tag{2.20}$$

$$N = 0.7 - (0.18)\, 10^{(0.38\, P/P_{CR})} \tag{2.21}$$

and for convection he developed:

$$\frac{h_{FC}}{h_{LO}} = \left\{\left[(1-X) + 1.2\, X^{0.4} \left(\frac{\rho_\ell}{\rho_v}\right)^{0.37}\right]^{-2.2} + \left[\frac{h_{GO}}{h_{LO}} (1 + 8(1-X)^{0.7} \left(\frac{\rho_\ell}{\rho_v}\right)^{0.67}\right]^{-2}\right\}^{-0.5} \tag{2.22}$$

These results were combined as:

$$h = \sqrt[3]{h_{FC}^3 + h_{NB}^3} \qquad (2.23)$$

The above equations were developed from experiments performed on cryogenic fluids in both horizontal and vertical tubes. Steiner indicates that no experimental data were known for comparison of horizontal tube nucleate boiling; however, vertical-tube data of other authors do not correspond well with his correlation, especially at low heat fluxes.

C. TUBE-BUNDLE STUDIES

1. Pure-Component Boiling

Studies by several authors, Chan and Shoukri [Ref. 27], Wallner [Ref. 28] and Jensen and Hsu [Ref. 29] suggest that in bundles of smooth tubes, the boiling performance is improved on the upper tubes. Generally all tubes show some improvement, but lower tubes in a bundle approach single-tube performance. Chan and Shoukri studied vertical, in-line, heated tubes immersed in R-113 and observed that the effect is most pronounced at low to moderate heat fluxes and tends to approach single-tube nucleate-boiling data at high heat fluxes [Ref. 27]. Several mechanisms have been proposed to explain the increase in the heat-transfer performance. Using R-11, Wallner [Ref. 28] observed that for triangular-pitch and square-pitch bundles (pitch to

diameter ratio of 1.33), the circulation flow in tube bundles tends to create a strong convective flow. This convective flow improved performance on all tubes, but the improvement is greatest on the upper tubes. For example, he noted that at low to moderate heat fluxes (approximately 1000 W/m^2), vapor agitation improved the heat-transfer performance on upper tubes by up to 50 percent above that of the bottom tubes.

Cornwell and Schuller [Ref. 30] conducted photographic studies of boiling of R-113 in bundles and suggested that bubbles departing from lower tubes impact tubes above, then slide around the surface of these tubes. This results in a disruption of the thermal boundary layer and a faster bubble growth rate, thus improving the heat-transfer performance.

On the other hand, Chan and Shoukri [Ref. 27] showed that, at high heat fluxes (greater than 40 kW/m^2), the agitation effect was negligible and was offset by the detrimental effect caused by a vapor blanket surrounding the upper tubes. The phenomenon of vapor blanketing has been observed by several authors for smooth-tube and enhanced-tube bundles. Robinson and Katz [Ref. 31] studied boiling of R-12 on the outside of four vertical tubes within a bundle of 16 smooth tubes. In their study, refrigerant gas was injected beneath the bundle so as to observe the effect of two-phase flow. Agitation due to the gas resulted in a

35 percent increase in the boiling coefficient for the bottom tube. For the upper tube, which had significant vapor blanketing prior to gas injection, the increase in boiling coefficient was less than 4 percent. In a study of R-11, Muller [Ref. 32] studied various effects within an 18-tube, finned-tube bundle. He observed that for the upper tubes in the bundle, up to a moderate heat flux (20 kW/m^2), the two-phase cross-flow improved heat transfer. At high heat fluxes, the enhancement due to two-phase agitation became insignificant as upper tubes experienced vapor-blanketing. This blanketing appears to represent a maximum enhancement point where increases in the heat-transfer performance by two-phase agitation is surpassed by the reduction in convective heat transfer when the fluid is predominately vapor vice liquid.

Studies of enhanced tubes in bundles by Yilmaz et al. [Ref. 33] indicate that the "bundle effect," i.e., the improvement in performance going from a single tube to a bundle, experienced for smooth tubes cannot necessarily be achieved for enhanced surfaces. The explanation for why the bundle effect does not improve porous-surface tubes as much as measured for smooth tubes is twofold. First, Fujita et al., proposed that the porous surface has a much greater rate of nucleation and nucleation site density; therefore, one would expect the rising two-phase flow stripping bubbles off of upper tubes to contribute much less to the

heat-transfer improvement, as shown in studies of smooth and enhanced tube bundles with boiling R-113 at 0.1 and 0.5 MPa [Ref. 33]. Second, Yilmaz et al. [Ref. 12] suggest that there is possible nucleate boiling suppression caused by the increased quality flow on the upper tubes. In an attempt to use single-tube data to predict bundle behavior, Palen et al. [Ref. 34] noted that the circulation must be accurately modeled. They compared single plain tubes, plain tube bundles as well as single tubes and bundles of the GEWA-T enhanced surface. In general, they noted approximately a 50 percent decrease in wall superheat in the plain tube bundle versus the single plain tube, as shown in Figure 2.3. For the GEWA-T surface, however, both the tube bundle and the single tube performed with less superheat than smooth tubes. One noteworthy observation is that at heat fluxes above 80 kW/m^2, the enhanced tube bundle performance approaches that of the single enhanced tube, although the bundle performed slightly better at low heat-fluxes. Palen et al., observed that for the reentrant surface studied (GEWA-T), the amount of heat-transfer improvement was inversely related to number of tubes, heat flux and system pressure.

The negligible improvement observed in the GEWA-T surface in going from a single tube to a tube bundle as compared with that for the smooth tube is due to effects of vapor stripping. In a smooth tube bundle, two-phase flow

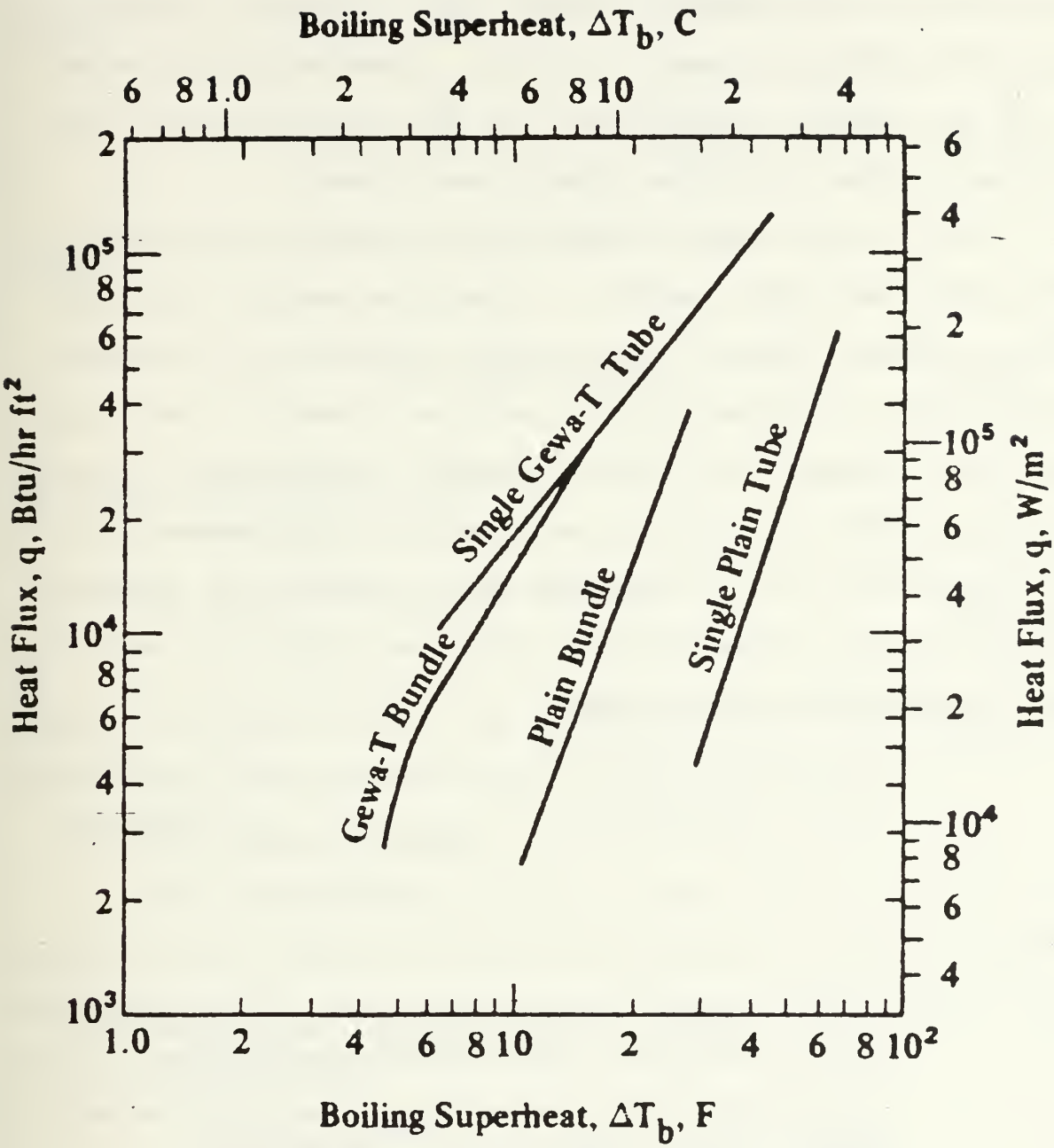

Figure 2.3 Comparison of Performance of Single Enhanced and Plain Tubes to that of Enhanced and Plain Tube Bundles with p-Xylene at 103 kPa [Ref. 12]

rising from lower tubes tends to strip bubbles from the tube surface, hence increasing heat transfer. Due to the construction of the GEWA-T surface, the stripping action is mitigated by the T-shaped fin tips. Consequently, bubbles are not as readily carried away from the heated surface, and enhancements due to bundle effects are reduced.

Due to the added complexities of operating within a bundle such as vapor quality, forced convection and wake effects behind tubes, correlations having any general applicability for tube bundles were not found in the open literature. Jensen [Ref. 29], however, has applied a Chen-type correlation to predict heat-transfer performance of a tube bundle in R-113 subjected to an externally induced convective flow. He modified F, the flow factor, by use of a momentum analogy and developed:

$$F = (\theta_L^2)^{m/(2-n)} , \qquad (2.24)$$

where:

- m is the Reynolds number exponent in the single-phase convective heat-transfer correlation,
- n is the Reynolds number exponent in the single-phase friction factor in a Blasius-type correlation for the tube bundle, and
- θ_L^2 is the liquid-only two-phase friction multiplier.

Jensen utilized the suppression-factor expression developed by Bennett [Ref. 35] for down flow in a tube bundle:

$$S = (k/F\ h_{conv}\ X_o)(1-\exp(-Fh_{conv}X_o/k)) , \qquad (2.25)$$

where

$$X_o = 0.041(\sigma/g(\rho_\ell - \rho_v))^{0.5} \qquad (2.26)$$

and h_{conv} is obtained from

$$Nu = 0.137\ Re^{0.692}\ Pr^{0.34} \qquad (2.27)$$

Jensen indicated that the application of the Chen-type correlation overpredicted data by about 20 percent.

2. Boiling of Mixtures

No correlations or data were found in the open literature for boiling of miscible mixtures in tube bundles, thus emphasizing the need for the primary objective of the present investigation.

III. EXPERIMENTAL APPARATUS

A. SINGLE-TUBE APPARATUS

1. Overview

A schematic of the single-tube apparatus is shown in Figure 3.1. The details pertaining to the design and assembly of this apparatus are discussed by Karasabun [Ref. 36], and only a brief discussion is provided in this thesis.

The apparatus uses two Pyrex-glass tees for the evaporator and condenser. Boiling takes place on a single tube immersed in a pool of refrigerant liquid in the lower tee (1). R-114 vapor passes through a riser and then condenses on the outside of a copper tubing coil in the upper tee (2). The R-114 liquid returns to the evaporator by gravity through a perforated tube located at the bottom, which runs the entire length of the evaporator.

In order to provide adequate cooling of the condenser, a 50:50 (by volume) solution of water and ethylene glycol was used. This solution was maintained between -17 ^{o}C and -13 ^{o}C by means of a 1/2-ton, R-12 refrigeration plant (7). The pump (8) provides a flow through the condenser coil and this flow can be finely controlled by means of valve VC. Since the pump is of the positive-displacement type (to provide a high delivery

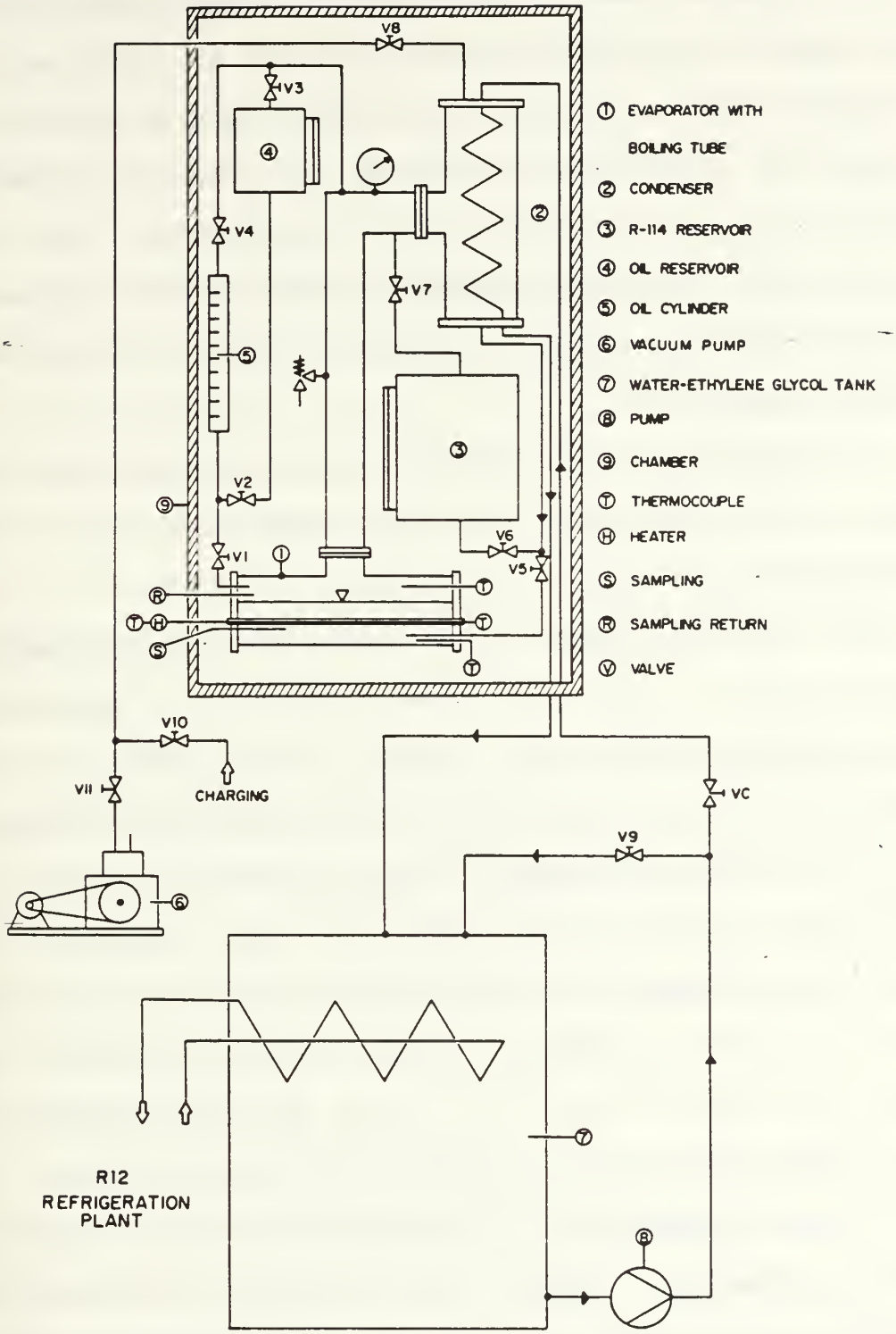

Figure 3.1 Schematic of Single-Tube Apparatus

head), a by-pass line is provided thorough valve V9 to prevent overloading of the pump in case of minimum flow through the condenser coil. The liquid in the evaporator is maintained at saturation conditions (2.2 ^{o}C) by adjusting the flow of the water/ethylene glycol mixture. The flow rate of this mixture controls both system pressure (maintained slightly above atmospheric) and R-114 condensate return temperature.

To facilitate successively increasing mass fractions of oil, an oil reservoir (4) and a graduated cylinder (5) are installed as shown in Figure 3.1.

The evaporator test tube is heated with an electric cartridge heater. This heater has a diameter of 6.4 mm and a heated length of 203.2 mm. Further, this heater is rated at 1000 W at 208 V, providing a maximum heat flux of 100 kW/m^2 at the tube surface having a diameter of 15.9 mm. Notice that if the heat input to the evaporator is decreased, for example, the flow through the condenser must also be decreased in order to maintain system pressure. As discussed by Sawyer [Ref. 37], owing to the considerable time lag (approximately 30 seconds) that exists between the change of valve positions and subsequent change in system saturation pressure, it was fairly difficult to achieve steady-state conditions. To alleviate this problem, Sawyer installed two auxiliary heaters on either side of the test tube. These heaters provided 600 W each at 208 V, and were

connected in parallel. Subsequently, when the heat input to the test tube was decreased, the input to the auxiliary heaters was increased by an equal magnitude, thus minimizing the effort necessary in manipulating valve VC to maintain steady-state conditions. The use of auxiliary heaters, however, provided erroneous enhancements to the boiling data (especially at low heat fluxes) on the test tube owing to the bubble agitation caused by the additional heaters. Sawyer successfully corrected this problem by placing a Plexiglas shield between the test tube and the auxiliary heaters, as shown in Figure 3.2. The tube heater and auxiliary heaters are individually controlled with variable transformers.

The test tubes, whether smooth or enhanced, had 76.2-mm-long, smooth unheated ends. The tubes are fitted in Teflon end plugs with O-rings as shown in Figure 3.3. The Teflon plugs are then attached to the aluminum end flanges with O-rings. Lastly, the flanges are gasketed to the ends of the evaporator tee as shown in the figure.

2. Instrumentation

Temperatures were measured using the thermal emf from copper-constantan (type-T) thermocouples made from 0.25-mm-diameter (30 gage) wire. Eight thermocouples were spaced both axially and circumferentially over the heated zone of the tube as shown in Figure 3.4. The liquid temperature was measured by two thermocouples symmetrically

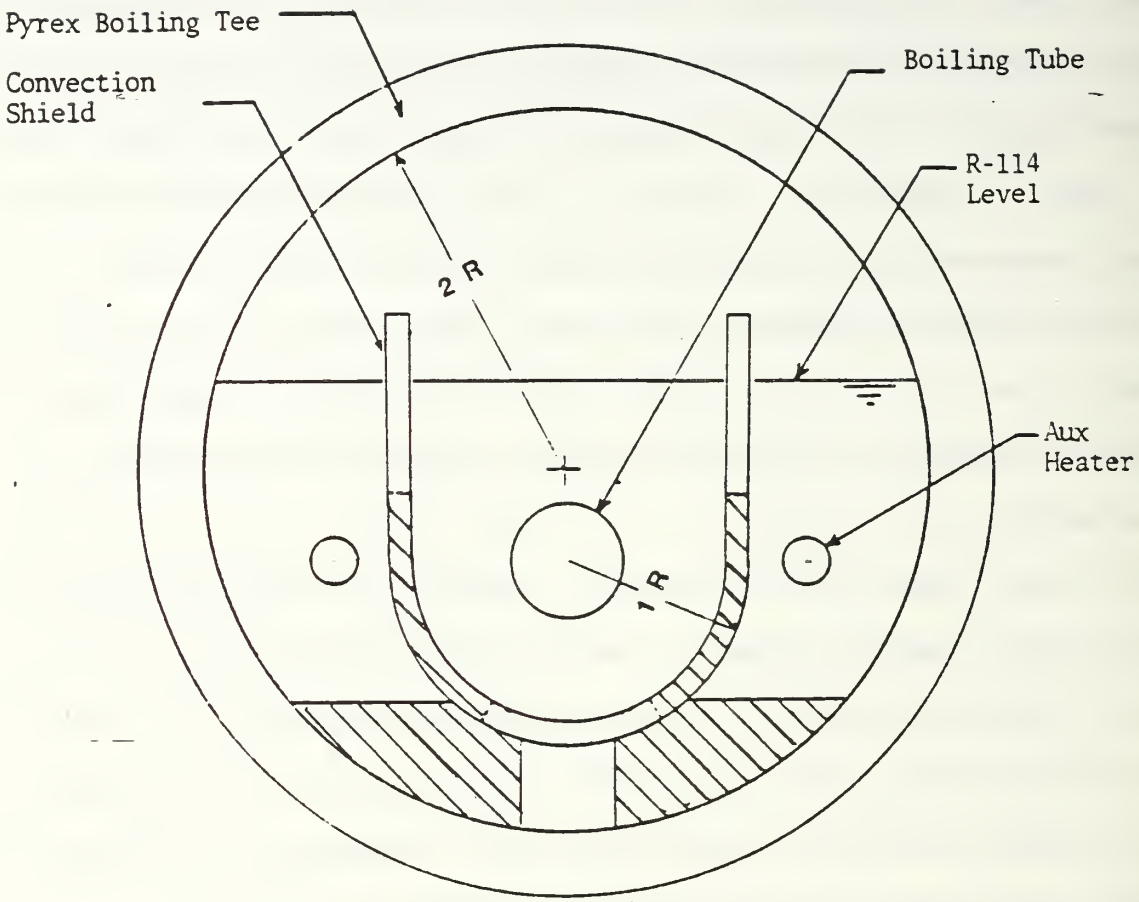

Figure 3.2 Schematic of Convection Shield Located within Evaporator

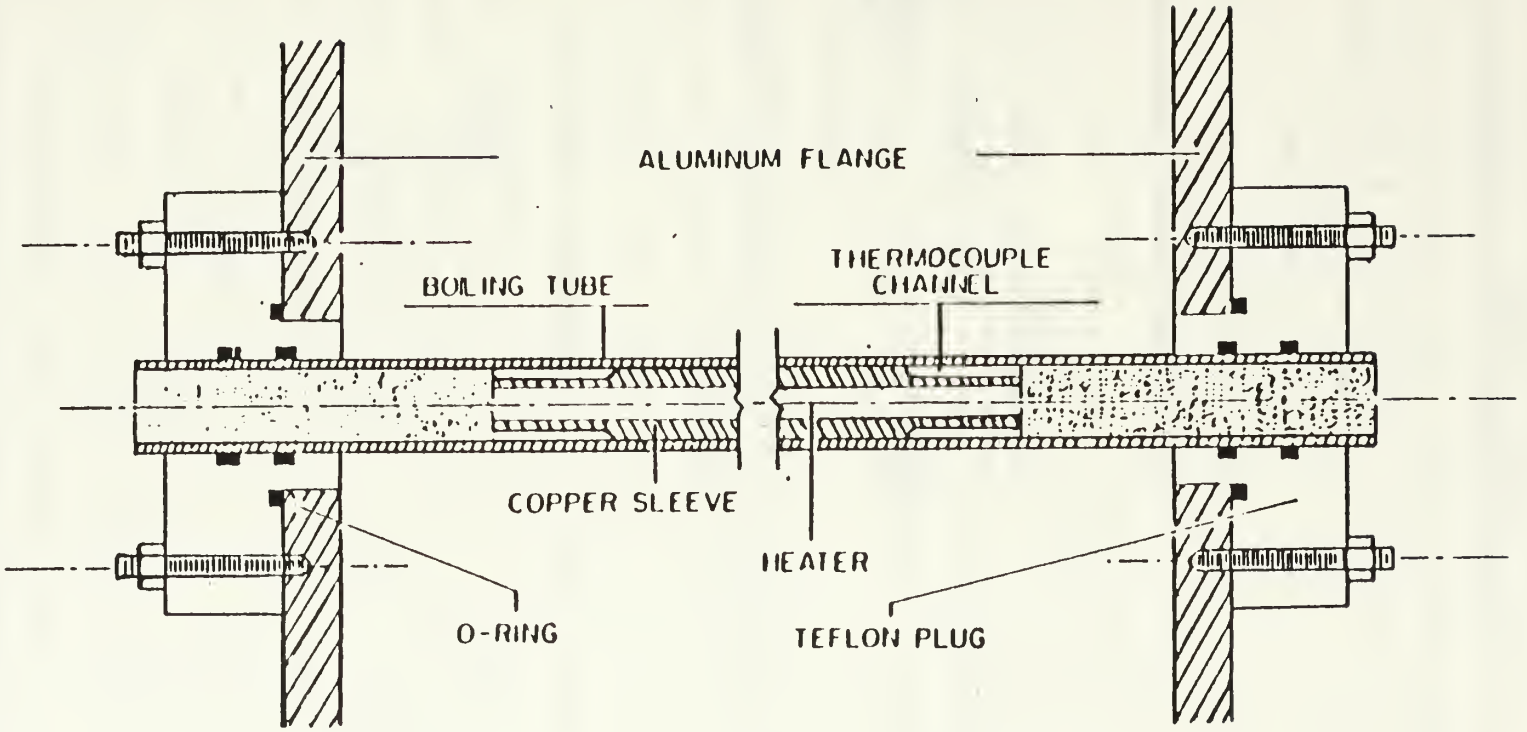

Figure 3.3 Sectional View of Boiling Tube used in Single-Tube Apparatus

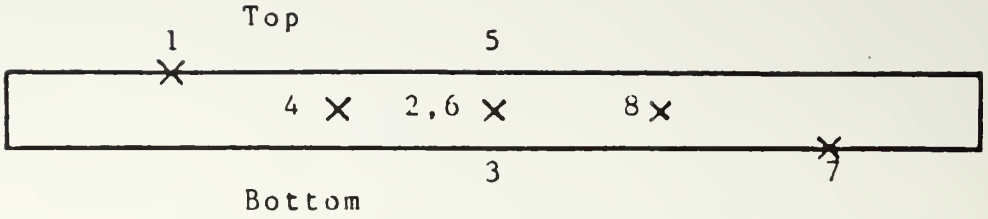

(a) View of the boiling tube thermocouple locations as seen from the front of the experimental apparatus.

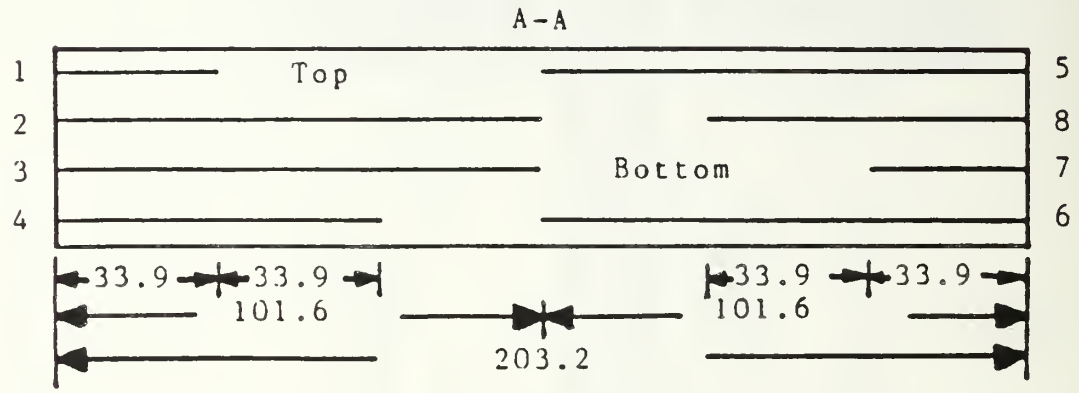

(b) Thermocouple sleeve unwrapped (at section A-A) to show the relative locations of the thermocouple channels (all dimensions in millimeters).

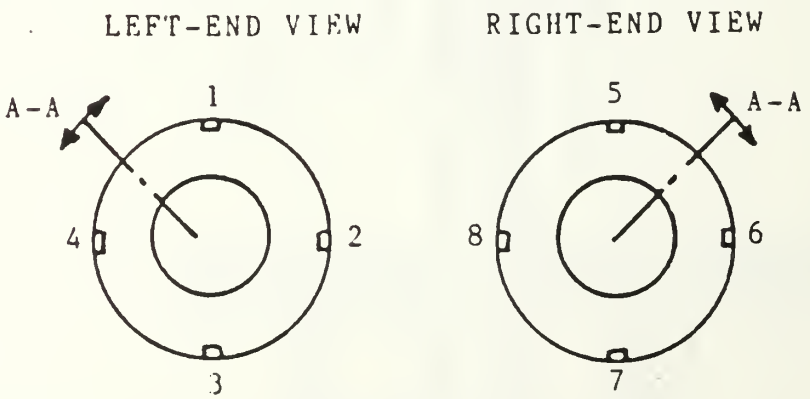

(c) End views of the boiling tube.

Figure 3.4 Thermocouple Locations of Instrumented Boiling Tube for Single Tube Apparatus

placed in thermocouple wells, which were located about 25 mm away from, and on either side of the test tube. Also, a single thermocouple was provided about 40 mm above the liquid surface at the axial midpoint to measure the vapor temperature.

The power-sensing device, described by Karasabun [Ref. 36], converts both the applied AC voltage and measured AC current into DC voltages readable by the HP-3497A Data Acquisition Unit. These sensors provided linear outputs from 0 to 5 V (DC) corresponding to 0 to 250 V (AC) and 0 to 10 A (AC), respectively. The HP-9826A computer then uses these values to calculate the power dissipated in the resistive heaters.

Due to the difficulty in measuring the saturation temperature and pressure brought about by radiative heat transfer through the glass tee, Wanniarachchi et al. [Ref. 2] found it necessary to utilize liquid temperature vice vapor temperature to represent saturation temperature. Wanniarachchi et al., noted that vapor temperature was consistently higher than the liquid temperature. The assumption that radiative heat transfer was the interfering cause was substantiated by observing an 80% reduction in the measured difference between the vapor and liquid temperatures when a stainless steel shield was provided around the vapor-space thermocouple well. Unfortunately, this shield made the vapor thermocouple insensitive to

transients. Since the ability to detect transients was desirable, the shield was removed. Later modifications were made to the apparatus and system pressure was measured with a mercury-in-glass manometer. The saturation temperature corresponding to the measured pressure was found to be about 0.1 K (0.2 ^{o}F) smaller than the average liquid temperature. For this apparatus, the liquid temperature represents the saturation temperature well within the accuracy of the measurements.

3. Data Acquisition and Reduction

A Hewlett-Packard 9826A computer and a Hewlett-Packard 3497A Automatic Data Acquisition Unit were used for all data acquisition. The HP-9826A was used to control the HP-3497A and provided for both repeated discrete system monitoring as well as data storage and processing. The HP-3497A was used to scan all the instrumented channels and system parameters, which were then displayed on a video monitor via the HP-9826A. The displayed temperature information included saturation temperature, vapor temperature and sump temperature, updated approximately every eight seconds. To facilitate data collection a data reduction program (DRP1) was developed by Karasabun [Ref. 36]. Subsequent improvements were made to this program and DRP6 comprises the most recent version. Data presented continuously on the video monitor allowed the operator to adjust cooling water flow to the condenser to

achieve the desired steady-state conditions. Once steady-state conditions were reached, and the researcher was satisfied that the apparatus was sufficiently free of perturbations and transients, the data collection option in program DRP6 was selected. Subsequent to channel scanning and data collection, the output data were printed for the researcher to review for acceptance. If the data were free of unreasonable or erratic values (such as would occur with sudden nucleation on the tube surface while the data were actually being collected), the data were stored on a floppy disk. For an individual set of collected data, the system sampled each channel 20 times and the average value was computed to minimize the effect of short-term fluctuations on the measurements.

B. TUBE-BUNDLE APPARATUS

1. Overview

The tube-bundle apparatus consists primarily of two large stainless steel shells and their associated piping and electrical systems. As shown in Figure 3.5, a 208 V (AC) power supply provides electrical power to the evaporator heaters via three variable transformers and a switch panel. The condenser is cooled by sets of instrumented and auxiliary condenser tubes. As shown, pumps circulate a water/ethylene glycol mixture from a large sump to the condenser tubes. The sump is cooled by an 8-ton refrigeration plant.

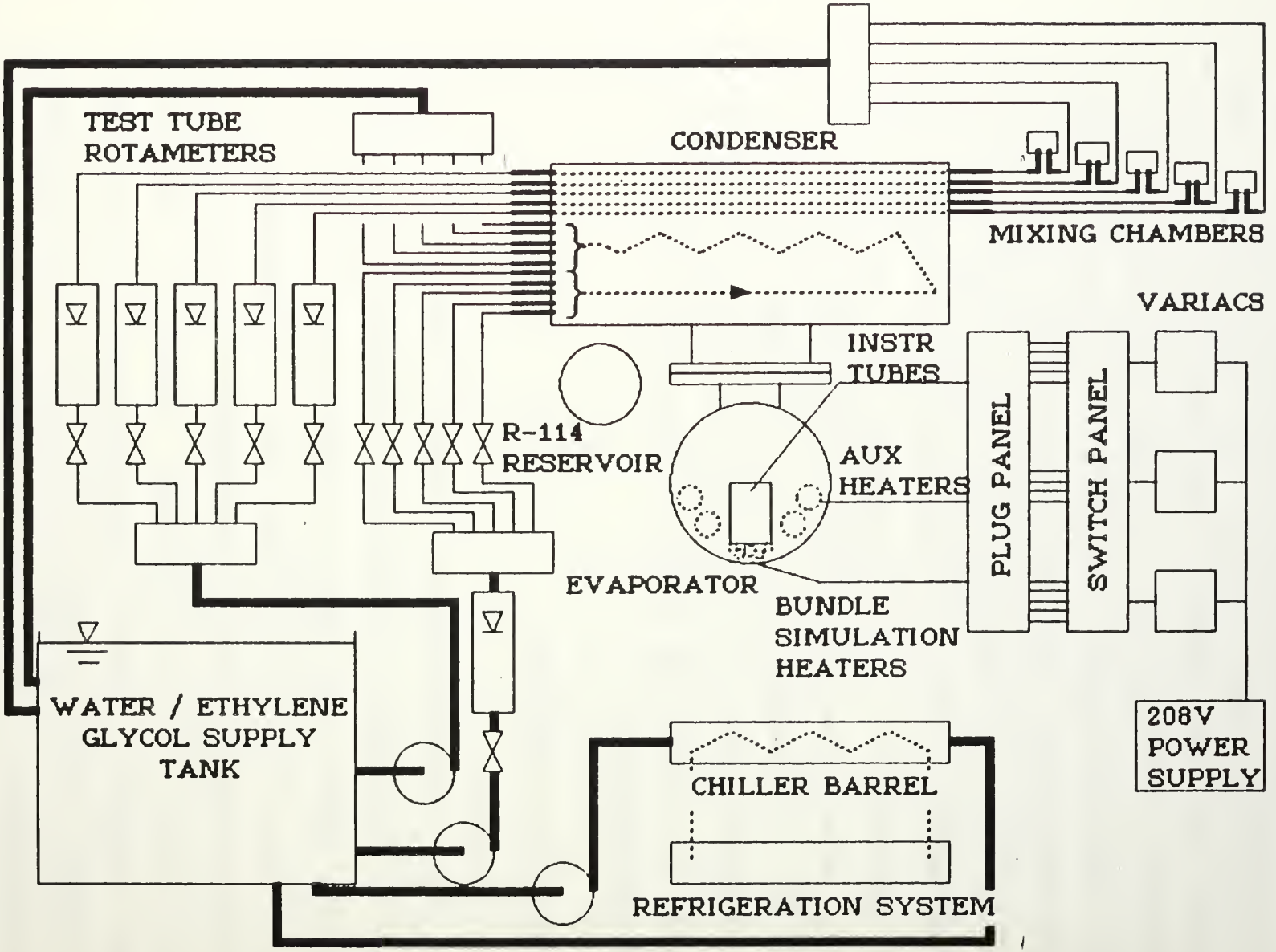

Figure 3.5 Schematic of Multi-Tube Apparatus

These shells were fabricated by rolling 6.35 mm (0.25 in) thick stainless steel plates. Wherever possible, all joints were double-welded (inside and outside) to minimize the likelihood of leakage. As can be seen from Figures 3.6 to 3.10, both shells have an external diameter of 0.61 m (24 in). While the evaporator has a length of 0.254 m (10 in), the condenser has a length of 1.28 m (50.4 in). The larger condenser length was necessary to yield a large enough coolant flow temperature rise so that this rise could be measured with a good deal of reliability.

Zebrowski [Ref. 38] provides details for the design of the condenser shell and its components. Both shells were designed for an absolute pressure of 308 kPa (44.7 psi). Notice that at a room temperature of 22 ^{o}C (72 ^{o}F), the absolute pressure within the apparatus (saturation condition for R-114) would be about 205 kPa (29.7 psi).

Similar to the single-tube apparatus discussed earlier, the multi-tube apparatus undergoes a closed-loop operation with the evaporator located below the condenser, thus allowing gravity flow of condensate from the condenser to the evaporator. As can be seen in Figure 3.12, the vapor generated within the evaporator enters the condenser through the interconnecting riser, and the vapor distributes both axially as well as circumferentially around the stainless steel shroud and travels to the top of the condenser shell. Figure 3.13 shows the details of the vapor shroud and

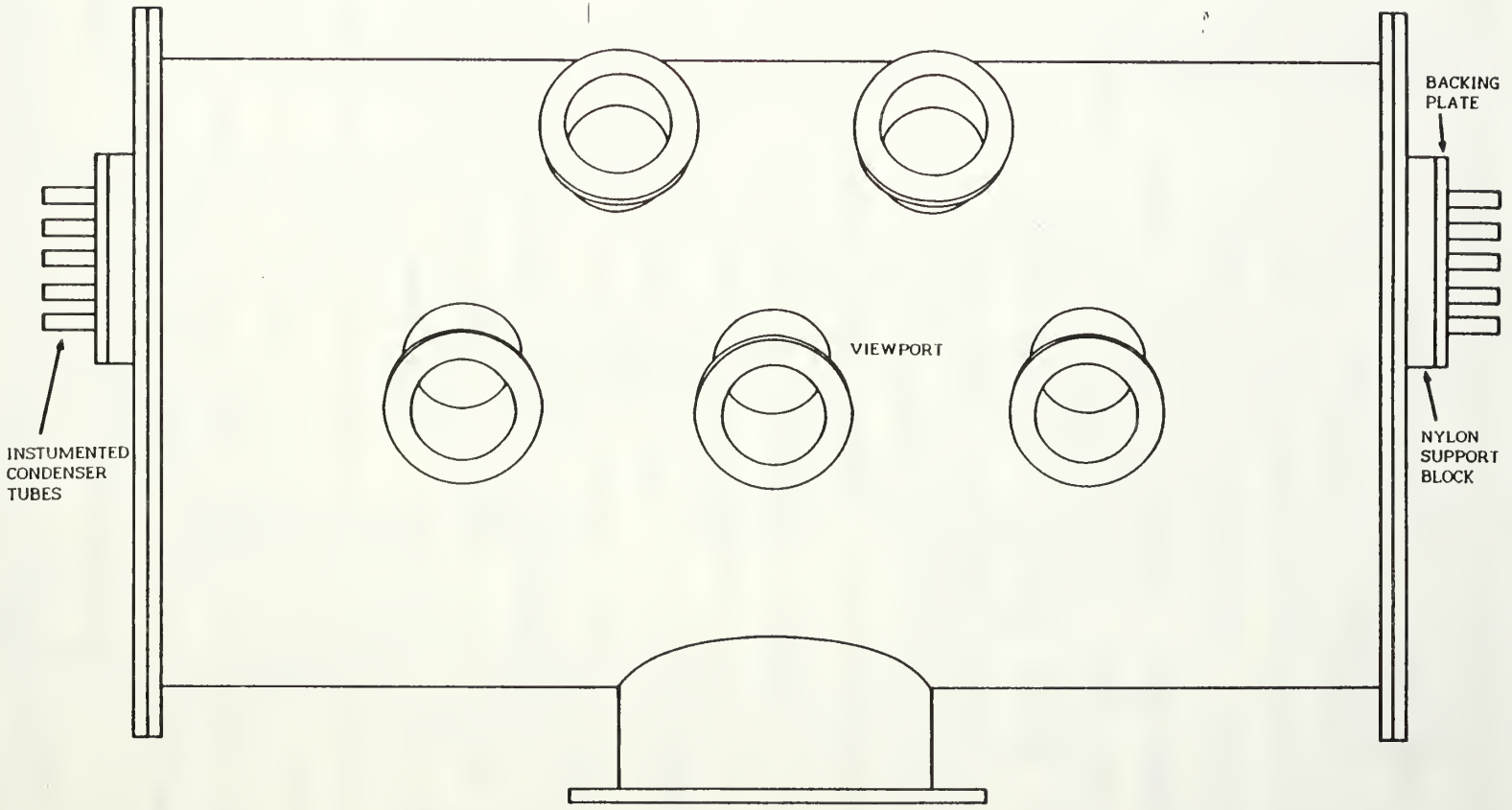

Figure 3.6 Front View of Multi-Tube Apparatus Condenser

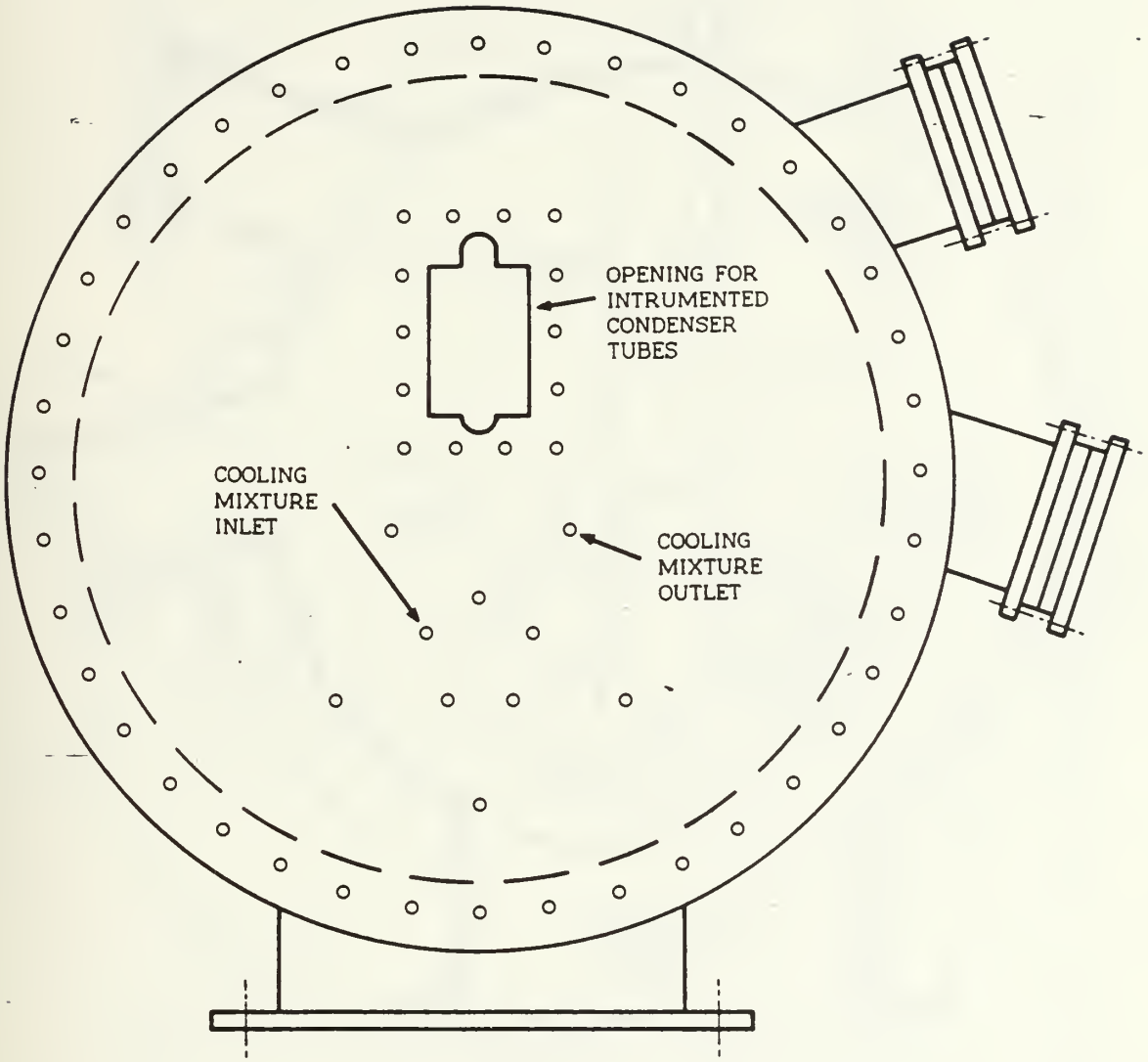

Figure 3.7 End View of Multi-Tube Apparatus Condenser

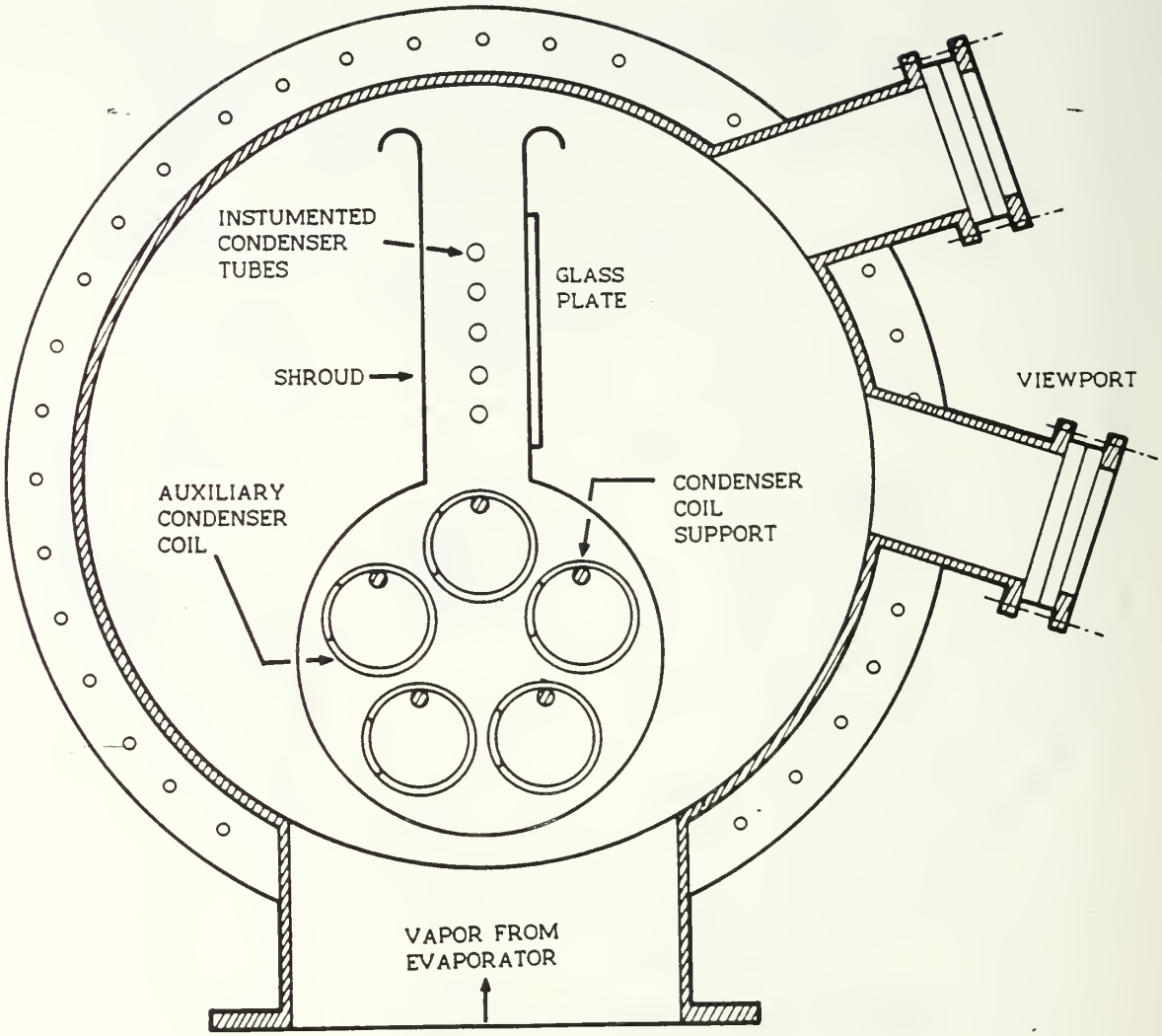

Figure 3.8 Sectional View of Multi-Tube Apparatus Condenser

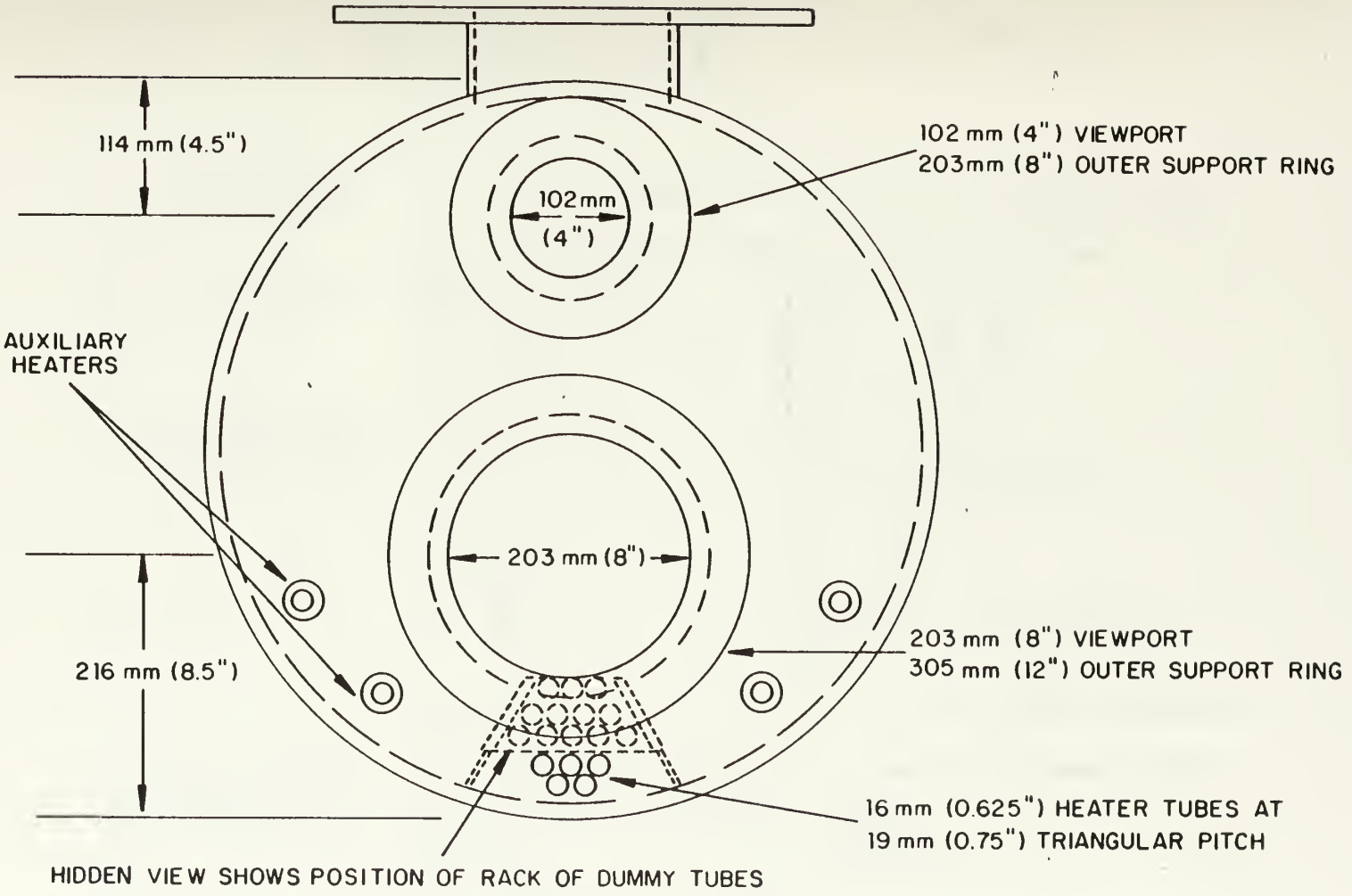

Figure 3.9 Front View of Multi-Tube Apparatus Evaporator

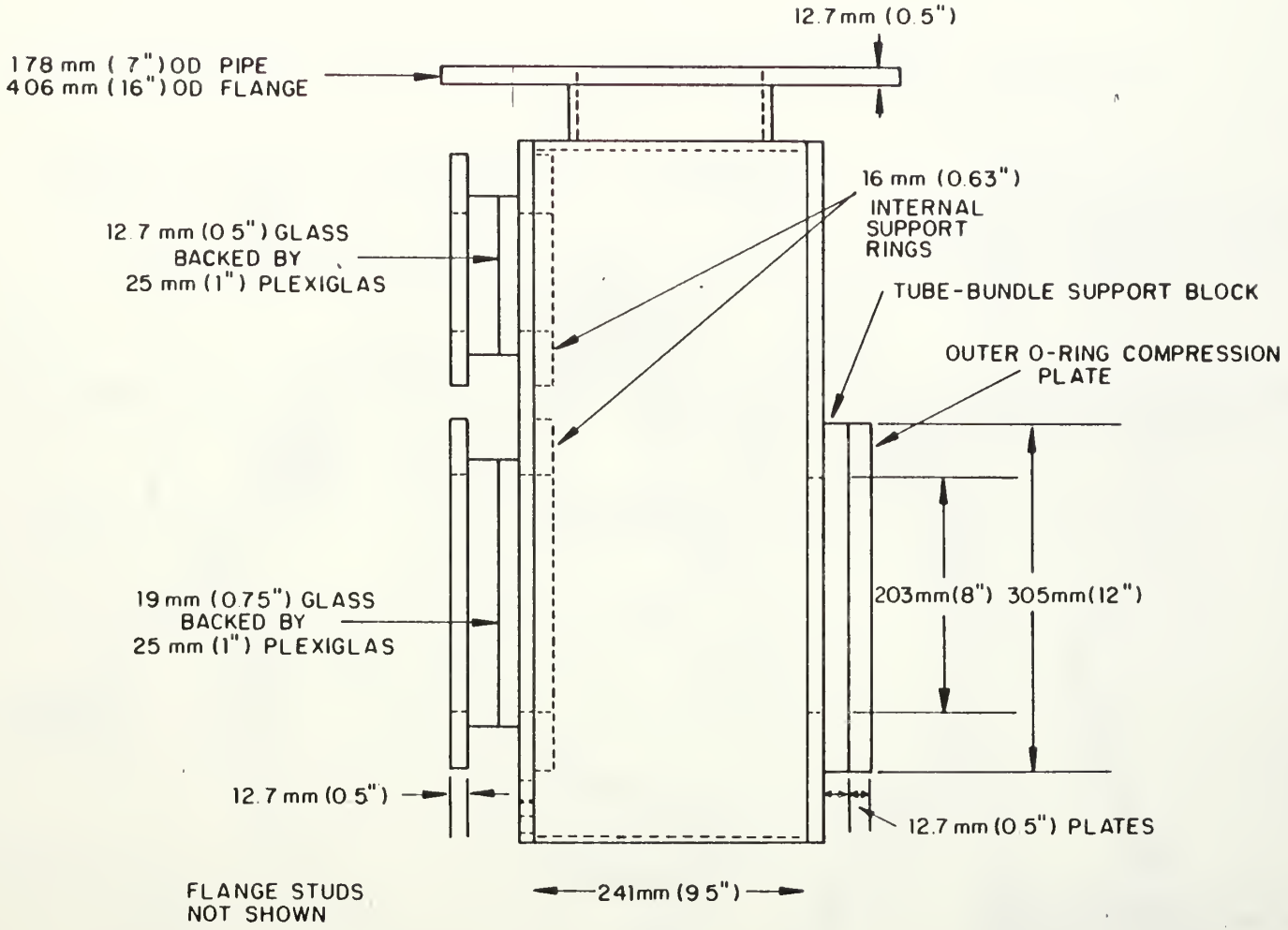

Figure 3.10 End View of Multi-Tube Apparatus Evaporator

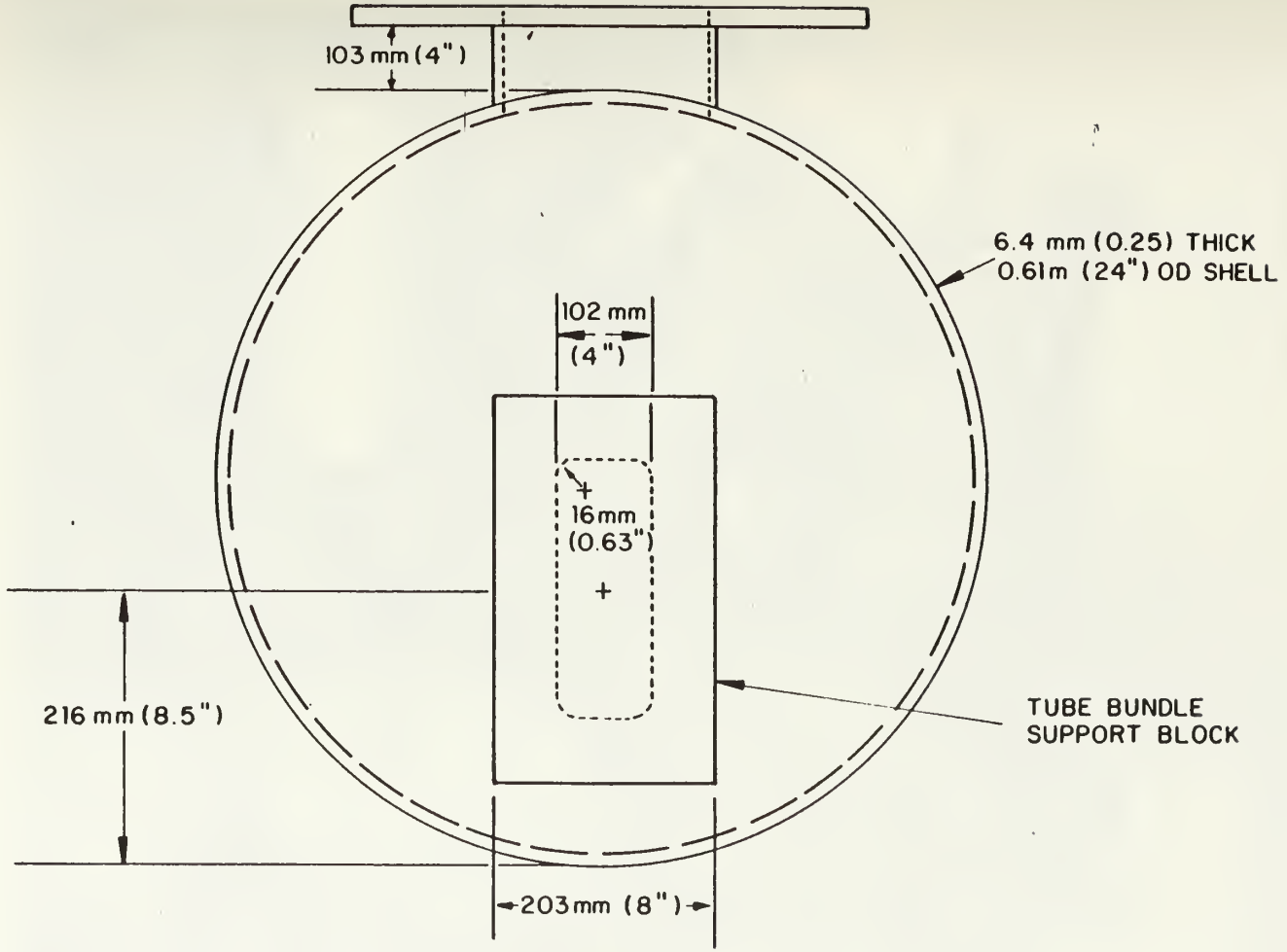

Figure 3.11 Rear View of Multi-Tube Apparatus Evaporator

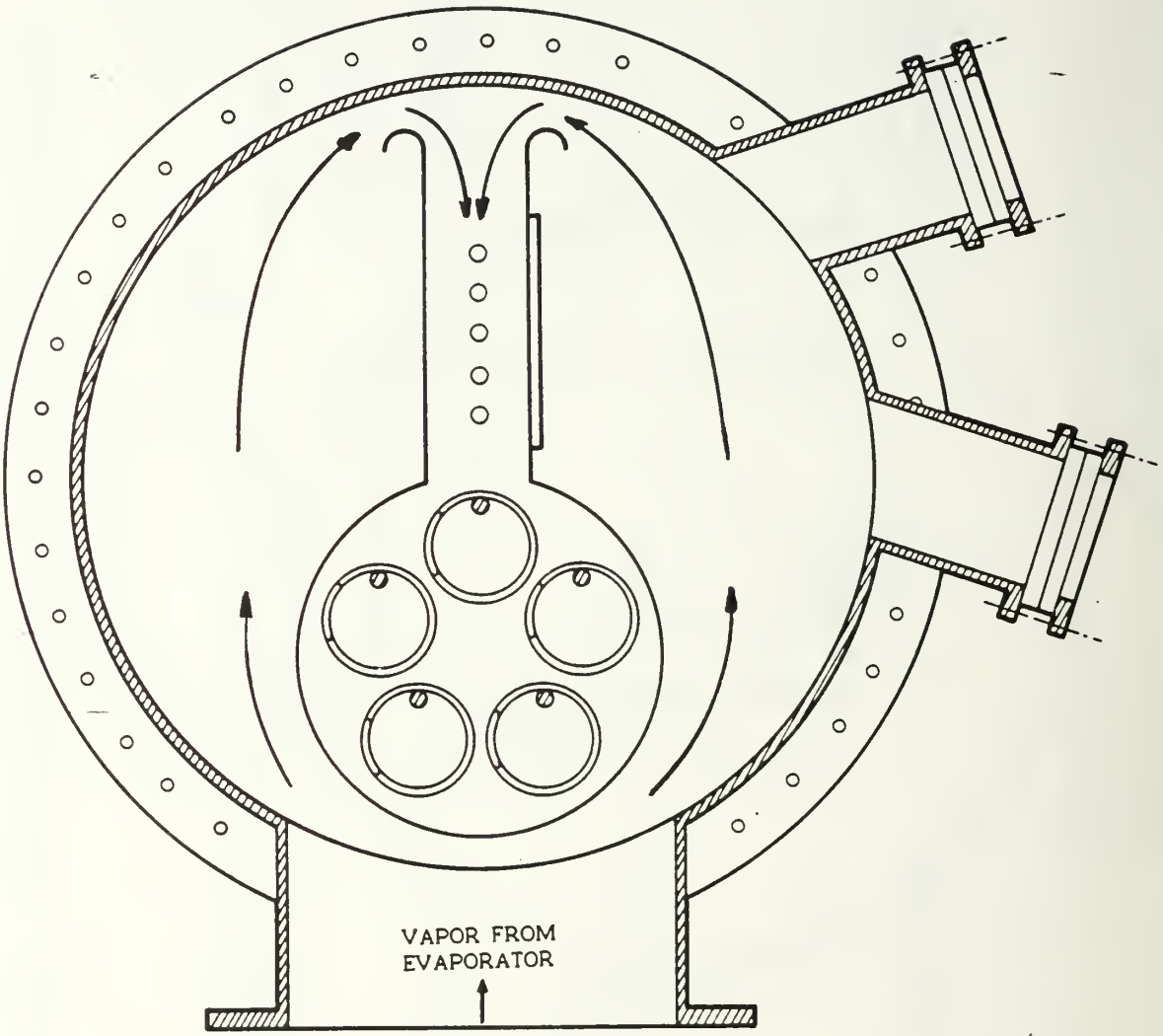

Figure 3.12 Sectional View of Multi-Tube Apparatus Condenser Showing Vapor Flow Path into Instrumented Section

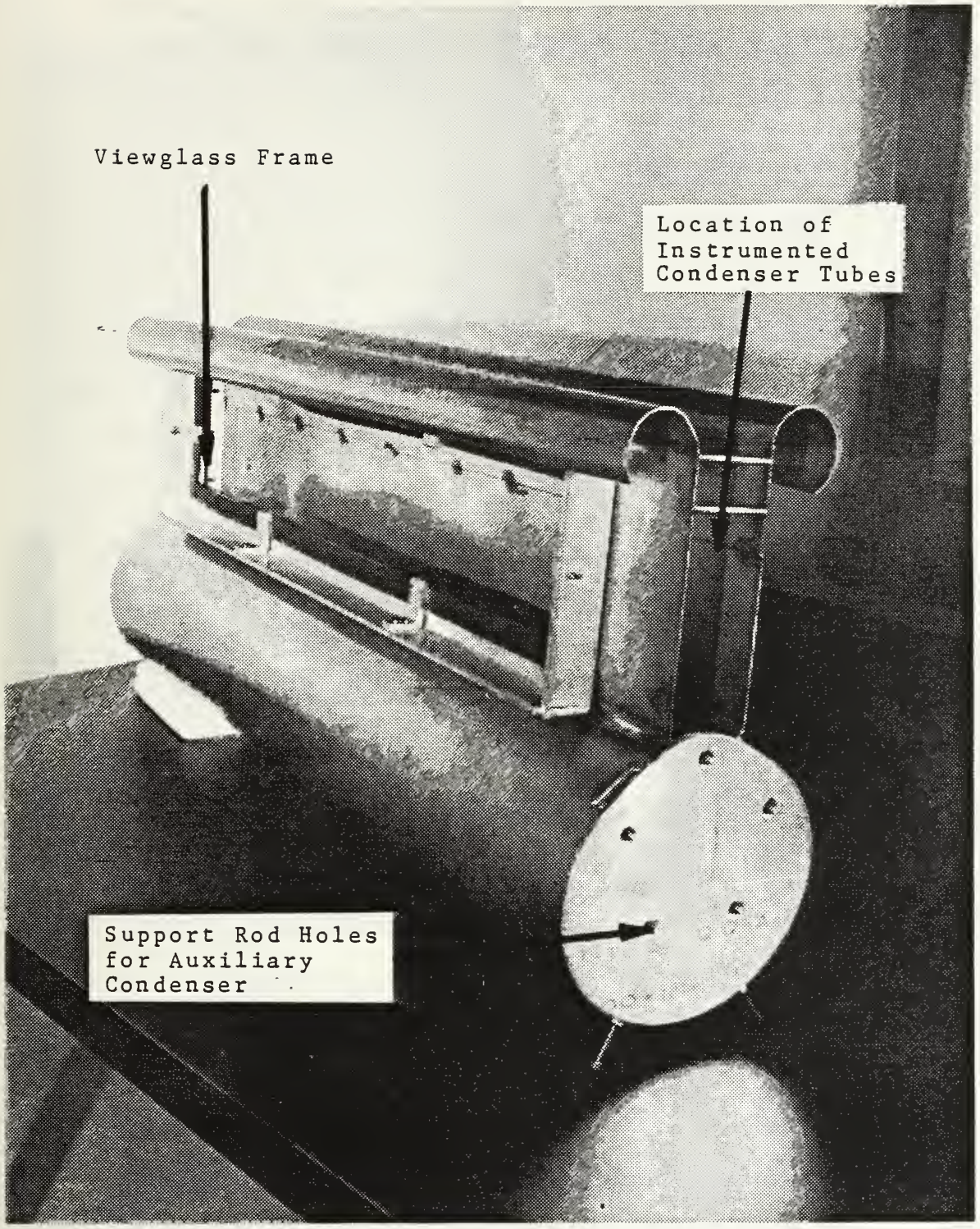

Figure 3.13 Photograph of Vapor Shroud

Figure 3.14 shows the shroud installed in the condenser. At this point, the vapor flows downward across the five, instrumented, horizontal condenser tubes mounted in a vertical line. After a portion of the vapor flow has condensed on the primary tubes, the remaining vapor condenses within the secondary condenser. The secondary condenser consists of five individual copper coils. Both condenser sections are cooled by a 40:60 (by volume) solution of water and ethylene glycol, maintained at approximately -16 ^{o}C (3.2 ^{o}F) in a 1.8 m^3 (64 ft^3) sump. This sump temperature is maintained by means of an 8-ton refrigeration system. While each of the primary condenser tubes is provided with a separate calibrated rotameter and a valve, all five secondary condenser coils are controlled with one large rotameter and a single valve.

The condensate collected at the bottom of the shroud travels axially and drains at the two ends. As shown in Figure 3.15, the condensate is returned to the evaporator by the same piping that is used to deliver vapor flow. Under normal operation of the apparatus, valves V1, V2, V5 and V6 are closed. However, before dismantling the system for re-tubing, valves V1 an V2 would be opened to divert condensate flow to the R-114 liquid reservoir (see Figure 3.16).

Heat was added to the evaporator in three ways (see Figure 3.17). The primary method was by 17 heated tubes located within the test section. Note that the five tubes

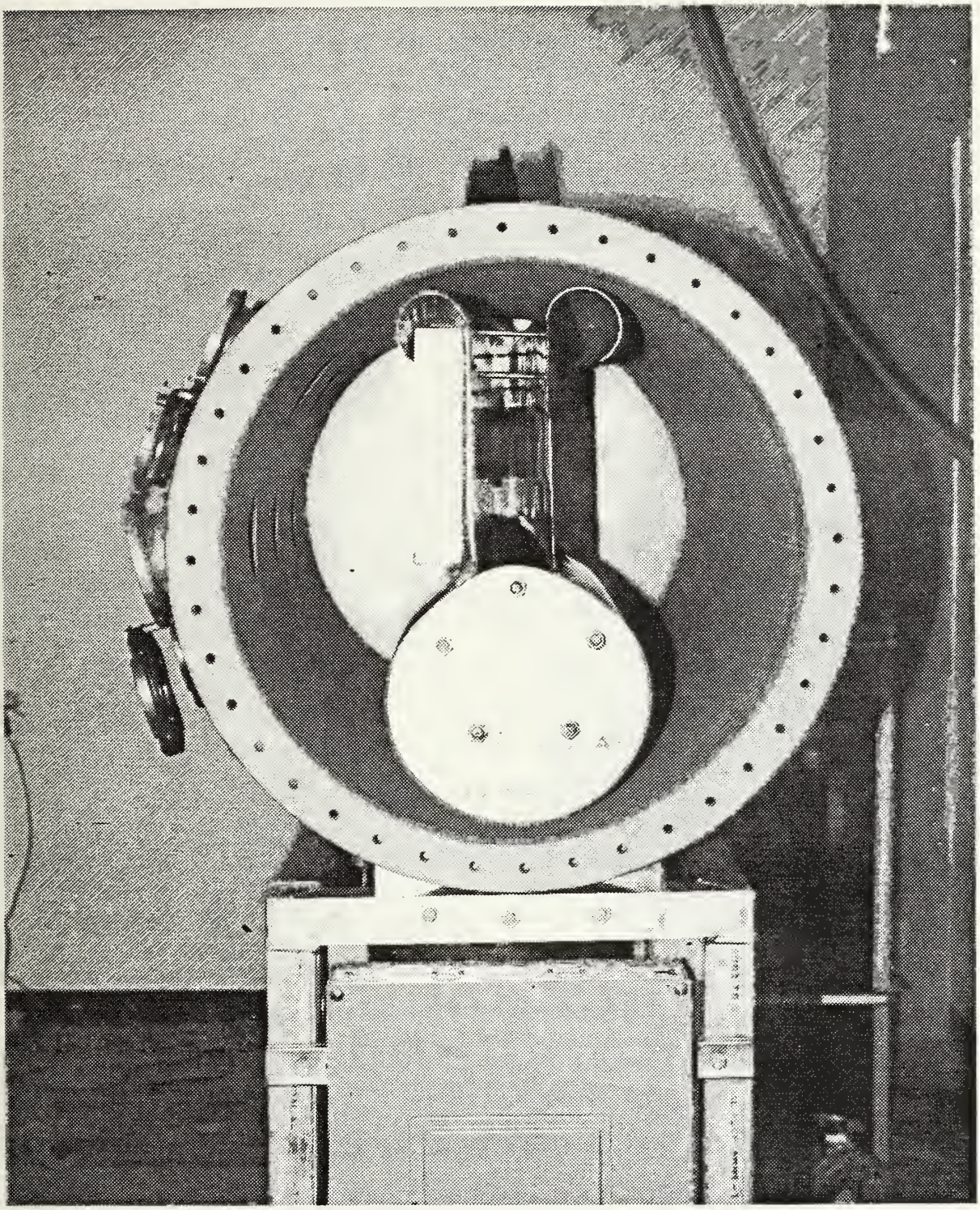

Figure 3.14 Photograph of Vapor Shroud Inserted into Condenser

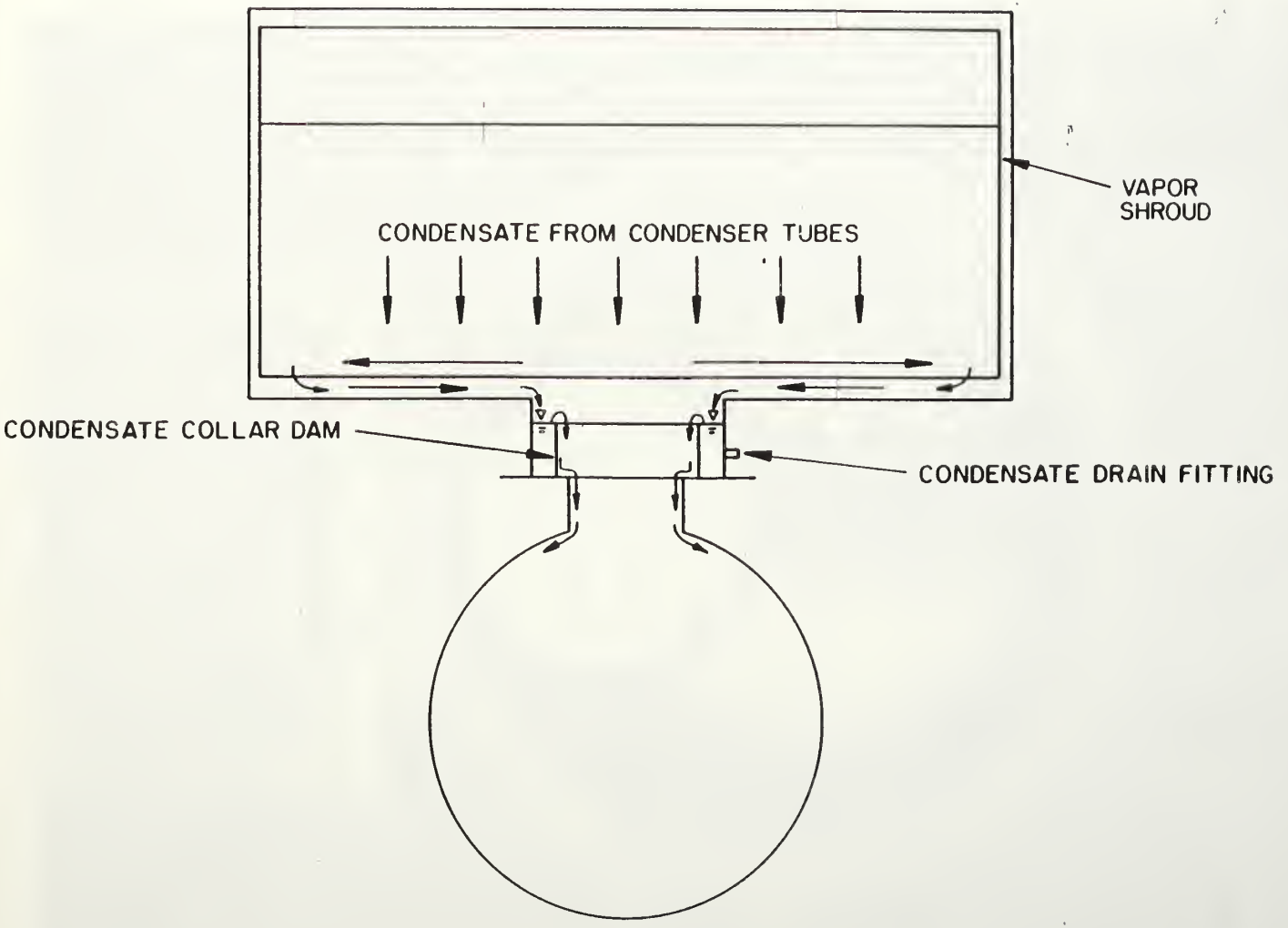

Figure 3.15 Sectional Schematic of Multi-Tube Apparatus Showing Condensate Return Path

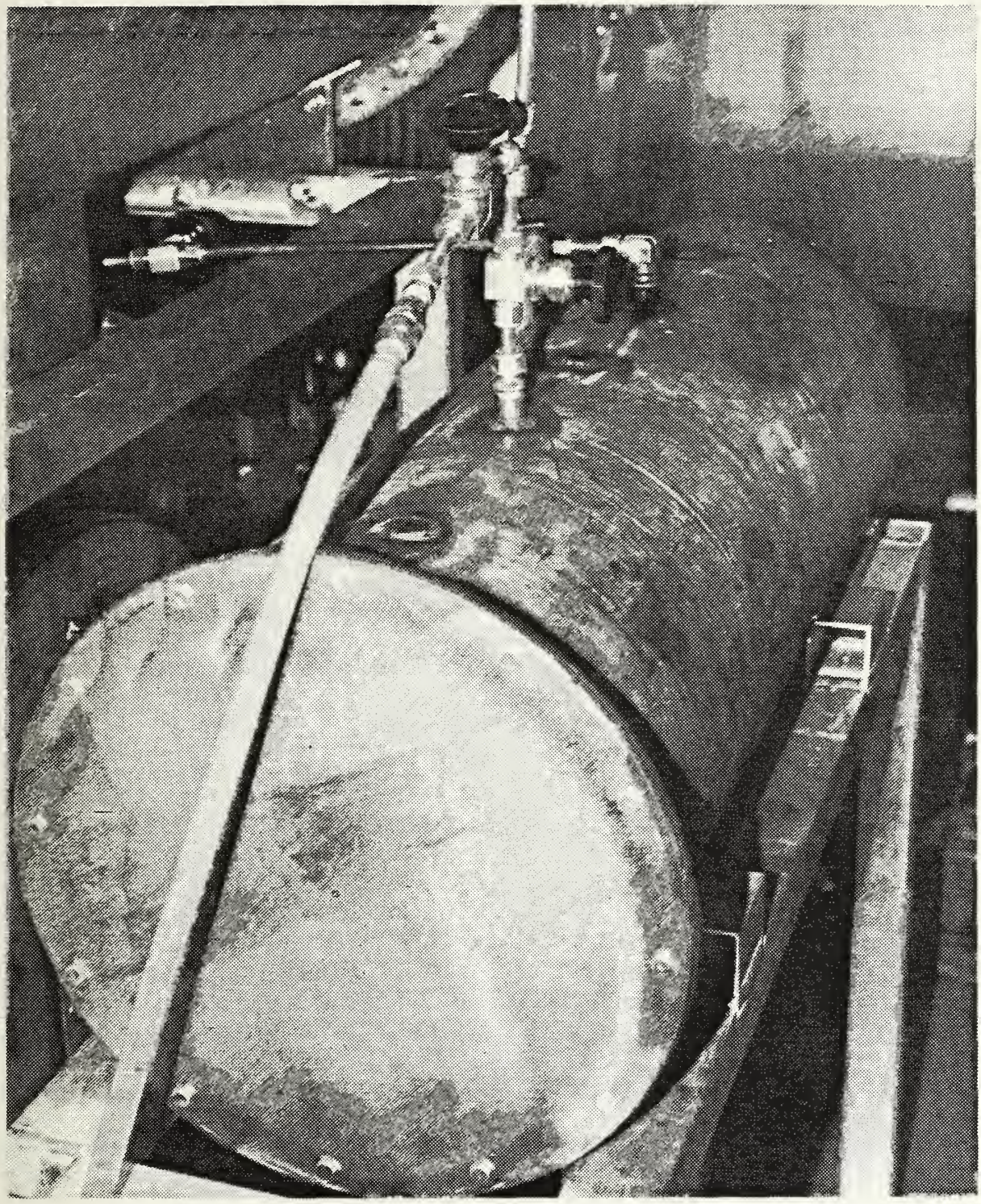

Figure 3.16 Photograph of R-114 Liquid Reservoir

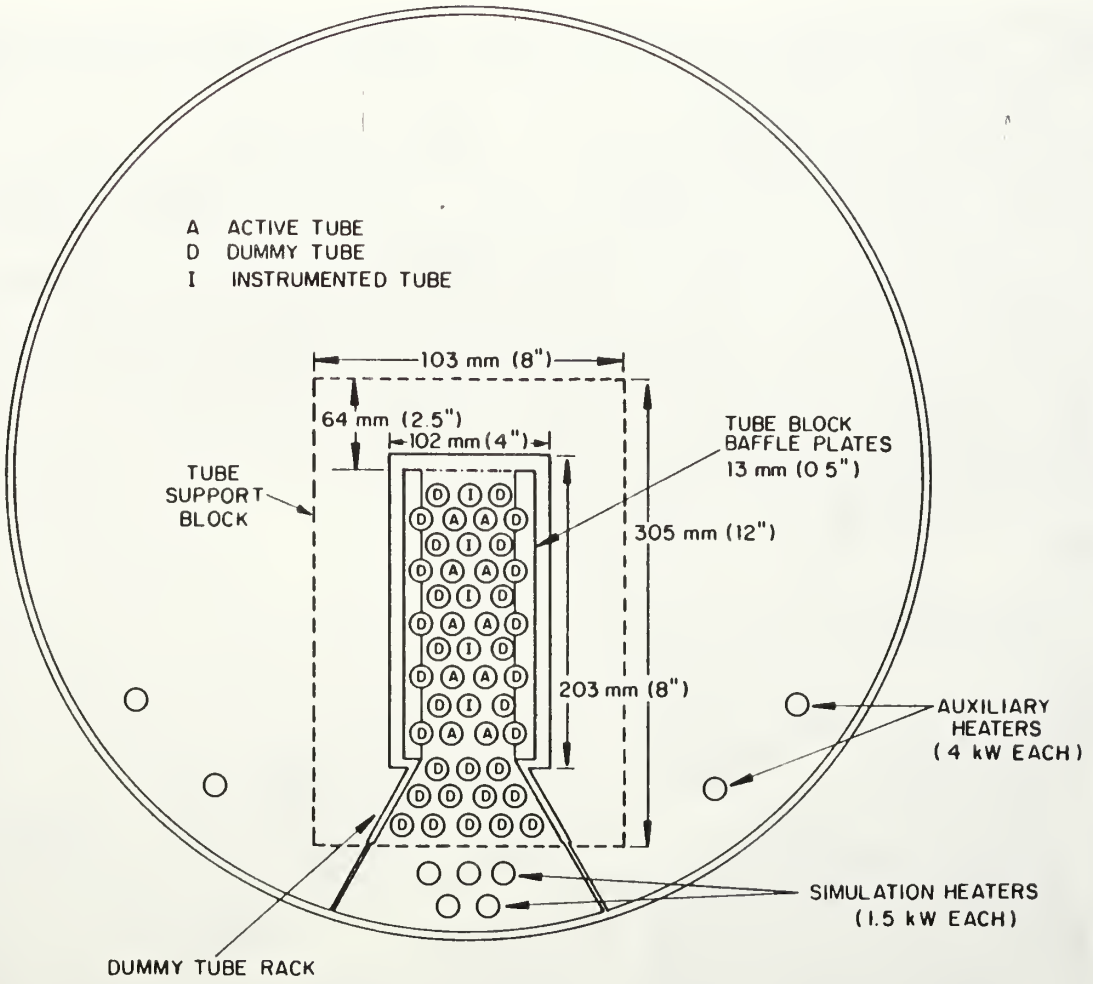

Figure 3.17 Sectional View of Multi-Tube Evaporator Showing Tube Bundle, Dummy Tube Rack and Simulation Heaters

(denoted by "I") representing the control column are also provided with instrumentation to measure wall temperatures as will be discussed later in this section. The secondary method was by four large auxiliary heaters located on the evaporator periphery whose purpose is to allow a constant total heat input to the evaporator so as to generate a constant vapor velocity in the evaporator riser and a constant operating pressure. The tertiary method is heating through a set of five heaters in a simulation section located directly beneath the test section (see Figure 3.17). The purpose of this simulation section is to generate a rising two-phase flow into the test section simulating greater evaporator inlet quality and/or large tube bundles. Each of the means of heat addition are controlled by three 208-V, 75-A variable transformers as shown in Figures 3.5 and 3.18. In addition, the tubes in the test section are individually switched, allowing for studies of from one to five instrumented tubes.

All tubes in the evaporator are cantilevered from the back of the apparatus and are mounted in a tube support block (see Figure 3.19). The tube support block serves to align the tubes, which are sealed using O-rings, and also provides side baffle plates. The baffle plates provide flow orientation and also isolates the test tubes from agitation effects induced by the auxiliary heaters. The active and instrumented tubes are surrounded on the sides by dummy

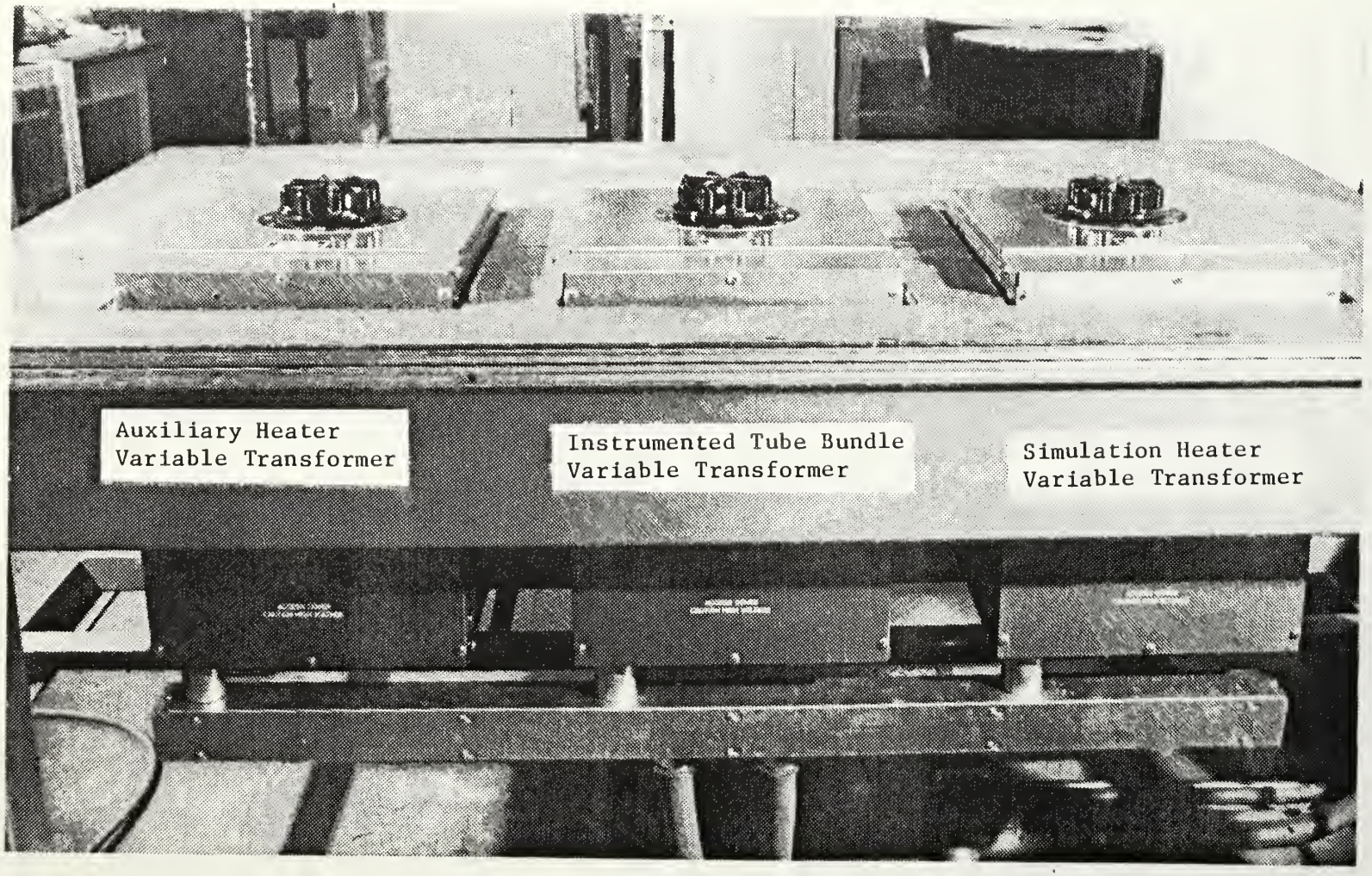

Figure 3.18 Photograph of 208 V, 75-A, Variable Transformers Used to Control Heat Addition

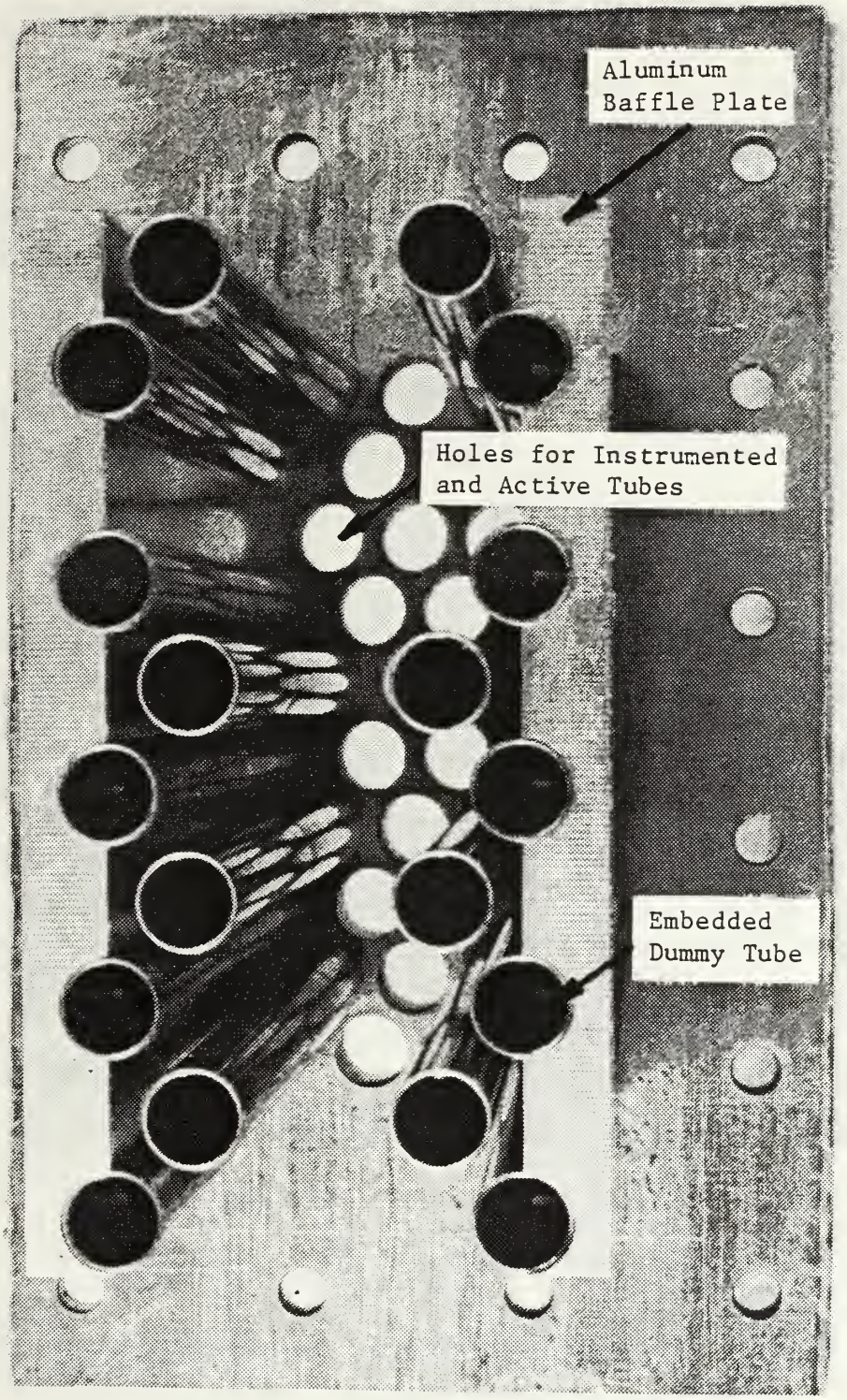

Figure 3.19 Photograph of Tube Bundle Support Block without Instrumented and Active Tubes

tubes whose purpose is strictly to provide flow orientation comparable to that which would be expected within a large bundle. Note that dummy tubes are nested within the baffle plates so as to minimize flow around the instrumented section along the baffle walls. Placed directly between the support block baffle plates and the simulation heater section is a dummy-tube block (see Figure 3.20). This block is fabricated from aluminum plate stock and solid aluminum rod. The purpose of this block is twofold. The block is designed to collect all rising two-phase flow generated by the simulation tubes and direct it into the test section. Secondly, the rods are 15.9 mm (0.625 in) in diameter and are spaced at 19 mm (0.75 in) intervals in a triangular-pitch arrangement, which therefore orients the flow into the test section as would be expected in a large multi-tube bundle.

Both the evaporator and condenser are equipped with various viewports as shown in Figures 3.6 to 3.11. The viewports consist of a 12.7 mm (0.5 in) thick Pyrex glass backed by a 12.7 mm (0.5 in) thick Plexiglas, except for the 0.241 m (9.5 in) diameter evaporator viewport which has a 19.1 mm (0.75 in) thick glass. The glass was used to prevent crazing of the Plexiglas by refrigerants, and the Plexiglas plate placed over the glass gave added strength.

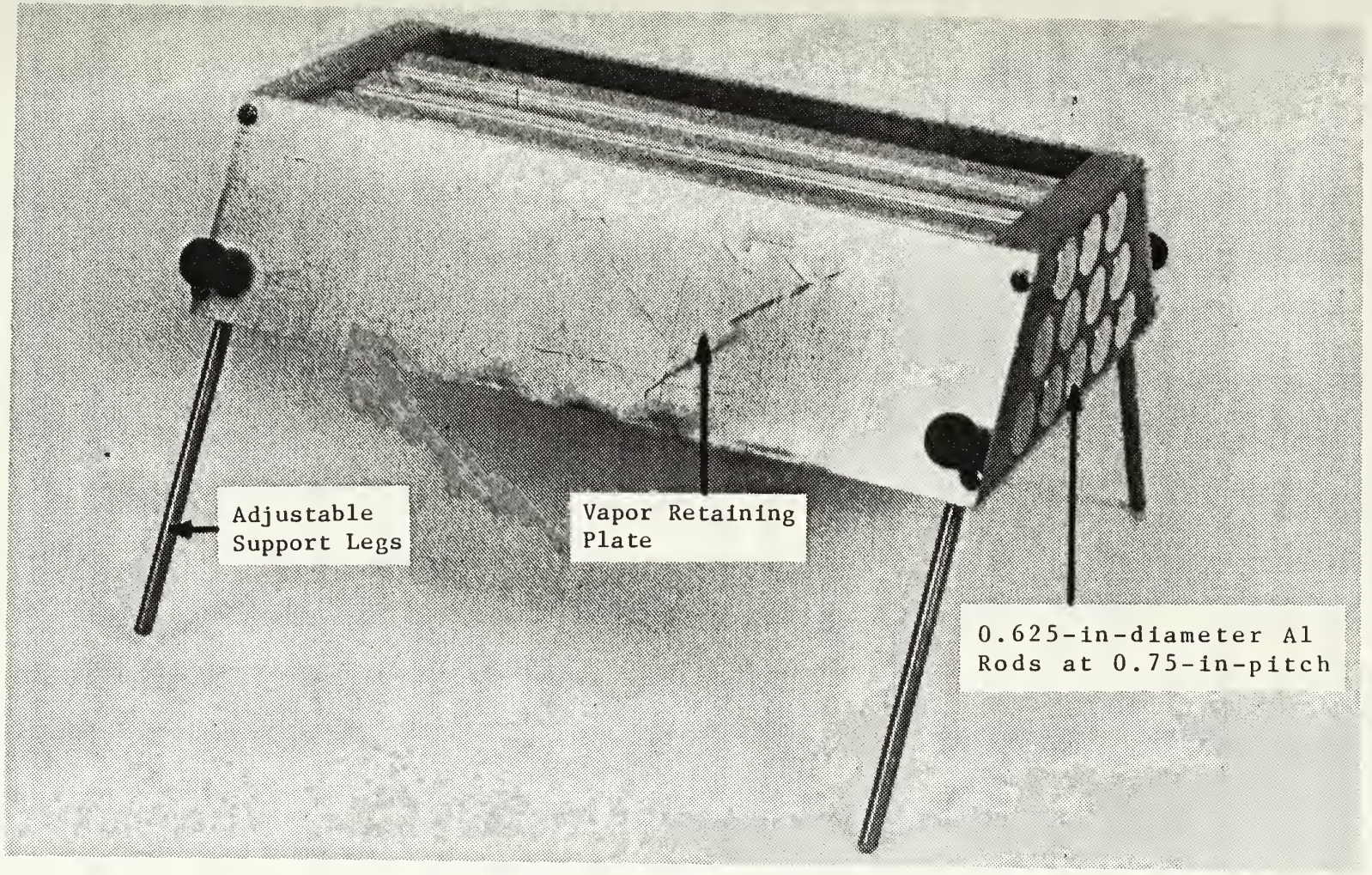

Figure 3.20 Photograph of Dummy Tube Rack

2. Tube-Bundle Ancillary Systems

Components and equipment external to the R-114 tube-bundle experimental apparatus include the following: (1) an R-114 storage and transfer system, (2) an oil storage and injection system, (3) a condenser cooling and flow control system, and (4) a cooling liquid (40:60 water/ethylene glycol) sump, (5) various piping, and (6) an 8-ton refrigeration plant.

The R-114 liquid reservoir consists of a stainless steel cylinder supported in an aluminum frame (see Figure 3.16). The height of the tank is configured so as to allow addition of R-114 liquid to the evaporator and to also allow for the condensate to be diverted from the condenser to the reservoir by gravity. Note that as shown in Figure 3.15, R-114 liquid drains from the condenser and is collected in a collar at the evaporator/condenser connecting flange. This collected fluid is drained into the storage tank through a diverter valve (V1). Notice that lines of connecting tubing are fitted with two valves. Valves were installed at the tubing couplings of each component of the apparatus. The additional valves provided improved system reliability and allowed for the independent isolation of major system components.

The oil storage tank is located above the evaporator mounted to the apparatus support frame. The amount of oil to be injected is measured in a calibrated Plexiglas

cylinder. The appropriate volume of oil was first drained into the calibrated cylinder, and then injected into the evaporator by an induced differential pressure.

The cooling fluid is pumped through the condenser coils by two pumps driven by 1/2-HP electric motors (see Figure 3.21). One pump provides flow through the five instrumented tubes and is controlled by five individual valves and flow rotameters. The other pump provides flow to the five auxiliary coils and is controlled by a single valve and a rotameter. The rotameters are mounted on a display frame adjacent to the cooling liquid sump (see Figure 3.22). The gages, valves and rotameters were connected to the condenser tubes with flexible tubing.

Because it was desired to maintain the cooling liquid temperature constant, a large volume of liquid was necessary. The temperature control band of commercially available refrigeration plants was either too broad for experimental work or was prohibitively expensive. To provide for a thermal "damping" or capacitance, a large Plexiglas sump was used as a source of cooling liquid, and this sump was cooled by an 8-ton refrigeration plant located outside the building. The 40:60 water/ethylene glycol mixture was circulated to the refrigeration plant by a 3/4-HP pump through approximately 45.7 m (150 ft) of polyvinyl chloride (pvc) piping. The piping was insulated using 19 mm (0.75 in) thick foam rubber insulation.

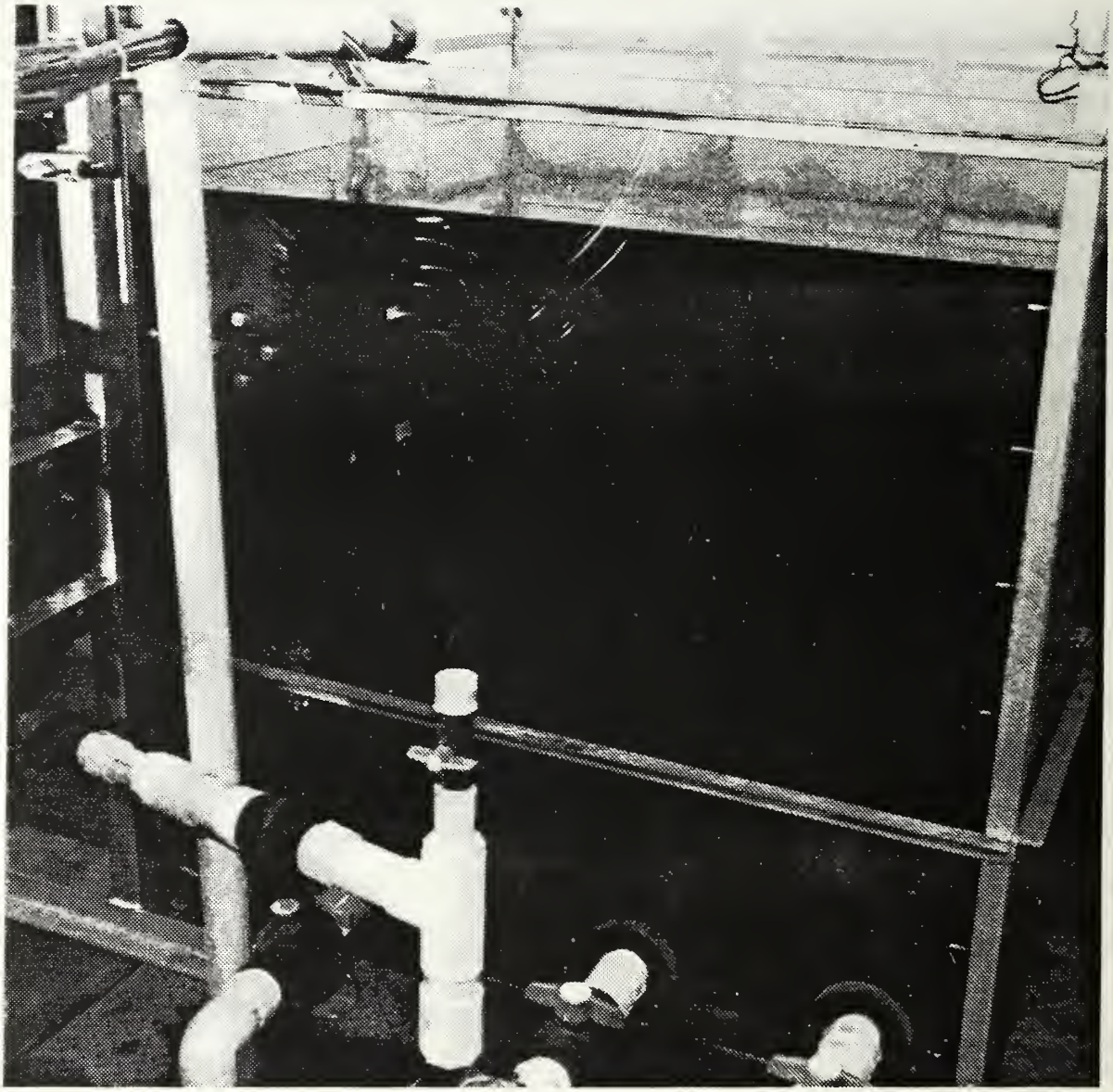

Figure 3.21 Photograph of Pumps and Water/ Ethylene Glycol Sump

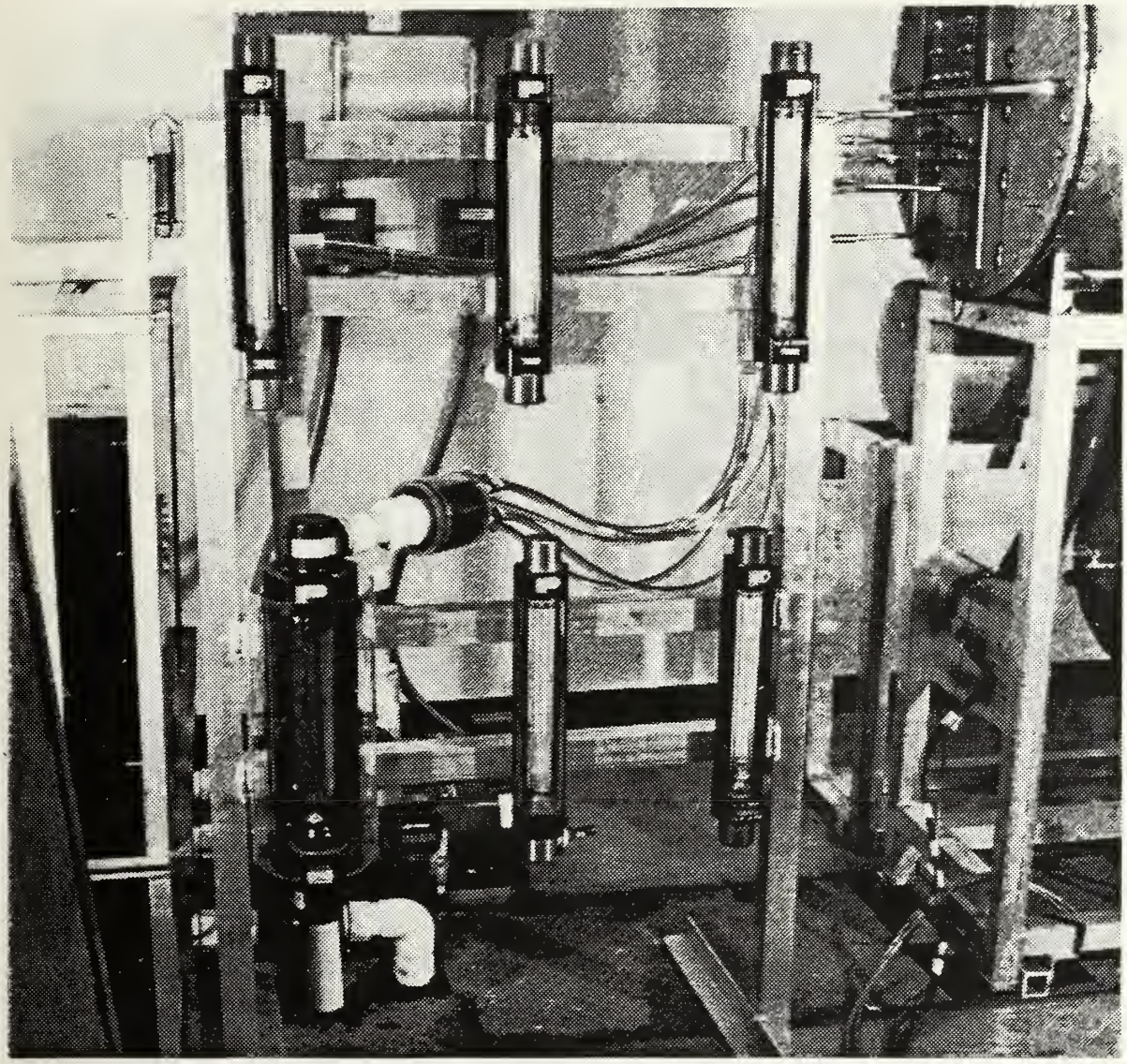

Figure 3.22 Photograph of Rotameter Gage Board

3. Instrumentation

The instrumentation used in the tube-bundle apparatus is similar in type to that used in the single-tube apparatus except much larger in scope.

As shown in Figure 3.17, the experimental tube bundle has a cross section of 102 mm x 203 mm (4 in x 8 in), and consists of 17 pairs of heater wires and 30 pairs of thermocouple leads. To avoid any induced interferences from the heater wires, the thermocouple wires were properly isolated wherever possible. For this purpose, grounded copper braided cables were used to ensheath the thermocouple leads.

Thermocouples were placed in six grooves (measuring 1 mm x 1 mm) machined on a copper sleeve. The circumferential and axial locations of these grooves are shown in Figures 3.23 and 3.24. A 6.35-mm-diameter x 203.2-mm-long heater was inserted into the sleeve and the outer surface was tinned by applying electrical heating. The tinned sleeve, with thermocouples and the heater, was inserted into the test tube. Thermocouple wells for measuring the vapor temperature, liquid temperature and condensate return temperature were placed as shown in Figures 3.25 and 3.26.

The measurement of power input to the electric heaters was carried out by means of root-mean-square sensors for voltage and current for each heater or group of heaters.

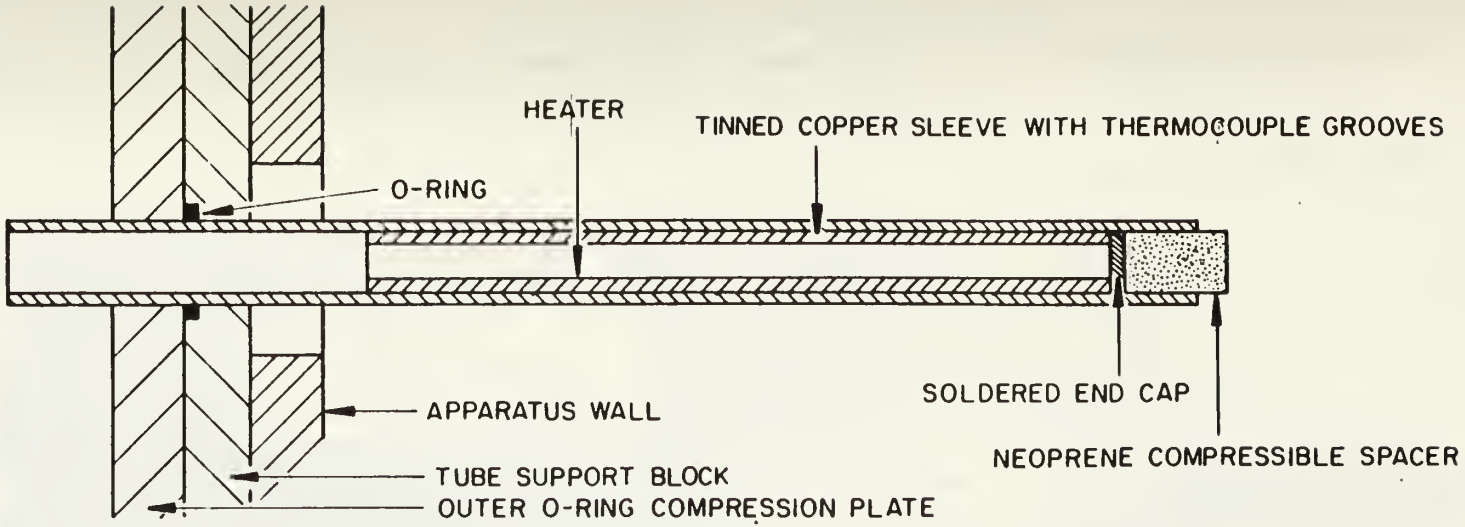

(a) BUNDLE HEATER TUBE SECTIONAL VIEW

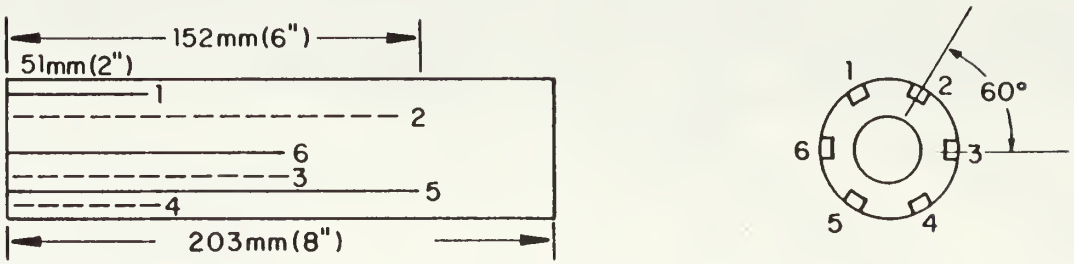

(b) THERMOCOUPLE LOCATIONS ALONG HEATED LENGTH

Figure 3.23 Thermocouple Locations of Instrumented Boiling Tube for Multi-Tube Apparatus

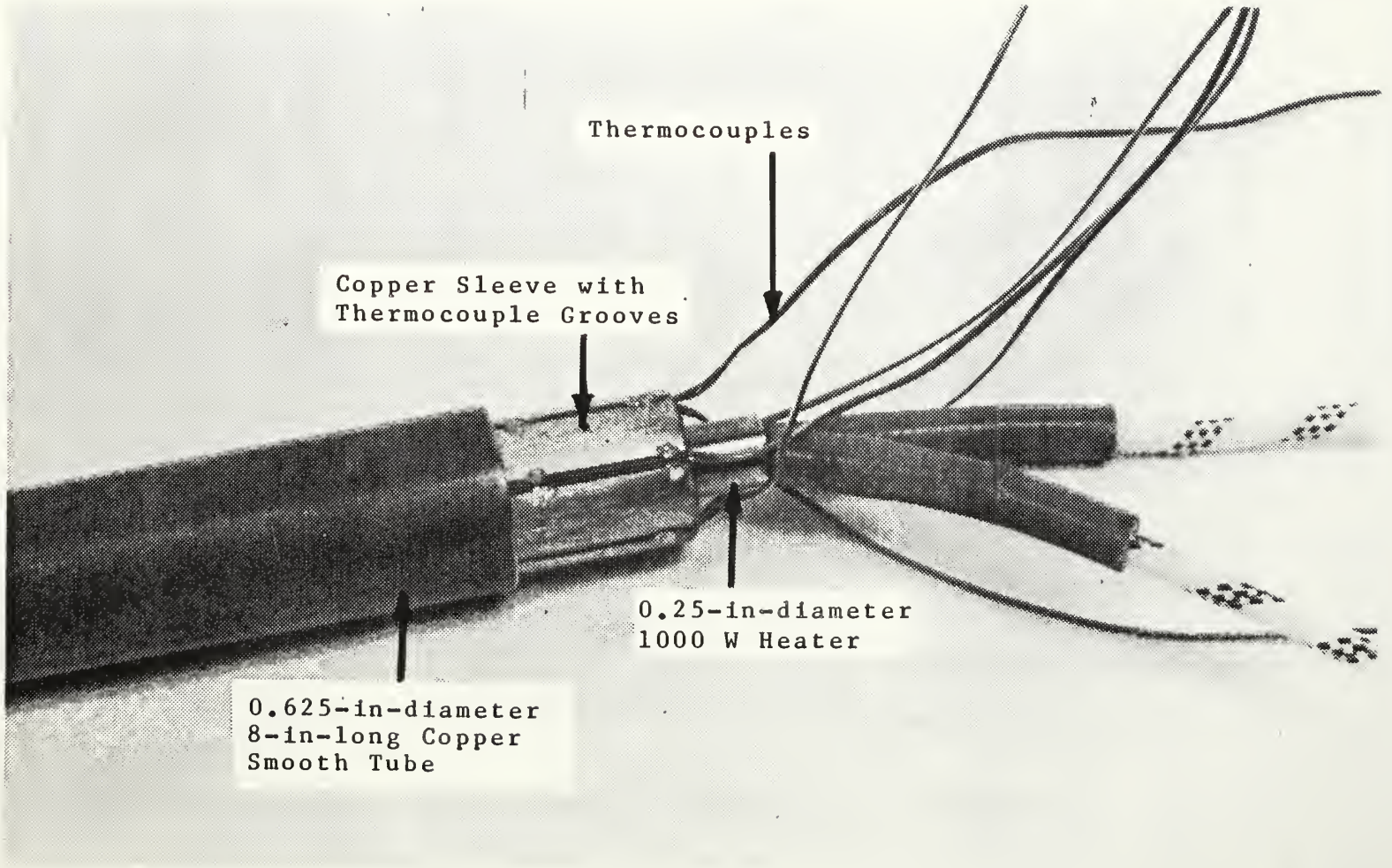

Figure 3.24 Photograph of Instrumented Test Tube for Multi-Tube Apparatus

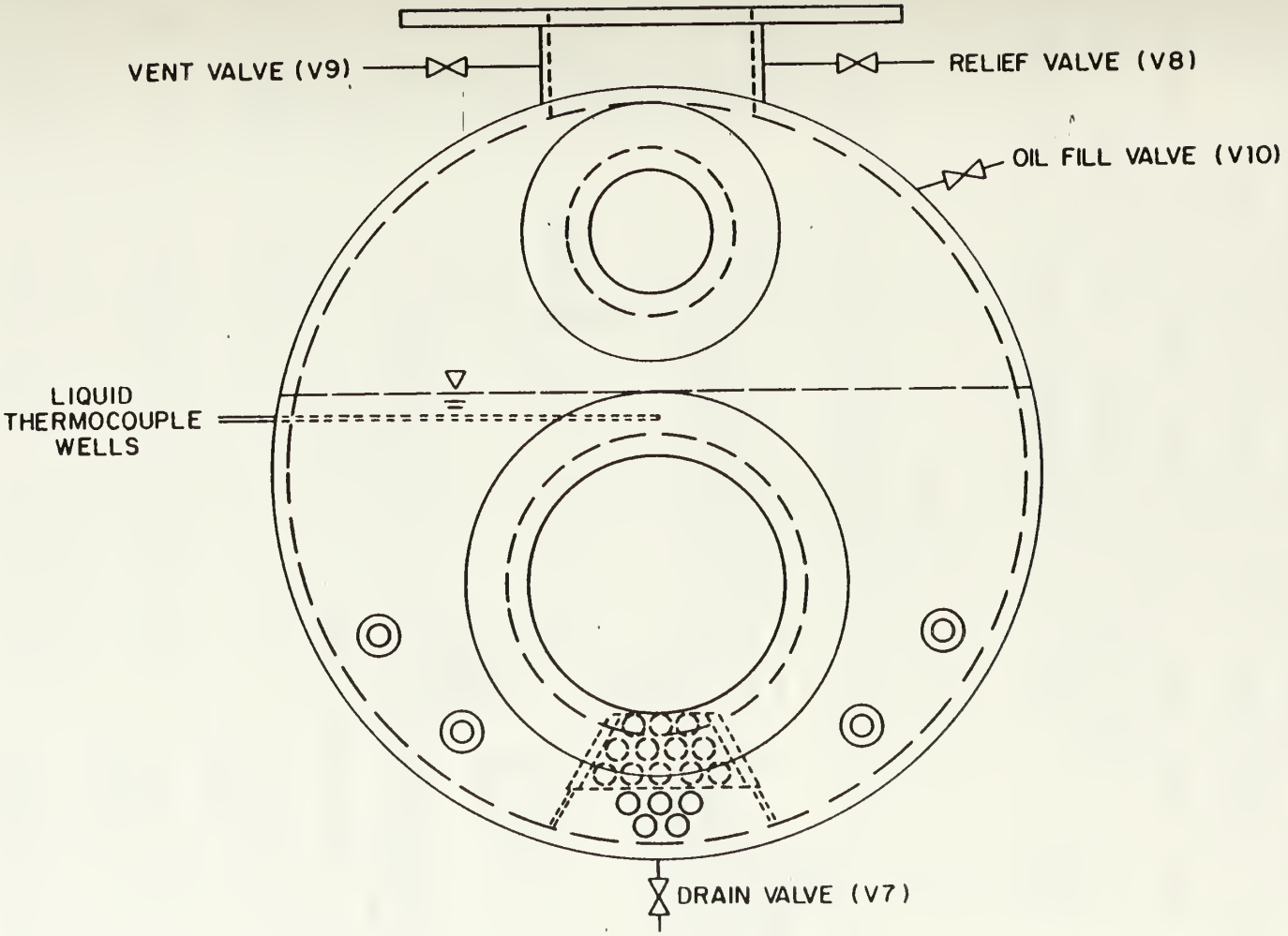

Figure 3.25 Front View of Multi-Tube Evaporator Showing Valves and Liquid Thermocouple Wells

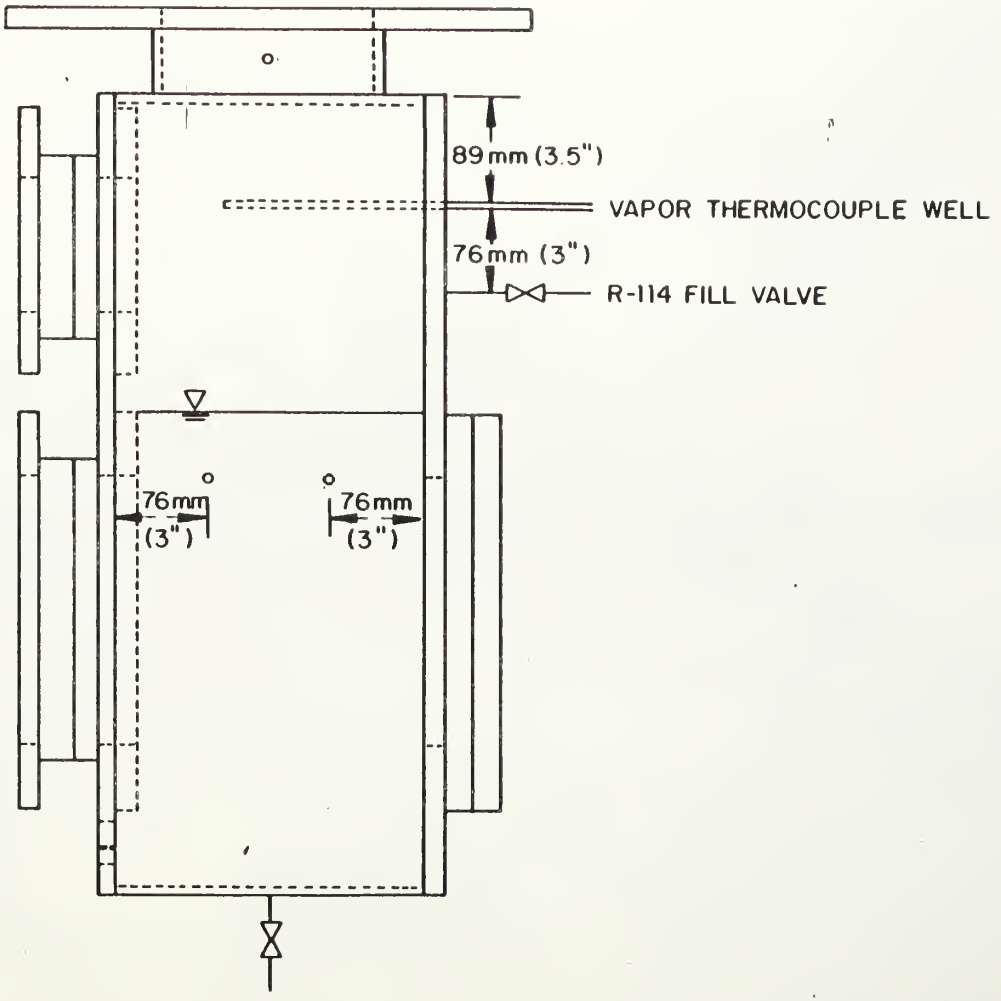

Figure 3.26 Side View of Multi-Tube Apparatus Evaporator Showing Vapor Thermocouple Well

Complete details of the type of sensors used are listed in Table 3.1 and Figure 3.27 shows the current and voltage sensors installed in the circuit breaker panel. As can be seen, each instrumented tube, designated by "I" in Figure 3.17, is provided with an individual current sensor. This sensor is capable of measuring 0-5 A (AC), and producing a linear output of 0-5 V (DC). On the other hand,

TABLE 3.1

SENSORS USED TO MEASURE HEATER VOLTAGES AND CURRENTS

Sensor	Input	Output	Remarks
1,3,5,7,9	0-5 A (AC)	0-5 V (DC)	Measures the current to each of the instrumented tubes.
2,4,6,8, 10	0-10 A (AC)	0-5 V (DC)	Measures the combined current to each pair of active tubes.
11	0-100 A (AC)	0-5 V (DC)	Measures the total current to all bundle-simulation heaters.
12	0-100 A (AC)	0-5 V (DC)	Measures the total current to all auxiliary heaters.
13	0-300 V (AC)	0-5 V (DC)	Measures voltage applied to bundle heaters.
14	0-300 V (AC)	0-5 V (DC)	Measures voltage applied to auxiliary heaters.
15	0-300 V (AC)	0-5 V (DC)	Measures voltage applied to bundle-simulation heaters.

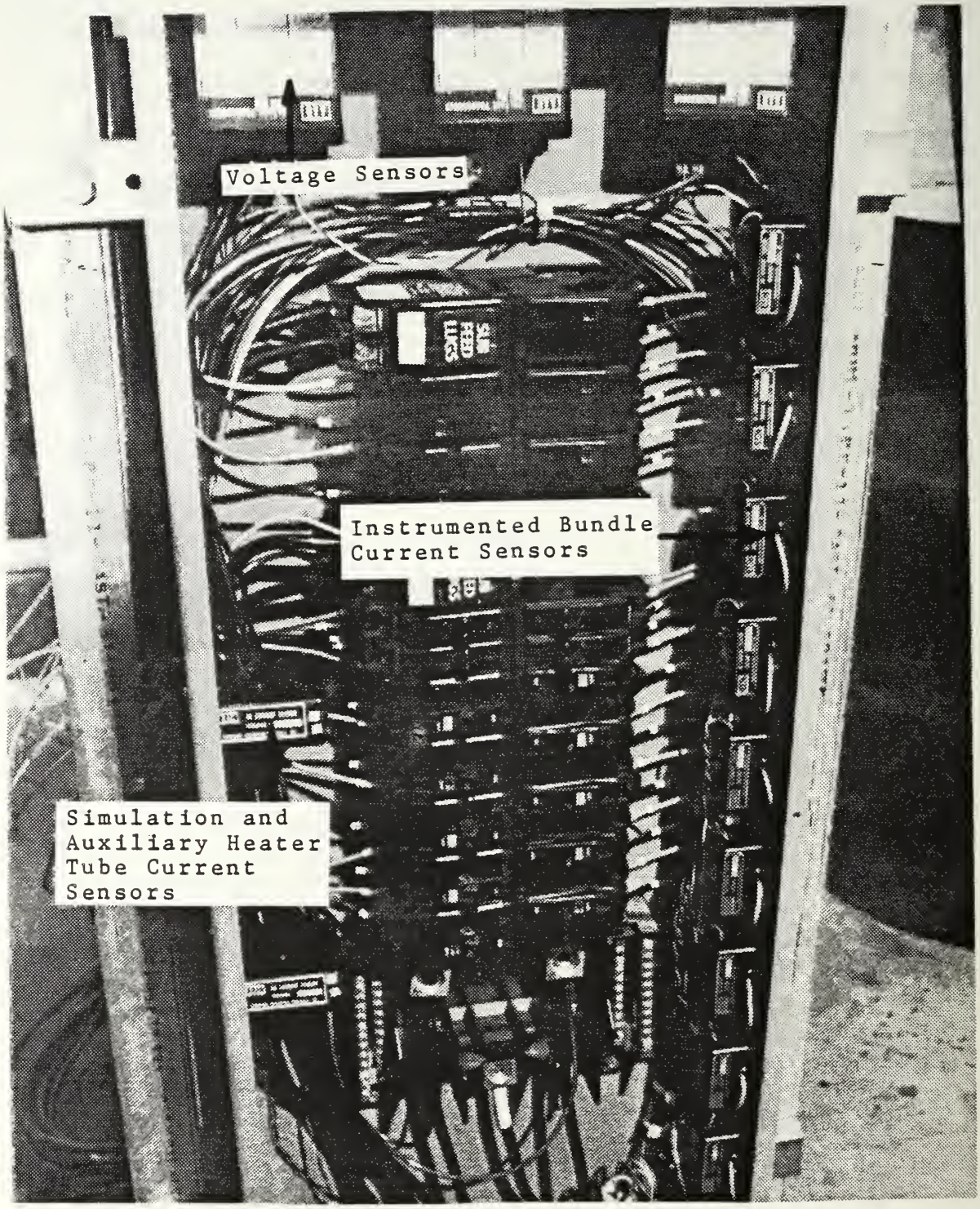

Figure 3.27 Photograph of Voltage and Current Sensors Installed in Circuit Panel

each pair of active tubes, designated by "A", are electrically connected in parallel. The combined current of each such pair of active tubes was measured using a separate current sensor. This sensor measures 0-10 A (AC), producing a linear output of 0-10 V (DC). In addition, two other current sensors were used to measure the combined current to the auxiliary heaters and the bundle simulation heaters. These sensors are rated to measure 0-100 A (AC) producing an output of 0-5 V (DC). As stated earlier, three variable transformers were used to power the instrumented and active tubes, the auxiliary heaters and the bundle simulation heaters. The individual voltage sensors were used to measure the output voltages of these transformers. These sensors are rated to measure 0-300 V (AC), producing a linear output of 0-5 V (DC). Since all these devices produce a 0-5 V (DC) output, they were easily readable by the HP-3497A data acquisition system.

4. Installation of Condenser Tubes

The installation of the auxiliary condenser coils was intended to be a permanent assembly that would require modifications only in rare circumstances. Prior to condenser assembly, these five coils were suspended on individual 12.7-mm-diameter support rods cantilevered from the left condenser end plate (see Figure 3.28). The ends of the auxiliary coils were coupled to compression fittings on the endplate. Note that unlike the test condenser tubes,

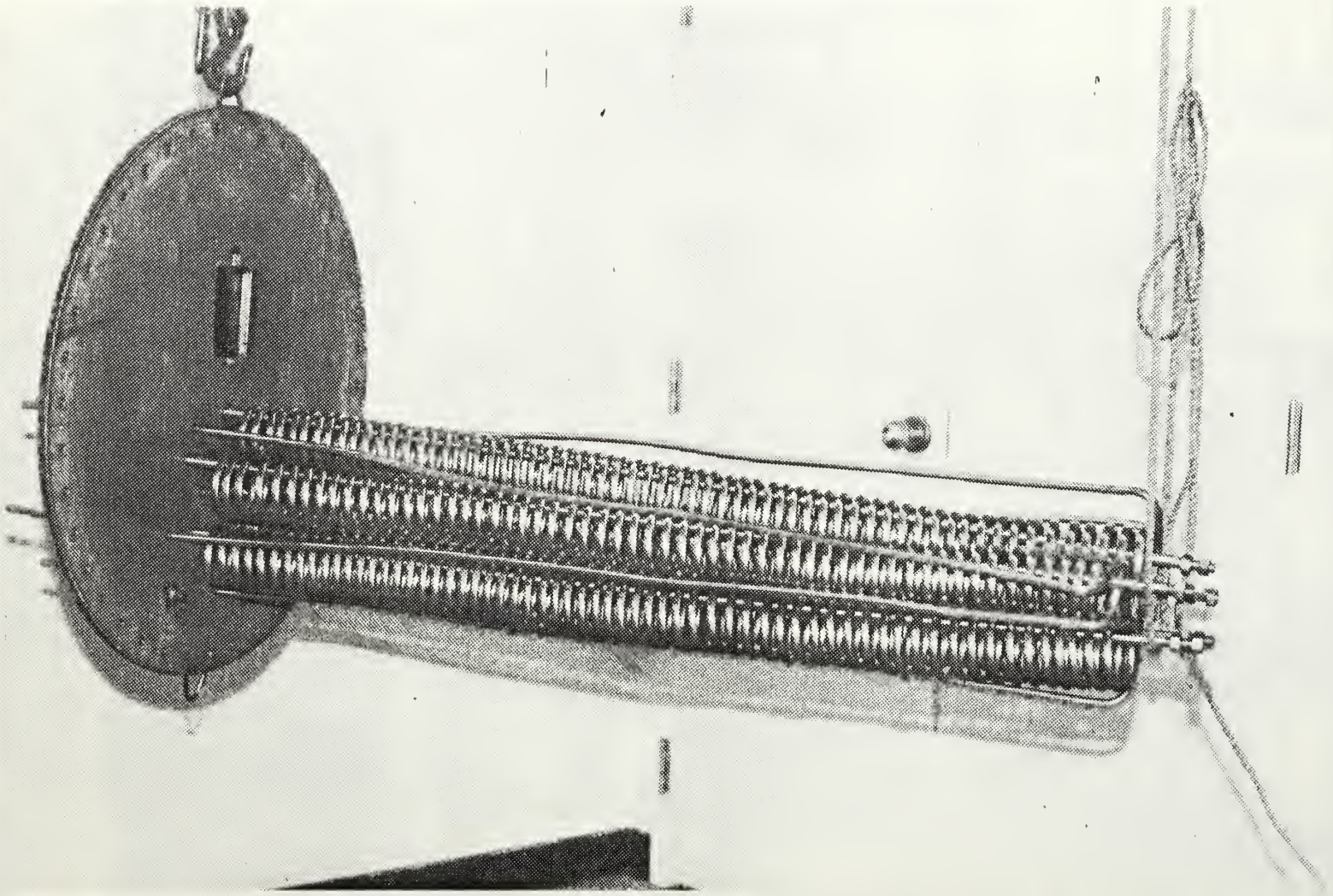

Figure 3.28 Photograph of Auxiliary Condenser Coils

the auxiliary tubes and outlets are directed through the same endplate. Next, the vapor flow shroud, with Pyrex viewglass installed, was slid over the auxiliary condenser tubes and their support rods. The shroud was attached to the endplate and supported on the free end by adjustable legs.

The pre-assembled auxiliary condenser section was next inserted into the condenser. This task was tedious, requiring utmost care so as to avoid breaking the glass plate attached to the shroud. After the shroud and coil supports were adjusted to a satisfactory alignment, the other condenser endplate was lifted into position. The endplates were then sealed to their respective flanges. Lastly a 0.91 m (36 in) long copper tube with axial perforations was inserted through the right endplate and fastened with a compression fitting. The perforated tube was used to withdraw noncondensing gases from the condenser.

The instrumented condenser tubes were individually pushed through the left 25 mm (1 in) thick nylon block and 12.7 mm (0.5 in) thick stainless steel plate. Once all five tubes were assembled in this manner, the unattached end of the tubes were passed through the access in the condenser endplates and centered along the Pyrex glass viewport. Next, the right side nylon and stainless steel plates were placed on the tubes. The tubes were sealed with O-rings compressed between the plates. Lastly, the instrumented

tube plates were secured to their respective studs and sealed to the condenser endplates.

5. Initial Overall Apparatus Assembly

After initial fabrication, the condenser and evaporator were coupled in the machine shop. The various tubing accesses were plugged, viewports were installed and the basic apparatus was pressure tested. After cleaning, the shells were moved to the laboratory.

The auxiliary condenser tubes were assembled to the left endplate and the vapor shroud was installed as discussed previously. The left endplate was joined to condenser followed by the right condenser endplate.

The tubing for the R-114 reservoir was connected. All lines between components had two valves to facilitate isolation (see Figure 3.16). Next the water/ethylene glycol piping was connected from the sump to the circulation pump then to the gage board, and lastly to the condenser (see Figure 3.29).

All thermocouple wells described previously were installed next. Insulation was then placed over all accessible surfaces of the stainless steel shells, the piping and the sump. The tube support block with instrumented and active tubes was installed in the evaporator. The twist plugs to supply power to the heaters were checked for continuity and connected to the distribution panel. Prior to filling the apparatus with

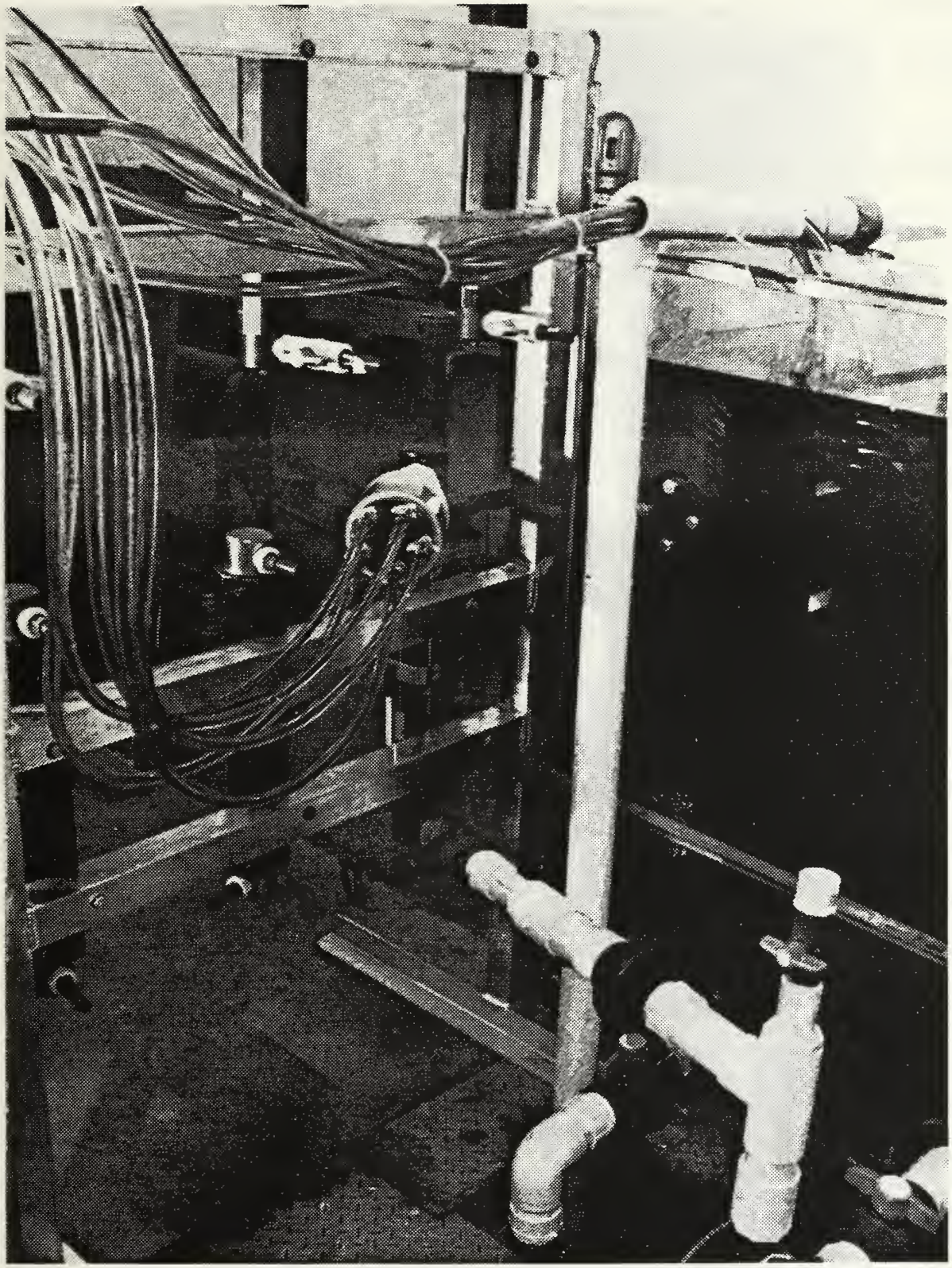

Figure 3.29 Photograph of Condenser Cooling Liquid Tubing

R-114, an overall system pressure test was conducted and leaks found were corrected.

The apparatus after initial assembly is shown in Figure 3.30.

6. Tube-Bundle Data Acquisition and Reduction

For the tube-bundle apparatus, approximately the same overall data-collection system was used as for the single-tube apparatus. A Hewlett-Packard 9826A computer was used to control a Hewlett-Packard 3497A Automatic Data Acquisition Unit; the data-acquisition unit used was expanded, however. The system used for the single-tube apparatus was equipped with 40 data channels while the larger bundle instrumentation required expansion to 80 data channels. Of the 80 channels, 60 were compensated for Type-T thermocouples, while the 20 remaining uncompensated channels were devoted to reading the outputs of the condenser coolant thermopiles and the voltage and current sensors. Table 3.2 shows a complete listing of all measurements automatically scanned by the data-acquisition system.

The DRP6 program, used for the single-tube apparatus, was enhanced to accommodate the extra thermocouple and sensor inputs. Additionally, the program was modified to provide a continuous reading of total heater power (from instrumented, simulation and auxiliary sections) so as to provide the researcher with the information

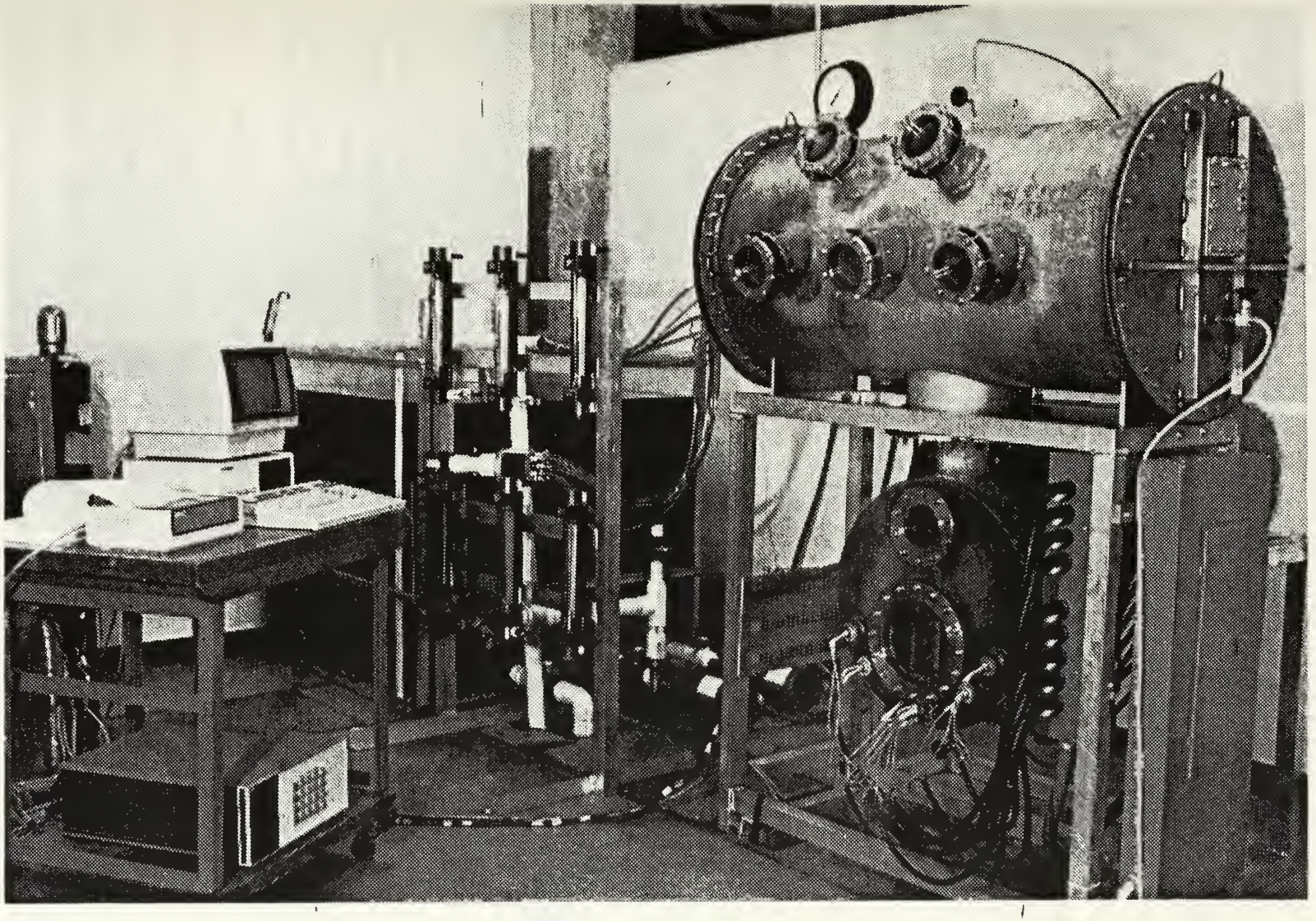

Figure 3.30 Photograph of Final Assembled Apparatus

TABLE 3.2

CHANNEL ASSIGNMENTS ON DATA ACQUISITION SYSTEM*

Channel Numbers	Measurement
0-1	Liquid Temperature
2	Vapor Temperature
3	Sump Temperature
4-9	Tube Wall Temperature of I_1
10-15	Tube Wall Temperature of I_2
16-21	Tube Wall Temperature of I_3
22-27	Tube Wall Temperature of I_4
28-33	Tube Wall Temperature of I_5
60-64	Input Current to I_1-I_5
65-69	Input Current to Pairs of Active Tubes
70	Input Current to Auxiliary Heaters
71	Input Current to Bundle-Simulation Heaters
72	Voltage across Bundle Heaters
73	Voltage across Auxiliary Heaters
74	Voltage across Bundle Simulation Heaters

*Channels 0-59 are compensated for Type-T thermocouples,
Channels 34-59 are reserved for instrumentation of the condenser, and
Channels 60-79 measure direct voltages.

necessary to maintain constant system temperature and pressure, as well as a constant vapor volume flow rate to the condenser.

IV. EXPERIMENTAL PROCEDURES

A. SINGLE-TUBE APPARATUS

1. Installation of Boiling Tube in the Apparatus

To remove surface oil, oxidation or other contaminants, the tubes were thoroughly cleaned with acetone. After the acetone had completely evaporated, the thermocouple and the heater leads were led through the Teflon plugs shown previously in Figure 3.3. Before assembly, a single aluminum flange and a Teflon plug were bolted to the Pyrex tee at one end. The test tube was then pushed through the pair of O-ring seals. Lastly, the remaining aluminum flange was bolted to the tee and the Teflon plug was pushed over the heater tube and screwed to the flange.

After the tube was in place and all appropriate fittings were tightened, the apparatus was evacuated with a vacuum pump to 29.0 in Hg. The apparatus was left undisturbed for at least two hours and if no pressure rise was observed, the apparatus was pressurized to 0.19 MPa (27 psi) with R-114 vapor. Next, using an automatic halogen leak detection (TIF 5000), all joints and fittings were inspected for R-114 leakage. The sensitivity of the detector was 3 ppm minimum concentration. Any leaks detected were fixed immediately.

2. General Operation

Prior to assembly, a scribe mark had been installed on the interior surface of the left flange at a level corresponding to 1600 cm^3 of R-114 liquid at 22 ^oC (72 ^oF). This level establishes an initial mass of R-114 in the apparatus of 2.5 kg. To this mass, successive measured volumes of oil were added so as to test the performance of the heater rube in varying oil concentrations.

Prior to operation, the 1/2-ton refrigeration plant was operated for between two to four hours in order to achieve a sump temperature of -12 ^oC or less. When starting the apparatus, the R-114 liquid was at room temperature and the system absolute pressure was approximately 172 kPa (25 psi). To start up the apparatus, the valve VC controlling flow of cooling fluid was slowly opened. The system pressure and temperature were slowly decreased as R-114 vapor condensed on the copper coils. Care was taken to ensure that the pressure decrease was slow enough to prevent nucleation from occurring prematurely on the test tube.

Once the system stabilized at a saturation temperature 2.2 ^oC (at approximately atmospheric pressure), the power to the test tube and auxiliary heater tubes was increased to the desired heat flux. Heat flux was increased by adjusting the output of two variable transformers and noting the measured power displayed on the video monitor. The flow of cooling fluid was increased simultaneously so as

to maintain saturation conditions. Once saturation conditions were restored, the conditions were maintained for at least five minutes prior to data collection to eliminate transient effects. Measurements were made for both increasing and decreasing heat-flux conditions.

3. Data-Reduction Procedures

All of the sensor input information provided to the data-acquisition system is manipulated to provide two basic data variables--temperature and heat flux.

The data-acquisition system receives AC voltage 0-300 V and current 0-10 A information on data channels with 0-5 V (DC) linear output as discussed previously. The data were converted to tube input heat according to the following equations:

$$V_{AC} = (300/5)V_{VS} \tag{4.1}$$

$$A_{AC} = (10/5)V_{AS} \tag{4.2}$$

where V_{VS} and V_{AS} refer to voltage signal and amperage signal voltages, respectively. V_{AC} and A_{AC} refer to the actual applied voltage and current in the heater, respectively.

Cartridge heaters are a resistive load; therefore, the product of applied voltage and current yields the total input power to the test tube.

The ordinary expression for heat flux is:

$$q = \frac{Q}{\pi D L} \tag{4.3}$$

but this equation must be modified to account for axial heat transfer beyond the instrumented length of the tube. The precise expression for heat flux from the instrumented tube becomes:

$$q = \frac{Q - 2Q_L}{\pi D L} \tag{4.4}$$

where Q_L refers to the axial heat loss along the smooth tube end. The development of the analytical expression for Q_L has been presented by Karasabun [Ref. 36].

The eight thermocouples provide temperature information at the interface between the tinned copper sleeve and the inner wall of the test tube. The average temperature is calculated from the arithmetic mean of all the thermocouples. Neglecting contact resistance, the outer wall tube temperature is obtained by employing Fourier's law of conduction with the known wall heat flux.

4. Oil Addition

Predetermined amounts of oil were measured by opening valves V2, V3 and V4 (see Figure 3.1) and allowing the desired volume of oil to fill the graduated cylinder. Flow to the condenser was re-initiated, without any heat

addition, and valves V2, V3 and V4 were closed. After a vacuum has been drawn in the apparatus, the flow was secured and valve V1 was opened allowing oil to enter the evaporator tee. The apparatus was cycled through several iterations of this procedure when adding increased amounts of oil.

5. Shutdown and Fluid Removal

Upon completion of a data series for an individual tube, the oil/R-114 mixture must be separated and the R-114 recovered. As shown in Figure 3.1, valve V5 was secured and valves V6 and V7 were opened. The cooling flow rate to the condenser was set at its maximum, and the condensate was directed to the R-114 reservoir. The distilling process was initially accelerated by energizing the auxiliary and tube heaters, with proper care exercised to ensure that no heater surface was uncovered while energized. With only ambient heat transfer, the R-114 liquid was transferred to the reservoir in about two hours. Next, the reservoir was isolated by securing valves V7 and V6, and condenser cooling flow was secured. After the apparatus reached equilibrium with ambient air, the absolute pressure rose to approximately 172 kPa (25 psi). The differential pressure was then used to expel the oil residue from a sampling petcock provided at the bottom of the evaporator. The oil residue was then expended and the evaporator tee and flanges were cleaned with acetone following the removal of the test tube and the evaporator flanges.

B. TUBE-BUNDLE APPARATUS

1. Installation of Evaporator Tubes and Tube Support Block

For the tube support block, 5 instrumented and heated tubes, 12 heated tubes and 18 dummy tubes were prepared. All heated tubes were prepared with tinned copper sleeves as shown in Figures 3.23 and 3.24. For the instrumented tubes, six thermocouple grooves were cut in the copper sleeves as discussed in Chapter III.

The tinned copper sleeve was inserted into the test tube by connecting the heater leads to a variable transformer and heating the sleeve so as to melt the solder. The temperature of the sleeve was monitored so that the solder was just slightly above its melting point, but not high enough to cause significant oxidation of the test tube surface.

The dummy tubes, which do not penetrate the tube support block, are connected to the plate by means of end plugs countersunk in the tube plate. The heated active and instrumented tubes penetrate the plate as shown in Figures 3.19 and 3.23, and are sealed with an O-ring compressed between two stainless steel plates. As shown in Figure 3.19, the side baffles are grooved to accept dummy tubes so as to more accurately model the hydrodynamics of a large tube bundle. The free end of the heater tubes are sealed with an end cap and lastly fitted with a compressible neoprene plug.

Prior to inserting the tube block, the rack of dummy tubes was placed above the simulation tubes as shown in Figure 3.17. During the initial installation of the tube support block, the front view glass of the evaporator (shown in Figures 3.9 and 3.10) was removed in order to guide the block into place. The tubes were then axially adjusted so that, with the view glass in place, the neoprene plugs were slightly compressed. The purpose of these plugs is to prevent two-phase flow from bypassing the instrumented section along the face of the viewport.

After the tube support block and front viewport were fastened securely, compressing their respective gaskets, the O-ring compression plate was slowly tightened, sealing the tubes.

2. Initial R-114 Trial Procedures

Baseline trials with the tube-bundle apparatus did not involve instrumented condenser tube operation. All R-114 vapor was condensed on the auxiliary condenser coils.

Using the installed variable transformers, various heat fluxes were applied to the top evaporator instrumented tube, with constant overall heat input maintained by adjusting the power to the auxiliary heaters. To observe bundle effects, the top instrumented tube was tested again with the entire bundle operating.

V. RESULTS AND DISCUSSION

A. SINGLE-TUBE RESULTS

As shown by Reilly [Ref. 39] (see Figure 5.1), the smooth-tube boiling data follow a characteristic boiling pattern. Smooth-tube data show natural-convection heat transfer up to a heat flux of approximately 12 kW/m^2 and a wall superheat of about 40 K, at which point the onset of nucleate boiling (ONB) occurs. The transition from natural convection to nucleate boiling was shown to be very abrupt. Notice that Figure 5.1 data by Reilly [Ref. 39] were taken at a saturation temperature of -2.2 ^oC compared to 2.2 ^oC used during the present investigation. Furthermore, Reilly took data also at 6.7 ^oC resulting in only up to 5 percent increase in the boiling heat-transfer coefficient compared to that at -2.2 ^oC.

For the finned tube with a fin density of 1024 fpm (26 fpi), as shown in Figure 5.2, ONB occurred at about 8 kW/m^2 in the pure-refrigerant case with delay in onset of nucleate boiling to about 22 kW/m^2 for the 10 percent oil case. The wall superheat to achieve ONB for the 1024 fpm (26 fpi) tube at 0 percent oil was approximately 7 K, as compared to 40 K for the smooth tube. Additionally, at a practical heat flux of 30 kW/m^2 with up to 10 percent oil, the nucleate boiling wall superheat for the finned tube was

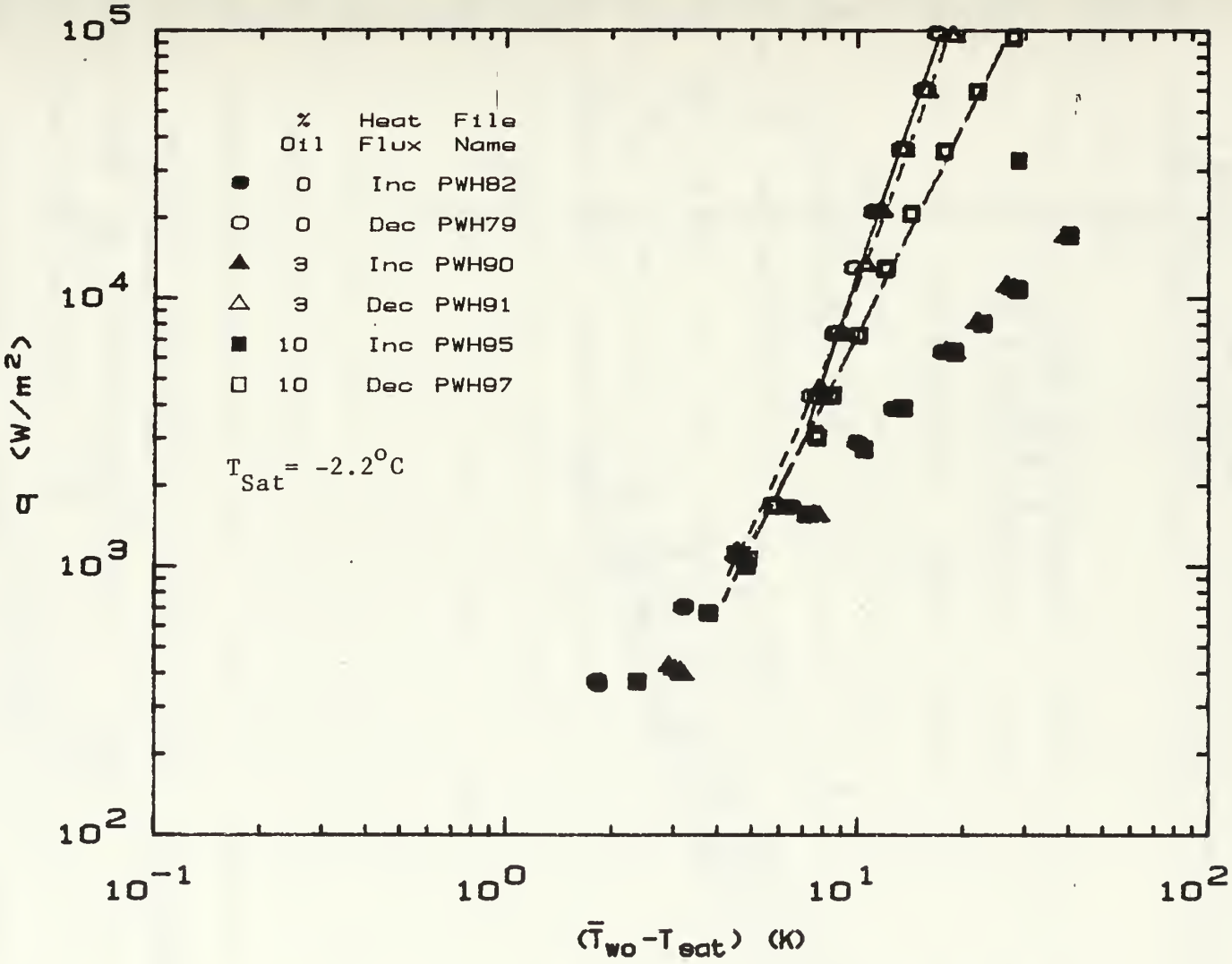

Figure 5.1 Heat-Transfer Performance of Smooth Tube [Ref. 39]

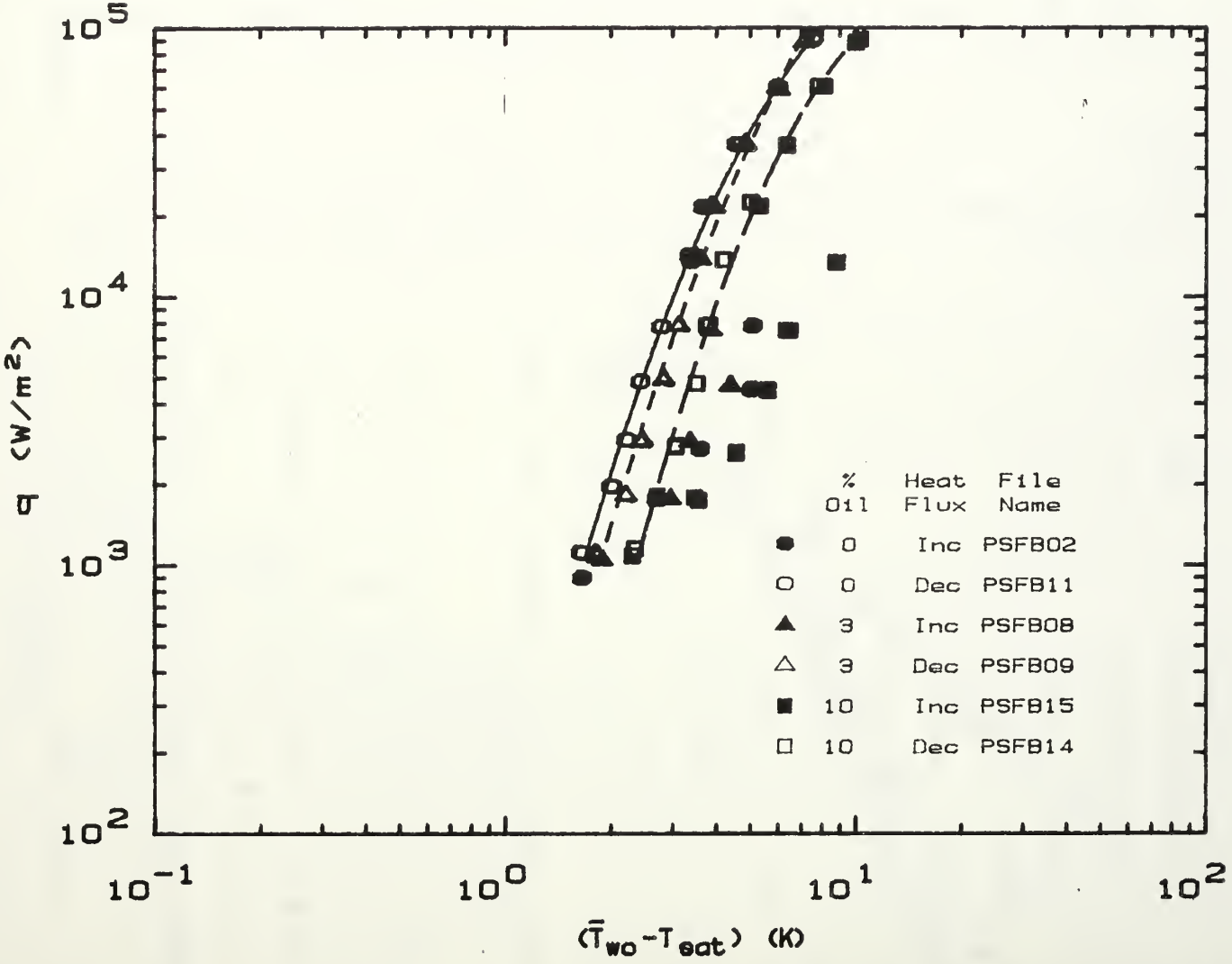

Figure 5.2 Heat-Transfer Performance of Finned Tube (1024 fpm (26 fpi))

less than 3 K whereas for the smooth tube, the wall superheat at an equal heat was 7 K for 0 percent oil and 8 K for 10 percent oil. As with the smooth-tube case, the 1024 fpm (26 fpi) tube showed an increase in wall superheat with increasing percentages of oil and a delay in onset of nucleate boiling.

The variation of the heat-transfer coefficient with heat flux for the finned tube (1024 fpm (26 fpi)) and smooth tubes are shown in Figure 5.3. For a practical heat flux of 30 kW/m^2, the finned tube yields enhancement ratios (i.e., the ratio of enhanced-tube pool-boiling coefficient to the value for the smooth tube at a specified heat flux) of 2.8, 2.6 and 2.6 for 0, 3 and 10 percent oil, respectively. Notice that these ratios are essentially the same, within the experimental uncertainty, indicating that both smooth and 1024 fpm (26 fpi) tubes are affected equally by the presence of oil. It is worth comparing these ratios with the area ratio (a value of 3.98 for this tube) due to finning (i.e., the ratio of finned tube external area to that of smooth tube having an outer diameter equal to the root diameter of the finned tube). Therefore, based on the actual external area of the finned tube, the boiling coefficient for pure-component case is only 70 percent of the value for the smooth tube. As stated by Palen et al. [Ref. 1] (see Chapter II), the boiling coefficient based on

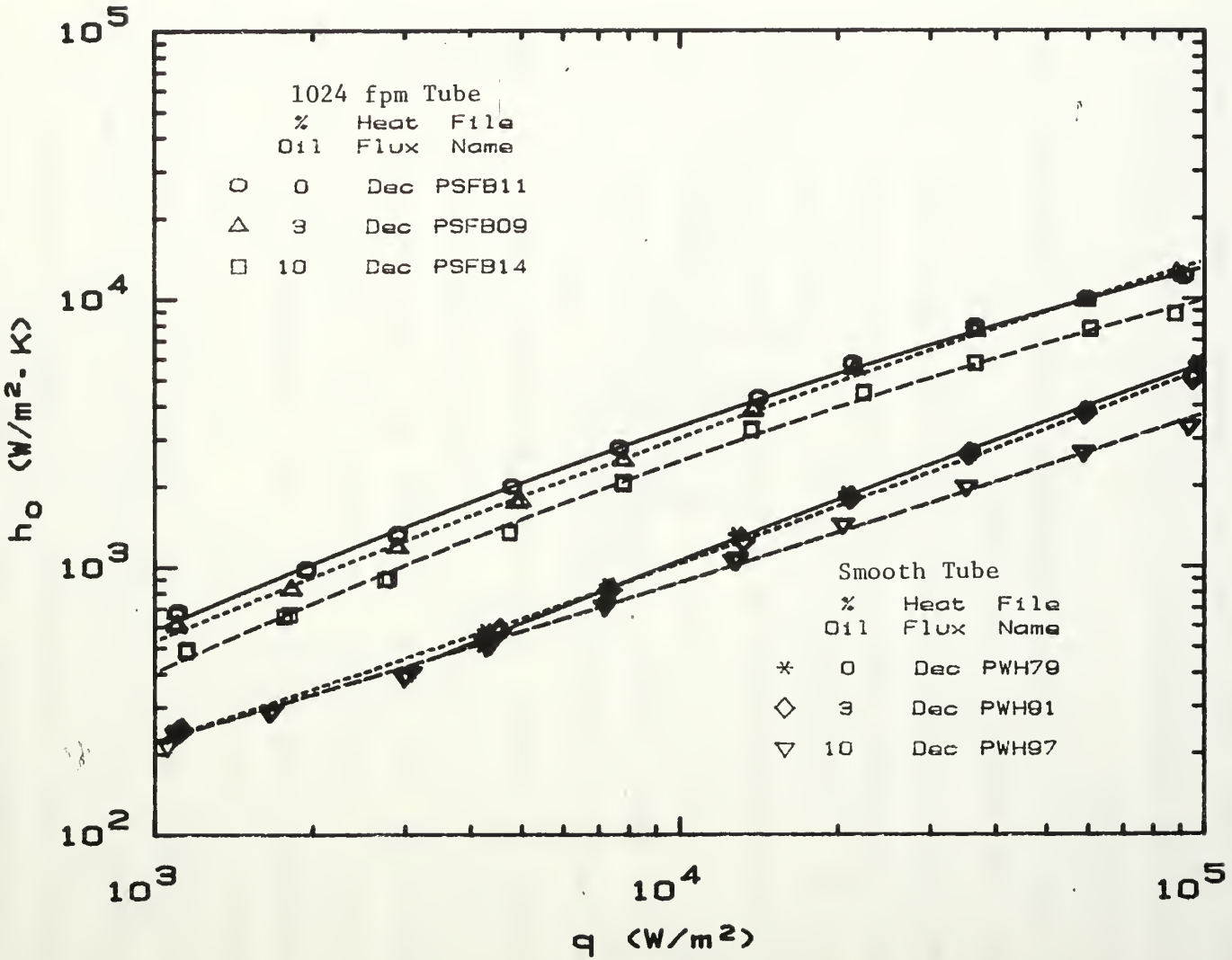

Figure 5.3 Heat-Transfer Performance of 1024 fpm (26 fpi) Tube Compared with Smooth Tube [Ref. 39]

the actual area is thus smaller than the smooth-tube value, but this reduction is more than offset by the increased area.

The variation of heat flux with wall superheat for the more densely finned tube (1575 fpm (40 fpi)) is shown in Figure 5.4. For this tube, the onset of nucleate boiling for 0 percent oil occurred at about 20 kW/m^2 and a wall superheat of about 11 K, which is about 50 percent greater than that for the 1024 fpm (26 fpi) tube, although better than for the smooth tube. An explanation is not known for this unexpected observation in the onset of nucleate boiling for these two finned tubes. For all concentrations of oil, the 1575 fpm (40 fpi) tube had greater wall superheats in the natural-convection region than the 1024 fpm (26 fpi) tube, but with fully developed boiling the wall superheats of the 1575 fpm (40 fpi) tube were consistently less than for the 1024 fpm (26 fpi) tube.

The variation of the heat-transfer coefficient with heat flux for the finned tube (1575 fpm (40 fpi)) and smooth tubes are shown in Figure 5.5. The enhancement ratios for the 1575 fpm (40 fpi) tube at 0, 3 and 10 percent oil were 3.8, 3.5 and 3.2, respectively. The measurable decrease in enhancement ratio indicates that, like the smooth and 1024 fpm (26 fpi) tubes, increases in oil cause decreases in heat-transfer performance. When the area ratio of 6.2 is included in comparisons of pure-component performance, the

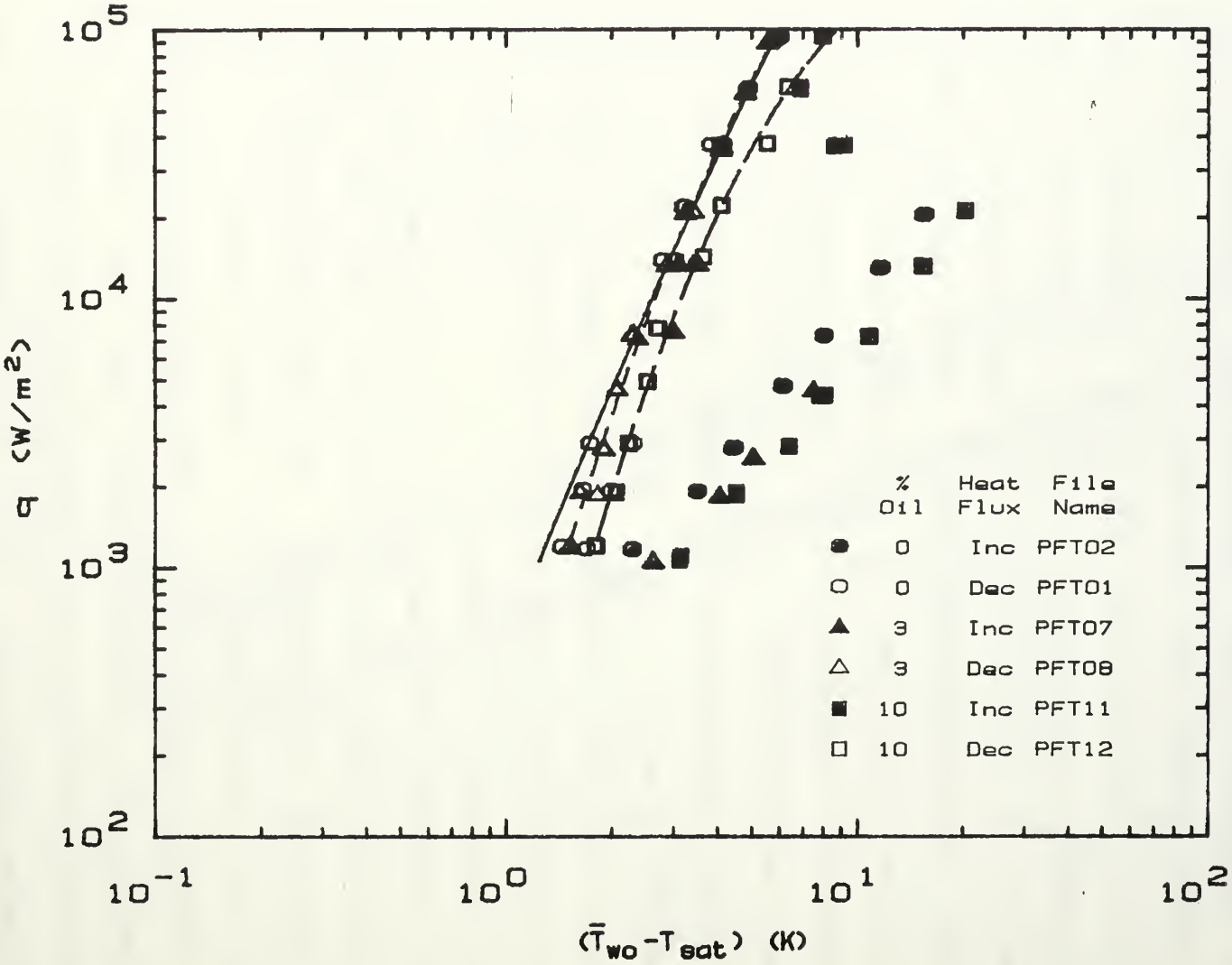

Figure 5.4 Heat-Transfer Performance of Finned Tube (1575 fpm (40 fpi))

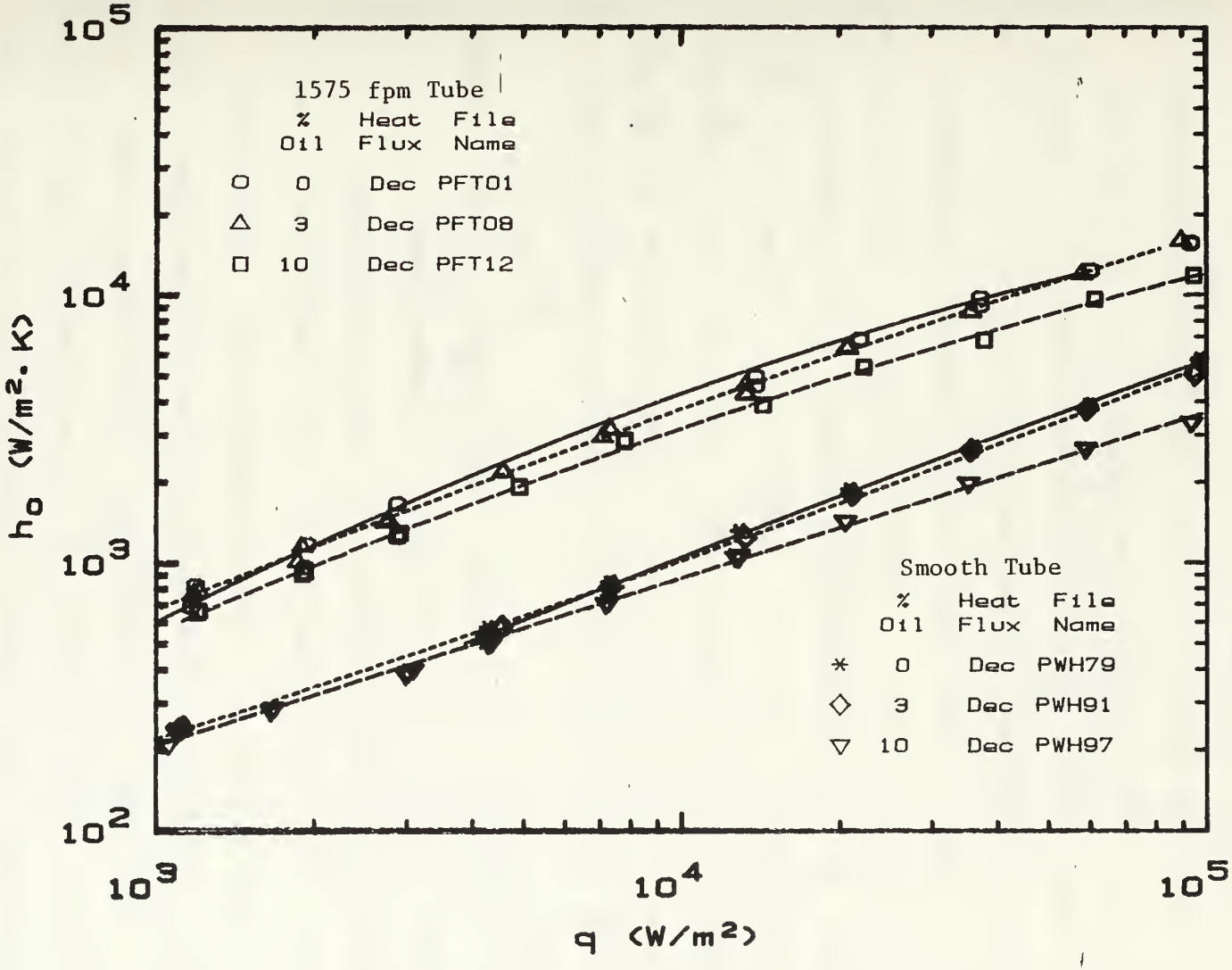

Figure 5.5 Heat-Transfer Performance of 1575 fpm (40 fpi) Tube Compared with Smooth Tube [Ref. 39]

1575 fpm (40 fpi) tube boiling coefficient is only 62 percent of that of the smooth tube. The decrease in local boiling coefficient is once again offset by the large area increase due to the fins.

As shown in Figure 5.6, for the Turbo-B test tube, ONB in the pure refrigerant case occurred at a heat flux of about 1 kW/m^2 and a wall superheat of about 4 K. This is a significant improvement over the smooth tube or the 1024 fpm (26 fpi) tube. Like other tubes studied, increasing oil concentrations caused a delay in ONB. For successive increases in oil concentrations from 0, 3 to 10 percent, the wall superheat, for a given heat flux, increased approximately one kelvin for each of the three oil additions. The variation of the heat-transfer coefficient with heat flux for the Turbo-B and smooth tubes are shown in Figure 5.7.

Like the 1024 fpm (26 fpi) and 1575 fpm (40 fpi) tubes, the Turbo-B tube showed decreases in enhancement ratio with increasing oil concentration. As shown in Figures 5.8, 5.9 and 5.10, the enhancement ratio for the Turbo-B tube was 5.2, 5.0 and 4.7 at 0, 3 and 10 percent oil, respectively.

Among the three tubes studied, the Turbo-B tube clearly shows the best heat-transfer performance under all conditions. At this point, it is worthwhile comparing the best-performing tube found during this investigation with the best-performing tube (the High Flux tube) found during

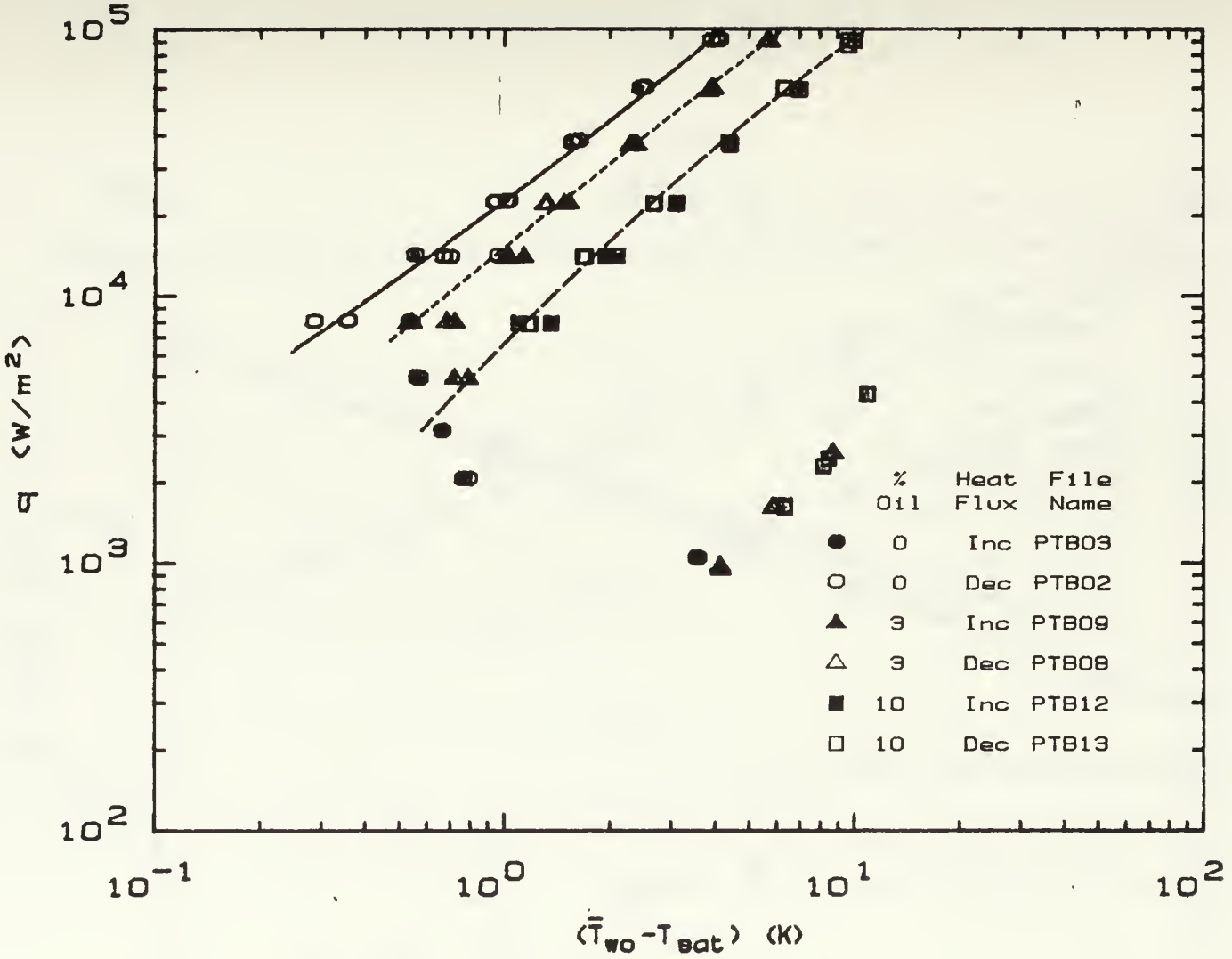

Figure 5.6 Heat-Transfer Performance of Turbo-B Tube

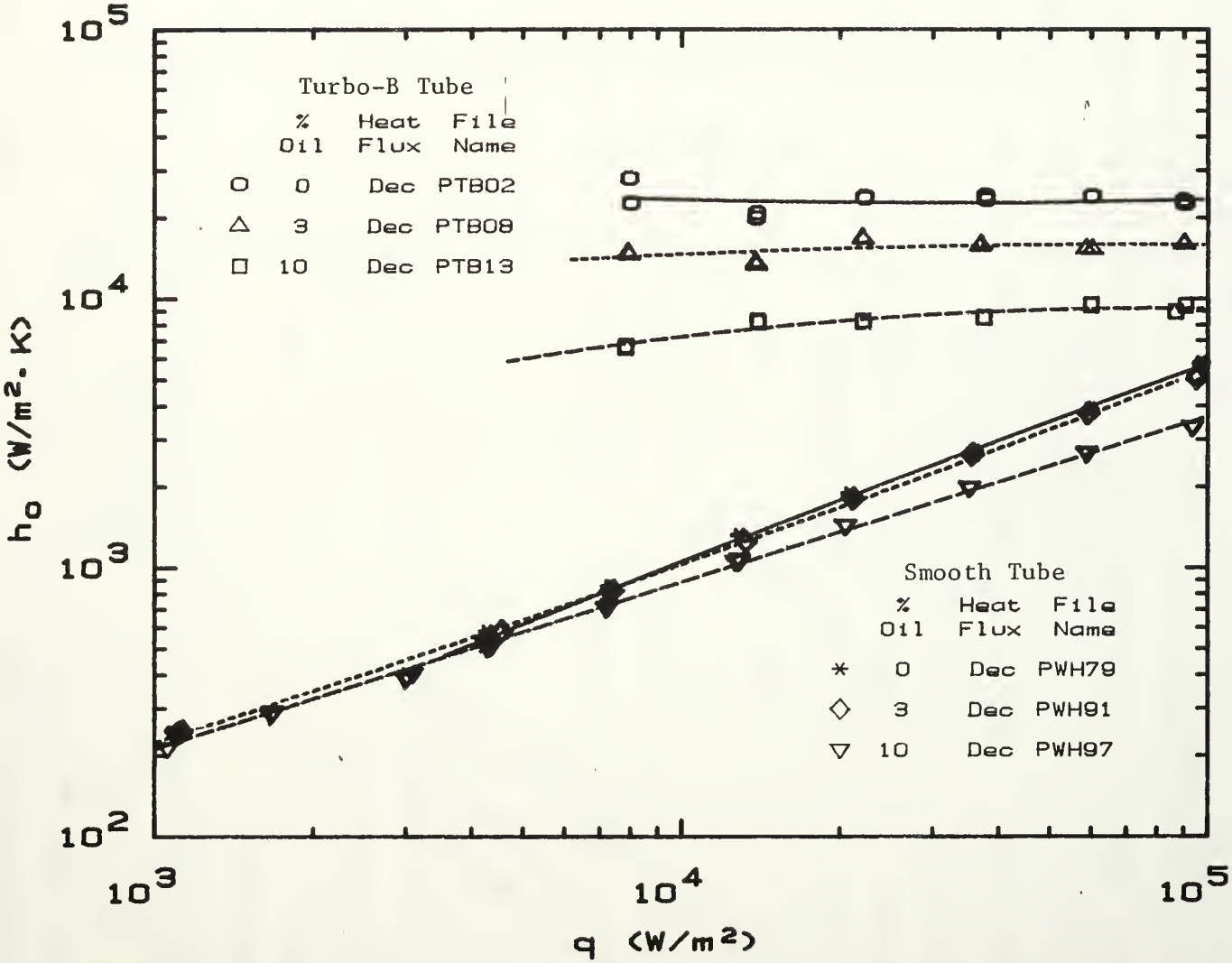

Figure 5.7 Heat-Transfer Performance of Turbo-B Tube Compared with Smooth Tube [Ref. 39]

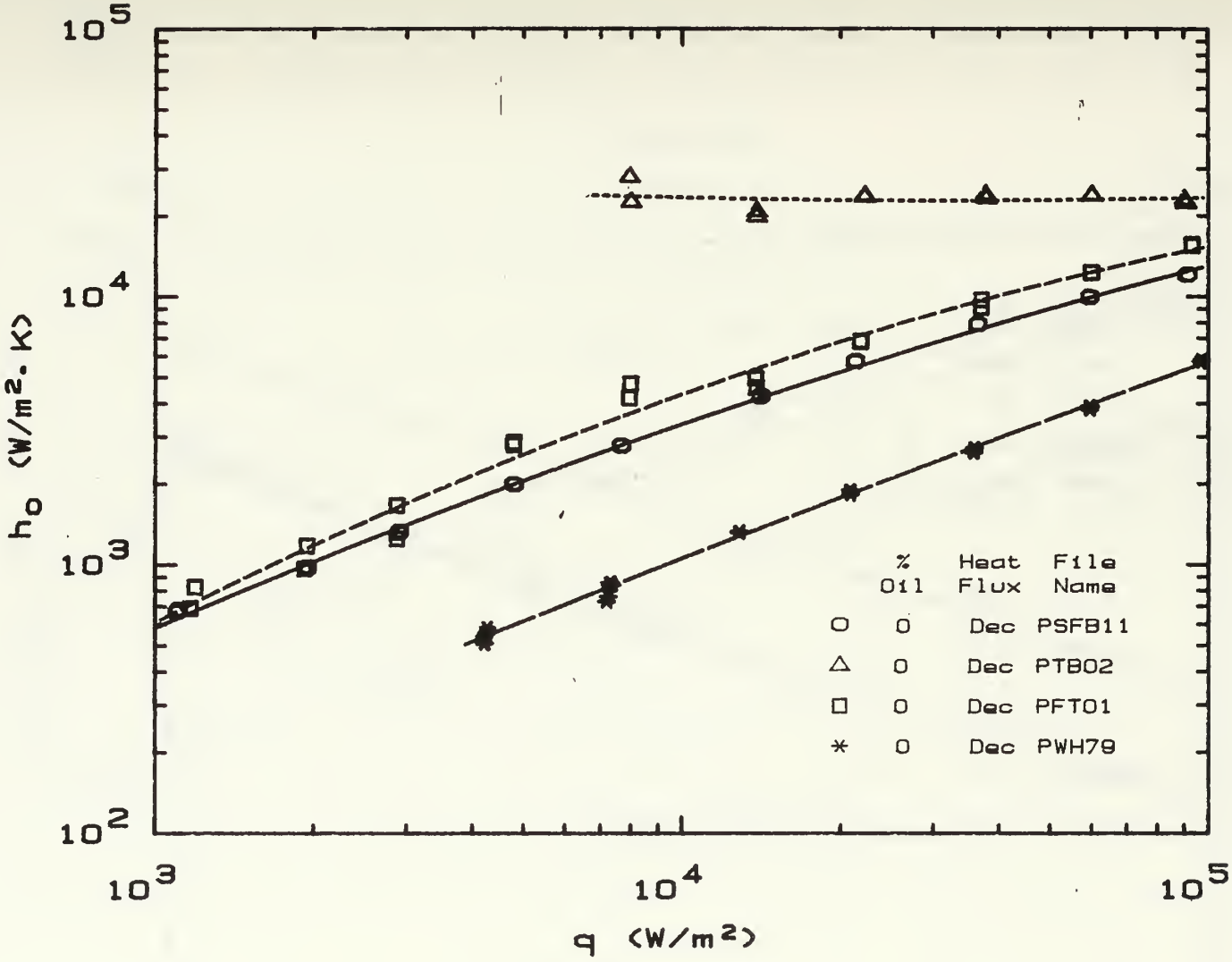

Figure 5.8 Comparison of Heat-Transfer Performance for 1024 fpm, 1575 fpm, Turbo-B and Smooth [Ref. 39] Tubes at 0 Percent Oil

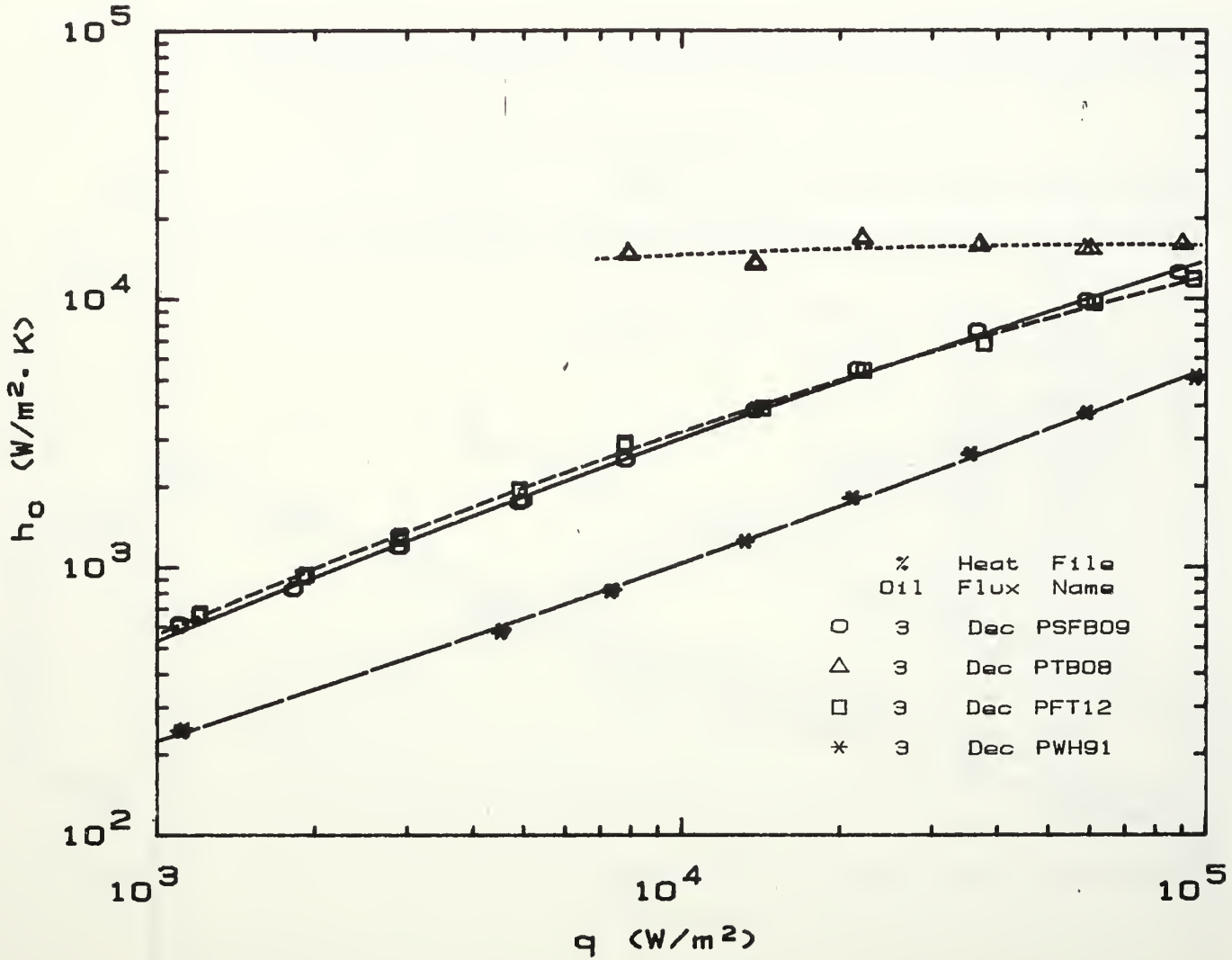

Figure 5.9 Comparison of Heat-Transfer Performance for 1024 fpm, 1575 fpm, Turbo-B and Smooth [Ref. 39] Tubes at 3 Percent Oil

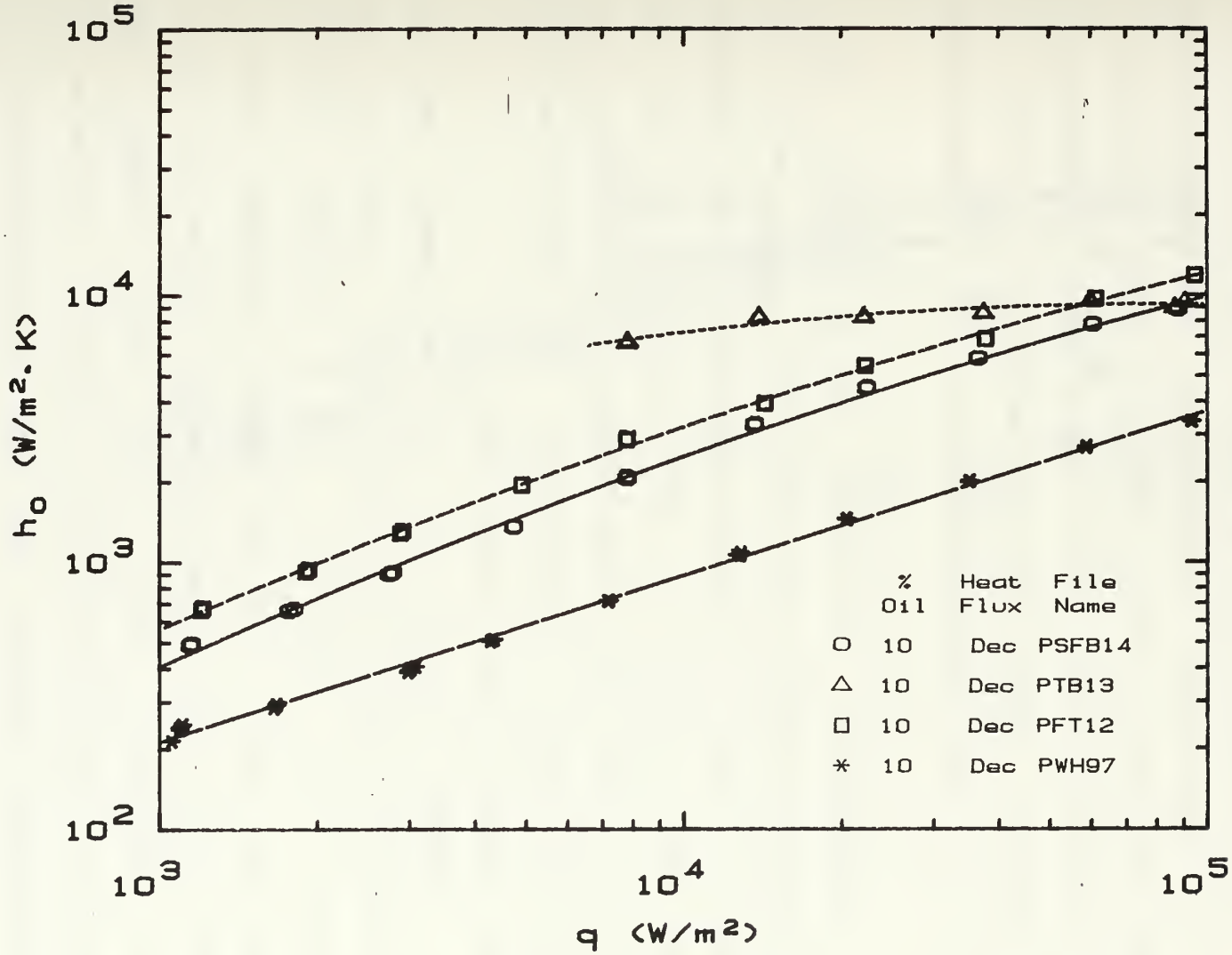

Figure 5.10 Comparison of Heat-Transfer Performance for 1024 fpm, 1575 fpm, Turbo-B and Smooth [Ref. 39] Tubes at 10 Percent Oil

previous investigations [Ref. 39], using the same apparatus. Figure 5.11 compares the performance of these two tubes.

A direct comparison of the Turbo-B and High Flux tubes at oil concentrations of 6 percent or more is difficult because the heat-transfer coefficient of the High Flux tube decreases drastically at heat fluxes in excess of 40 kW/m^2. This is believed to be due to the choking of nucleation sites by the oil. Notice that the reentrant cavity size of the High Flux tube is much smaller than that of the Turbo-B tube.

The heat-transfer coefficient of the Turbo-B tube, remained nearly constant over the studied range, while for the High Flux tube it increased with heat flux for mixtures with less than 3 percent oil. With 0 and 3 percent oil, the Turbo-B tube shows better heat-transfer performance up to 40 kW/m^2 and 60 kW/m^2, respectively, after which the High Flux tube outperforms the Turbo-B tube.

The observed decrease in tube performance as oil concentration is increased is attributable, in part, to the phenomenon of oil migration. As a miscible mixture undergoes pool boiling, the more-volatile component (R-114) vaporizes at the tube surface, thereby leaving the less-volatile constituent (oil). This action causes the concentration of the less-volatile component to increase at the heat-transfer surface. This high oil concentration at the tube wall requires the R-114 liquid to diffuse towards

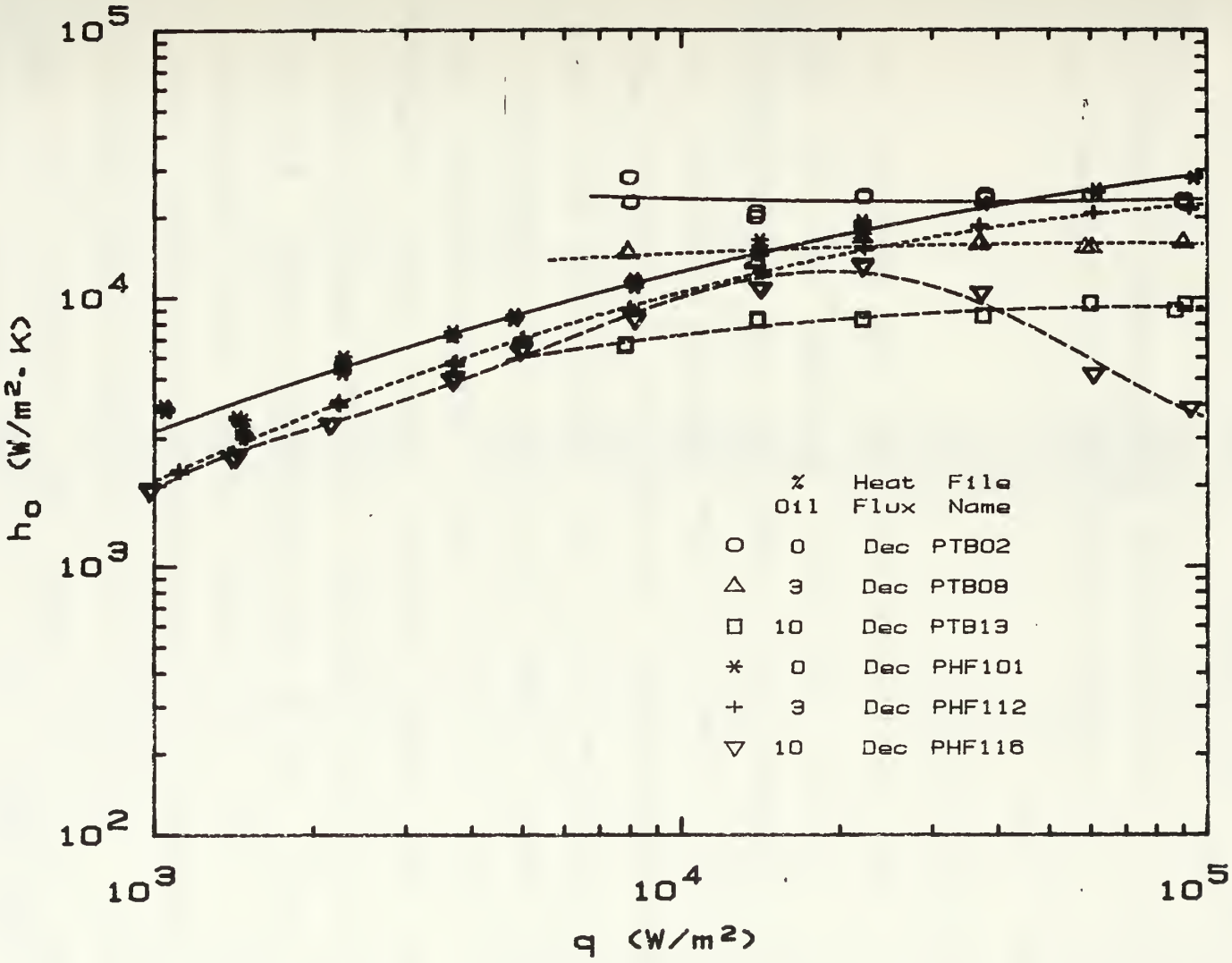

Figure 5.11 Comparison of Turbo-B Tube and High Flux Tube [Ref. 39] Heat-Transfer Performance at 0, 3 and 10 Percent Oil

the wall, as the oil must simultaneously diffuse away from the tube. Therefore, in addition to requiring enough superheat to promote nucleate boiling, additional energy is required to establish the diffusion transport of the components near the wall.

A summary of data collection runs is shown in Table 5.1. A summary of pool-boiling coefficient and enhancement ratio is shown in Table 5.2.

B. TUBE-BUNDLE RESULTS

Due to the very limited time that was available after debugging of the tube-bundle apparatus and the data-reduction programs, only two data runs were performed using the tube bundle. These runs were performed on smooth 0.625-in-diameter copper tubes. The first run measured the heat-transfer performance of the top, instrumented tube, while all of the other 16 tubes (both active and instrumented, as shown in Figure 3.16) in the bundle were in operation. That is, while the electric currents through these 16 heaters were not individually measured, the same voltage was applied as was applied to the top instrumented tube. For this preliminary study, the current through the top instrumented tube was assumed to be representative of that in all of the heated tubes. Therefore, total heat input to the bundle was considered to be 17 times that measured in the top instrumented tube. The second run measured the heat-transfer performance of the same top tube discussed above,

TABLE 5.1

SUMMARY OF DATA COLLECTION RUNS

Tube	% Oil	File Name	Number of Data Points	Heat-Flux Condition
Finned	0	SFB11	20	DEC
(26 fpi)	0	SFB02	20	INC
	1	SFB04	20	DEC
	1	SFB05	20	INC
	2	SFB06	20	DEC
	2	SFB07	20	INC
	3	SFB09	20	DEC
	3	SFB08	20	INC
	6	SFB12	18	DEC
	6	SFB13	20	INC
	10	SFB14	20	DEC
	10	SFB15	20	INC
Finned	0	FT01	20	DEC
(40 fpi)	0	FT02	20	INC
	1	FT04	20	DEC
	1	FT03	23	INC
	2	FT06	23	DEC
	2	FT05	20	INC
	3	FT08	22	DEC
	3	FT07	22	INC
	6	FT09	16	DEC
	6	FT10	23	INC
	10	FT12	20	DEC
	10	FT11	27	INC
Turbo-B	0	TB02	13	DEC
	0	TB03	19	INC
	1	TB04	14	DEC
	1	TB05	17	INC
	2	TB06A	12	DEC
	2	TB06B	19	INC
	3	TB08	12	DEC
	3	TB09	20	INC
	6	TB10	17	DEC
	6	TB11	18	INC
	10	TB13	12	DEC
	10	TB12	18	INC
Single Tube in Bundle	0	BST01	18	Bundle Operating
	0	BST02	20	Bundle Secured

TABLE 5.2

POOL-BOILING COEFFICIENTS AT A PRACTICAL HEAT FLUX OF 30 kW/m^2

Tube	% Oil	Pool-Boiling Coefficient (kW/m^2K)	Enhancement Ratio
Smooth	0	2.4	1.0
	3	2.3	1.0
	10	1.9	1.0
Finned	0	6.8	2.8
26 (fpi)	3	6.0	2.6
	10	5.0	2.6
Finned	0	9.0	3.8
40 (fpi)	3	8.0	3.5
	10	6.0	3.2
Turbo-B	0	12.0	5.2
	3	11.5	5.0
	10	9.0	4.7

except all other heaters in the bundle were turned off. Notice that during both of these runs, the auxiliary heaters were in operation to maintain the same total heat input to the evaporator constant. Boiling took place at approximately 3 ^{o}C.

Figure 5.12 compares the heat-transfer performance of the top tube in the bundle (with all other tubes not in operation) with the smooth tube data of Reilly [Ref. 39] for the smooth tube in the single-tube apparatus. As can be seen, the present data agree with that of Reilly within 10 percent for heat-flux values in excess of 10 kW/m^2. Thus the agreement is quite good for all practical heat-flux values (10-40 kW/m^2). However, the present data show up to 70 percent lower wall superheat values than the data of Reilly for heat-flux values less than 10 kW/m^2. While the exact mechanisms for the observed discrepancy are not known, the extraneous bubbles that were present throughout the bundle, resulting from not insulating the apparatus for this preliminary study, may have been responsible for this improved performance at low heat-flux values.

Figure 5.13, a graph of heat flux versus wall superheat, shows the bundle effect on the top tube in the bundle. As can be seen, the wall superheat decreases by up to 37 percent when the entire bundle was in operation compared to the case with only the instrumented tube in operation. This

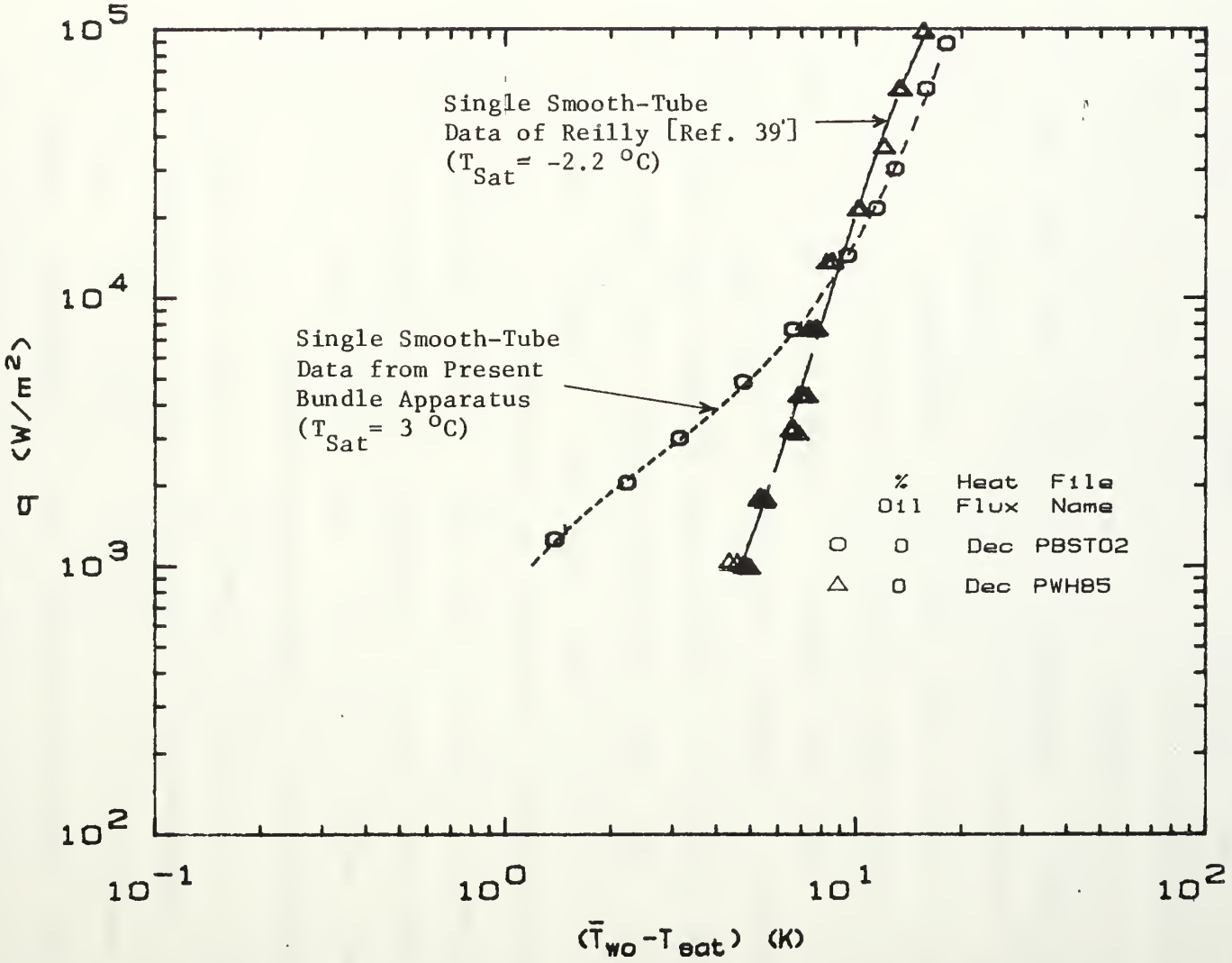

Figure 5.12 Comparison of Single Smooth-Tube Data from Bundle Apparatus with Single Smooth-Tube Data from Single-Tube Apparatus

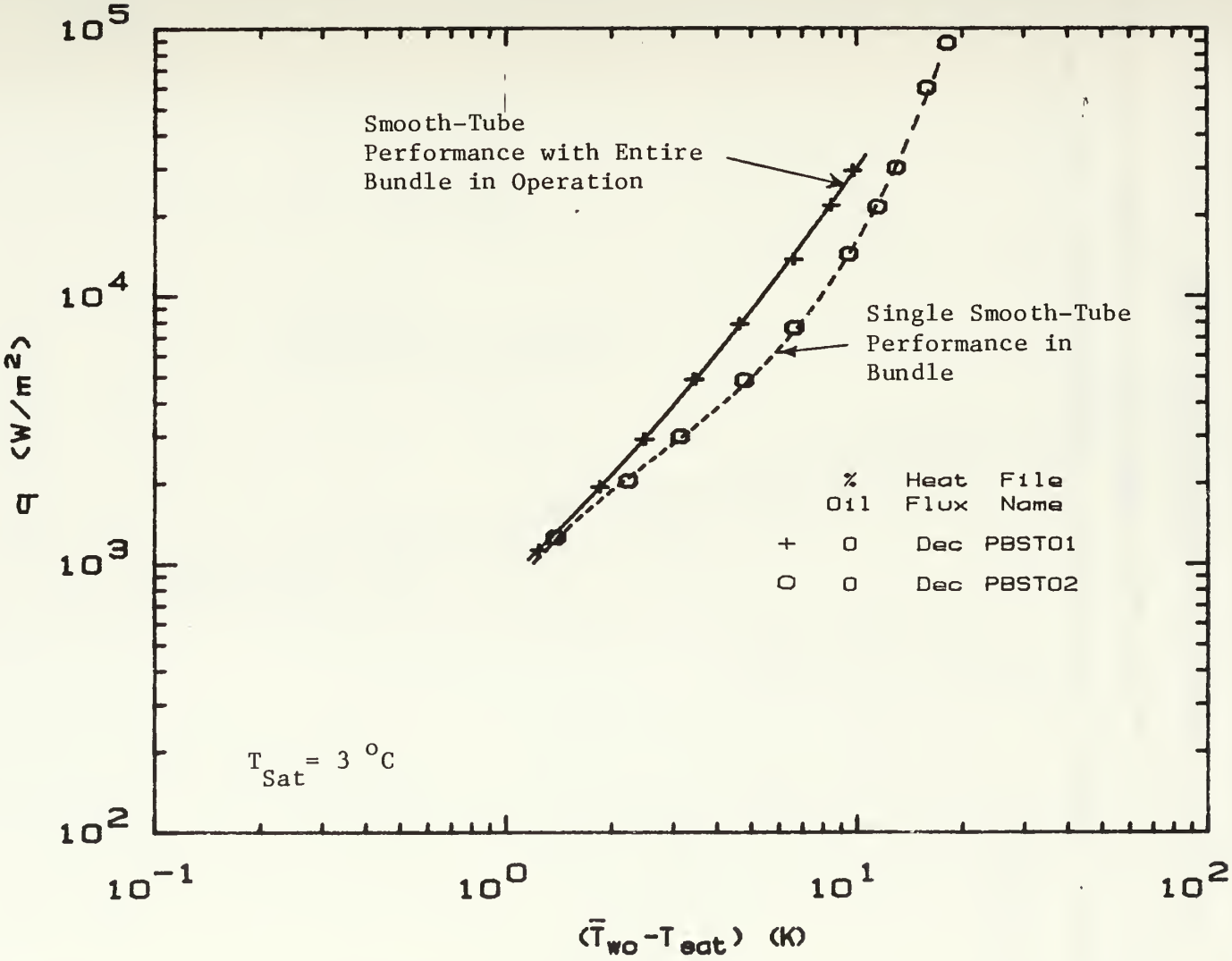

Figure 5.13 Comparison of Top-Tube Heat-Transfer Performance with and without Entire Bundle Operating (Version I)

enhancement is obviously a result of convective bubble-stripping action, as discussed in Chapter II. Notice that the two curves appear to merge at very low heat fluxes (because of diminishing bundle effect) and at very high heat fluxes (possibly a result of vapor blanketing).

Figure 5.14 shows the same comparison as Figure 5.13 on a different basis; pool-boiling heat-transfer coefficient versus heat flux.

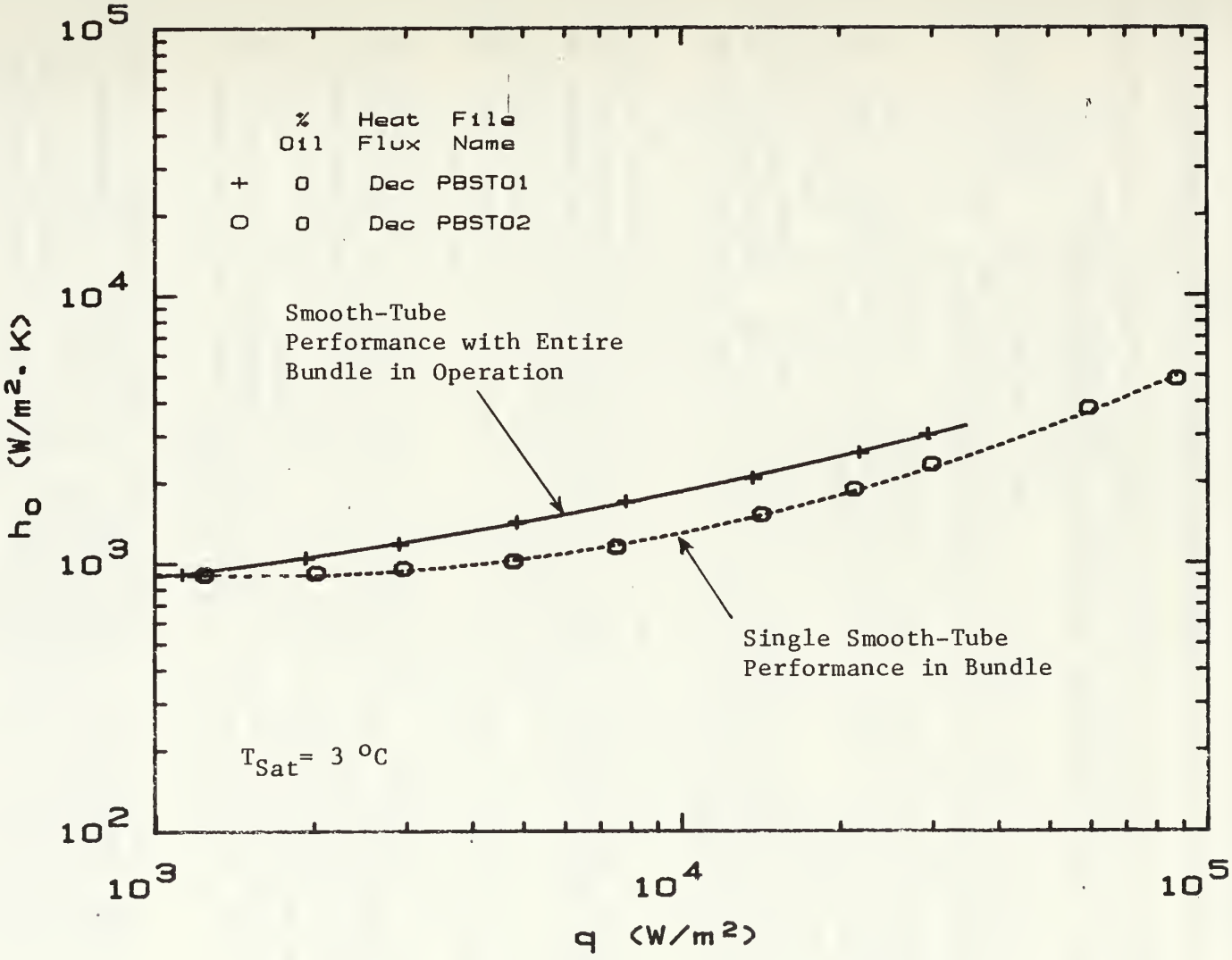

Figure 5.14 Comparison of Top-Tube Heat-Transfer Performance with and without Entire Bundle Operating (Version II)

VI. CONCLUSIONS AND RECOMMENDATIONS

A. CONCLUSIONS

Considering the data gathered during this investigation for boiling of R-114 in both a single-tube and a multi-tube apparatus, the following conclusions are reached:

1. A multi-tube apparatus was successfully designed, assembled and tested for the study of boiling and condensation of R-114 within tube bundles.

2. Preliminary tests were performed on the top tube of a smooth-tube bundle with and without the other tubes in operation. These tests showed up to a 40 percent enhancement in the nucleate pool-boiling coefficient owing to the favorable bundle effect. However, this bundle effect diminished at low heat fluxes (due to the lack of bubble agitation), and at high heat fluxes (due to vapor blanketing).

3. Of the tubes studied during this investigation using the single tube apparatus, the Turbo-B tube showed the best performance, both for the pure-component case as well as at oil concentrations up to 10 percent. Also, for this tube, the nucleate pool-boiling coefficient was fairly insensitive to the heat flux regardless of the oil concentration.

4. At a practical heat flux of 30 kW/m^2, the 1024 fpm finned tube, the 1575 fpm finned tube and the Turbo-B tube resulted in enhancements of the boiling heat-transfer coefficient of 2.8, 3.8 and 5.2, respectively, for the pure-component case. With 3 percent oil, these ratios were decreased to 2.6, 3.5 and 5, while with 10 percent they were further reduced to 2.6, 3.2 and 4.7, respectively.

5. At a practical heat flux of 30 kW/m^2, the Turbo-B tube showed essentially the same pool-boiling enhancements as the previously tested High Flux tube. However, the Turbo-B tube outperformed the High Flux tube at lower heat fluxes, while the High Flux tube showed superior performance at higher heat fluxes with oil concentrations of 6 percent or less.

B. RECOMMENDATIONS

Based on the results of the single-tube and multi-tube experiments, and on the experience gained in the assembly and preliminary data trials with the multi-tube apparatus, the following recommendations are made:

1. The investigation of bundle effect on the top tube in the bundle apparatus should be continued so as to study the enhancement mechanisms observed during preliminary data trials.

2. Increase the concentration of ethylene glycol in the cooling fluid sump and reduce the fluid temperature. This temperature change will enable the condenser to maintain steady-state conditions for higher evaporator heat inputs and will help offset flow limitations of existing circulation pumps.

3. Piping from the circulation pumps should be installed to allow cross connecting the pump discharges. This modification would allow more cooling fluid delivery to the condenser and thereby allow greater heat input from the evaporator.

4. A fixture or jig should be fabricated for the tube support block to maintain tube alignment on the free end of the cantilevered heated tubes.

5. To facilitate the operation of the variable transformers, and to assist in reaching steady state expeditiously, one or more of the following should be installed near the transformer controls: (1) a monitor reading heat input to the apparatus, (2) voltmeters displaying transformer output voltage, or (3) wattmeters for each variable transformer.

6. Install a cooling coil in the multi-tube R-114 reservoir to facilitate more rapid transfer of R-114 liquid from the condenser.

7. The cooling liquid flow control of the single-tube apparatus should be modified to include a valve allowing more precise flow control, especially at low flow rates. This modification would allow the operator to achieve steady-state conditions more readily.

APPENDIX A

UNCERTAINTY ANALYSIS

Using the data at a practical heat flux of 37 kW/m^2, an uncertainty analysis was performed on data run FT02 for the 1024 fpm (26 fpi) tube. The procedure below is based on the Kline-McClintock [Ref. 40] method. This method specifies that given a result (R), which is a function of variables (a,b,c), then the uncertainty in R is given by:

$$\frac{\delta R}{R} = \left[\left(\frac{\partial R}{\partial a}\cdot\frac{\partial a}{R}\right)^2 + \left(\frac{\partial R}{\partial b}\cdot\frac{\partial b}{R}\right)^2 + \left(\frac{\partial R}{\partial c}\cdot\frac{\partial c}{\partial R}\right)^2\right]^{1/2} . \qquad (A.1)$$

During this investigation the heat-transfer rate through the boiling tube was calculated by the equation:

$$Q = VI \qquad (A.2)$$

and the uncorrected heat flux through the tube is:

$$q = \frac{Q}{\pi D_o L} \qquad (A.3)$$

As discussed by Karasabun [Ref. 36], the actual heat flux through the tube should be corrected for heat transfer through the unenhanced ends. Since this correction is quite small (< 5%) and involves a complicated analysis procedure,

it was reasonable to assume the uncertainties in the corrected and uncorrected heat-flux values to be the same. Thus, the uncertainties were calculated using the uncorrected values for heat flux. Notice that this simplifying assumption was used only for the purposes of uncertainty analysis, and not for calculating the actual heat flux or the wall superheat.

Based on the above equations:

$$\frac{\delta Q}{Q} = \left[\left(\frac{\delta V}{V}\right)^2 + \left(\frac{\delta I}{I}\right)^2\right]^{1/2} \qquad (A.4)$$

and

$$\frac{\delta q}{q} = \left[\left(\frac{\delta Q}{Q}\right)^2 + \left(\frac{\delta D_o}{D_o}\right)^2 + \left(\frac{\delta L}{L}\right)^2\right]^{1/2} \qquad (A.5)$$

The heat-transfer coefficient is defined as:

$$h = \frac{q}{T_{Wo} - T_{sat}}, \qquad (A.6)$$

where

$$T_{Wo} - T_{sat} = T_{Win} - G - T_{sat}, \qquad (A.7)$$

and

$$G = \frac{Q \ln\left(\frac{D_o}{D_{in}}\right)}{2 \pi k L}. \qquad (A.8)$$

Following the method of Equation (A.1), the uncertainty in the Fourier conduction term (G) is:

$$\frac{\delta G}{G} = \left[\left(\frac{\delta Q}{Q}\right)^2 + \left(\frac{\delta k}{k}\right)^2 + \left(\frac{\delta L}{L}\right)^2\right]^{1/2} \qquad \text{(A.9)}$$

The resultant uncertainty in the heat-transfer coefficient is:

$$\frac{\delta h}{h} = \left[\left(\frac{\delta q}{q}\right)^2 + \left(\frac{\delta T_{Win}}{T_{Wo}-T_{sat}}\right)^2 + \left(\frac{\delta G}{T_{Wo}-T_{sat}}\right)^2 + \left(\frac{\delta T_{sat}}{T_{Wo}-T_{sat}}\right)^2\right]^{1/2} \qquad \text{(A.10)}$$

The individual uncertainty values are shown in Table A.1 with the resultant uncertainty in heat-transfer coefficient calculated to be about 4 percent.

TABLE A.1

UNCERTAINTY ANALYSIS FOR 1024 FPM (26 FPI) TUBE AT A HEAT FLUX OF 37 kW/m^2

		Remarks
$\frac{\delta V}{V}$	0.005	Sensor Accuracy
$\frac{\delta I}{I}$	0.005	Sensor Accuracy
$\frac{\delta Q}{Q}$	0.0071	Based on Eq. (A.4)
$\frac{\delta q}{q}$	0.0071	
$\frac{\delta k}{k}$	0.15	
$\frac{\delta L}{L}$	0.0005	
$\frac{\delta D}{D}$	0.005	
G	0.13	Based on Eq. (A.8)
$\frac{G}{G}$	0.15	Based on Eq. (A.9)
$\frac{\delta T_{Win}}{T_{Wo}-T_{sat}}$	0.021	
$\frac{\delta T_{sat}}{T_{Wo}-T_{sat}}$	0.018	
$\frac{\delta G}{T_{Wo}-T_{sat}}$	0.026	
$\frac{\delta h}{h}$	0.039	Based on Eq. (A.10)

APPENDIX B

LIST OF NOMENCLATURE

1. Nomenclature

A_{AC}	AC current through heaters	(A)
A_o	Outside area of smooth tube	(m^2)
A^*	Constant evaluated at P^*	
B_o	Coefficient used in Schlünder model	
C_F	Coefficient used in Steiner equation	
c_ℓ	Liquid specific heat	(J/kg·K)
c_{sf}	Coefficient depending on surface/ fluid combination	
C_q	Coefficient in Nakayama equation	
D	Diameter of tube	(m)
d_b	Bubble departure diameter	(m)
$(dP/dT)_{SAT}$	Slope of vapor pressure curve	($N/m^2 \cdot K$)
F	Two-phase Reynolds number	
f(P)	Function of pressure	
G	Fourier conduction term	
Gz	Graetz number	
g	Gravitational acceleration	(m/s^2)
g_c	Gravitational constant	
h	Heat-transfer coefficient	($W/m^2 \cdot K$)
h_{fg}	Specific enthalpy of vaporization	(J/kg)
k	Thermal conductivity	(W/m·K)
L	Length of tube	(m)

m	Reynolds number exponent in single-phase convective correlation	
N	Heat-transfer exponent in Steiner correlation	
N_A/A	Bubble population density	
n	Reynolds number exponent in single-phase friction-factor correlation	
Pr	Prandtl number	
P	Pressure	(N/m^2)
P^*	Reduced pressure P/P_{CR}	
Q	Heat-transfer rate	
q	Heat flux	(W/m^2)
Re	Reynolds number	
r	Exponent in Rohsenow correlation	
r_{VN}	Radius of trapped vapor nucleus	
S	Suppression factor	
s	Exponent in Rohsenow correlation	
T	Temperature	(K or ^oC)
U_o	Overall heat-transfer coefficient based on smooth-tube area	(m^2K/W)
V_{AC}	AC voltage across heaters	(V)
V_{AS}	Output voltage of current sensor	(V)
V_{AC}	Data signal voltage for volts AC	(V)
V_{VS}	Output voltage of voltage	(V)
X	Vapor quality	
$\tilde{X}_i$	Mole-fraction of component i in the liquid phase	
$\tilde{Y}_i$	Mole-fraction of component i in the vapor phase	

β	Mass-transfer coefficient	
δ	Matrix thickness	(m)
ΔP	Difference in vapor pressure corresponding to T_W and T_{sat}	(N/m^2)
ΔPe	Difference in vapor pressure corresponding to effective superheat	(N/m^2)
ΔT	Temperature difference or wall superheat, ($T_W - T_{sat}$)	(K or ^oC)
ΔTe	Effective superheat, with flow	(K or ^oC)
μ	Dynamic viscosity	($N \cdot s/m^2$)
ϕ	Relative vaporization rate	
ρ	Density	(kg/m^3)
σ	Surface tension	(N)
θ_L	Liquid only two-phase friction multiplier	

2. Subscripts

AX	Axial loss
B	Fully developed boiling
Bi	Incipient boiling
c	Corrected for tube end losses
conv	Convective
CR	Critical
ES	External Surface
FC	Forced convection
GO	Based on vapor physical properties only
in	Inner or inside
LH	Latent heat
LO	Based on liquid physical properties only

l	Liquid
NB	Nucleate boiling
o	Outside
PB	Pool boiling
sat	Saturation
v	Vapor
W	Wall

LIST OF REFERENCES

1. Palen, J.W., Yarden, A., and Taborek, J., AIChE Symposium Series, No. 118, Vol. 68, 1972.

2. Wanniarachchi, A.S., Marto, P.J. and Reilly, J.T., "The Effect of Oil Contamination on the Nucleate Pool-Boiling Performance of R-114 from a Porous-Coated Surface," ASHRAE Transactions, Vol. 92, Part 2, 1986.

3. Chongrungreong, S. and Sauer, H.J., Jr., "Nucleate Boiling Performance of Refrigerents and Refrigerant-Oil Mixtures," Journal of Heat Transfer, Vol. 102, pp. 701-705, November 1980.

4. ASHRAE Guide and Data Book, Chapter 18, pp. 281-291, 1963.

5. Helmick, R.L. et al., "Development of an Advanced Air Conditioning Plant for DDG-51 Class Ships," ASNE Journal, Vol. 99, No. 3, pp. 112-123, May 1987.

6. Rohsenow, W.M., "A Method of Correlating Heat Transfer Data for Surface Boiling of Liquids," Transactions ASME, Vol. 74, p. 969, 1952.

7. Sauer, H.J., Jr., Davidson, G.W. and Chongrungreong, S., "Nucleate Boiling of Refrigerant-Oil Mixtures from Finned Tubing," Joint ASME/AIChE National Heat Transfer Conference, Orlando, 1980.

8. Borishanski, V.M., "Correlation of Effect of Pressure on Critical Heat Flux and Heat Transfer," Heat Transfer and Hydrodynamics in Two Phase Flow, pp. 16-37, Pergamon, New York, 1969.

9. Mostinski, I.K., "Teploenergetika," British Chemical Engineering, Vol. 8, p. 580, 1963.

10. Collier, J.G., Convective Boiling and Condensation, McGraw Hill, 2nd Ed., 1985.

11. Marto, P.J. and Hernandez, B., "Nucleate Pool Boiling Characteristics of a Gewa-T Surface in Freon-113," AIChE Heat Transfer Symposium, Seattle, 1983.

12. Yilmaz, S., Palen, J.W. and Taborek, J., "Enhanced Boiling Surfaces as Single Tubes and Tube Bundles," 20th National Heat Transfer Conference, Milwaukee, Wisconsin, 1981.

13. Venart, J.E.S., Sousa, A.C.M. and Jung, D.S., "Nucleate and Film Boiling Heat Transfer in R11: The Effects of Enhanced Surfaces and Inclination," Eighth International Heat Transfer Conference, San Francisco, Vol. 4, pp. 2019-2024, 1986.

14. Wanniarachchi, A.S., Sawyer, L.M. and Marto, P.J., "Effect of Oil on Pool-Boiling Performance of R-114 from Enhanced Surfaces," Joint ASME/JSME Conference in Thermal Engineering, Hawaii, March 1987.

15. Tongze, M., et al., "Effects of Geometrical Shapes and Parameters of Reentrant Grooves on Nucleate Pool Boiling Heat Transfer from Porous Surfaces," Eighth International Heat Transfer Conference, San Francisco, Vol. 4, pp. 2013-2018, 1986.

16. Ayub, Z.H. and Bergles, A.E., "Pool Boiling from GEWA Surfaces in Water and R-113," Augmentation of Heat Transfer in Energy Systems, Vol. 52, pp. 57-64, 1985.

17. Nakayama, W., et al., "Dynamic Model of Enhanced Boiling Heat Transfer on Porous Surfaces," Advances in Enhanced Heat Transfer, pp. 31-43, 1979.

18. Czikk, A.M., and O'Neill, P.S., "Correlation of Nucleate Boiling from Porous Metal Films," Advances in Enhanced Heat Transfer, pp. 53-59, 1979.

19. Schlünder, E.U., "Heat Transfer in Nucleate Boiling of Mixtures," Eighth International Heat Transfer Conference, San Francisco, Vol. 4, pp. 2073-2079, 1986.

20. Pandey, S.K., Sharma, P.R. and Varshney, B.S., "Heat Transfer Studies During Nucleate Pool Boiling of Binary Liquid Mixtures," Eighth International Heat Transfer Conference, San Francisco, Vol. 4, pp. 2087-2092, 1986.

21. Shakir, S. and Thome, J.R., "Boiling Nucleation of Mixtures on Smooth and Enhanced Surfaces," Eighth International Heat Transfer Conference, San Francisco, Vol. 4, pp. 2081-2086, 1986.

22. Arshad, J. and Thome, J.R., "Enhanced Boiling Surfaces: Heat Transfer Mechanism Mixture Boiling," Joint ASME/JSME Conference, Honolulu, Vol. 1, pp. 191-197, 1987.

23. McManus, S.M., Marto, P.J. and Wanniarachchi, A.S., "An Evaluation of Enhanced Heat Transfer Tubing for Use in R-114 Water Chillers," Heat Transfer in Air Conditioning and Refrigeration Equipment, ASME, HTD-Vol. 65, pp. 11-19, December 1987.

24. Chen, J.C., "A Correlation for Boiling Heat Transfer to Saturated Fluids," Ind. and Eng. Chem., Process Design and Development, Vol. 5, No. 3, pp. 322-329, 1966.

25. Bergles, A.E. and Rohsenow, W.M., Journal of Heat Transfer, Vol. 80, p. 365, 1964.

26. Steiner, D., "Evaporation of Cryogenic Fluids in Vertical and Horizontal Tubes," Eighth International Heat Transfer Conference, San Francisco, Vol. 4, pp. 1853-1859, 1986.

27. Chan, A.M.C. and Shoukri, M., "Boiling Heat Transfer and Burnout Around Horizontal Tube Bundles," in Fundamentals of Phase Change: Boiling and Condensation, ASME, HTD-Vol. 38, pp.1-8, 1984.

28. Wallner, R., "Heat Transfer in Flooded Shell and Tube Evaporators," Fifth International Heat Transfer Conference, Tokyo, Vol. 5, pp. 214-217, 1974.

29. Jensen, M.K. and Hsu, J.T., "A Parametric Study of Boiling Heat Transfer in a Tube Bundle," Journal of Heat Transfer, Paper No. 86-F-398, 1986.

30. Cornwell, K. and Schuller, R.B., "A Study of Boiling Outside a Tube Bundle Using High Speed Photography," International Journal of Heat and Mass Transfer, Vol. 25, pp. 683-690, 1982.

31. Robinson, D.B. and Katz, D.L., "Effect of Vapor Agitation on Boiling Coefficients," Chemical Engineering Progress, Vol. 47, pp. 317-324, 1951.

32. Muller, J., "Boiling Heat Transfer on Finned Tube Bundles--The Effect of Tube Position and Intertube Spacing," Eighth International Heat Transfer Conference, San Francisco, Vol. 4, pp. 2111-2116, 1986.

33. Fujita, Y. and Ohta, H., "Boiling Heat Transfer and its Enhancement Technique," Report J-10, Faculty of Engineering, Kyushu University, Japan, 1986.

34. Palen, J.W., Taborek, J. and Yilmaz, S., "Comments to the Application of Enhanced Boiling Surfaces in Tube Bundles," Evaporation and Condensation, pp. 193-203.

35. Bennett, D.L., Davis, M.W. and Hertzler, B.L., "The Suppression of Saturated Nucleate Boiling by Forced Convection Flow," AIChE Symposium Series No. 199, Vol. 26, pp. 91-103, 1980.

36. Karasabun, M., An Experimental Apparatus to Study Nucleate Pool Boiling of R-114 and Oil Mixtures, M.S. Thesis, Naval Postgraduate School, Monterey, California, 1984.

37. Sawyer, L.M., Jr., The Effects of Oil Contamination on the Nucleate Pool-Boiling Behavior of R-114 from Enhanced Surfaces, M.S. Thesis, Naval Postgraduate School, Monterey, California, 1986.

38. Zebrowski, D., Condensation Heat-Transfer Measurements of Refrigerants on Externally Enhanced Tubes, M.S. Thesis, Naval Postgraduate School, Monterey, California, 1987.

39. Reilly, J.T., The Influence of Oil Contamination on the Nucleate Pool-Boiling Behavior of R-114 from a Structured Surface, M.S. Thesis, Naval Postgraduate School, Monterey, California, 1985.

40. Kline, S.J., and McClintock, F.A., "Describing Uncertainties in Single Sample Experiments," Mechanical Engineering, p. 3, 1953.

INITIAL DISTRIBUTION LIST

		No. Copies
1.	Defense Technical Information Center Cameron Station Alexandria, Virginia 22304-6145	2
2.	Library, Code 0142 Naval Postgraduate School Monterey, California 93943-5002	2
3.	Department Chairman, Code 69 Department of Mechanical Engineering Naval Postgraduate School Monterey, California 93943-5004	1
4.	Professor Paul J. Marto, Code 69Mx Department of Mechanical Engineering Naval Postgraduate School Monterey, California 93943-5004	3
5.	Professor A.S. Wanniarachchi, Code 69Wa Department of Mechanical Engineering Naval Postgraduate School Monterey, California 93943-5004	2
6.	Dr. B.H. Hwang, Code 2722V David W. Taylor Naval Ship Research and Development Center Annapolis, Maryland 21402	1
7.	Mr. R. Helmick, Code 2745 David W. Taylor Naval Ship Research and Development Center Annapolis, Maryland 21402	1
8.	Mr. N.R. Clevinger Product and Process Development Mgr. Wolverine Tube, Inc. P.O. Box 2202 Decatur, Alabama 35602	1
9.	Mr. and Mrs. Joseph L. Murphy 1602 Flower Road Schenectady, New York 12303	1

10. LCDR Thomas J. Murphy 2
Long Beach Naval Shipyard
Long Beach, California 90822

11. LCDR David Zebrowski 1
4116 N. Declaire Avenue
Chicago, Illinois 60641

Thesis
M9675 Murphy
c.1 Pool boiling of R-114/
oil mixtures from single
tubes and tube bundles.